Dissertation

Entwicklung eines multidimensionalen bioanalytischen Modellsystems für die gesicherte Identifikation der Auswirkungen von oxidativen Stressfaktoren auf den Organismus

submitted by

Bernhard Michael Wagner

for the Academic Degree of

Doctor of Medical Science

(Dr. scient. med.)

at the

Medical University of Graz

Klinisches Institut für Medizinische und Chemische Labordiagnostik

under the Supervision of

Ass.Prof. Priv.-Doz. Dr.rer.nat. Hubert Scharnagl

2014

Eidesstattliche Erklärung

Ich erkläre ehrenwörtlich, dass ich die vorliegende Arbeit selbstständig und ohne fremde Hilfe verfasst habe, andere als die angegebenen Quellen nicht verwendet habe und die den benutzten Quellen wörtlich oder inhaltlich entnommenen Stellen als solche kenntlich gemacht habe.

Declaration

I hereby declare that this thesis is my own original work and that I have fully acknowledged by name all of those individuals and organizations that have contributed to the research for this thesis. Due acknowledgement has been made in the text to all other material used. Throughout this thesis and in all related publications I followed the guidelines of "Good Scientific Practice".

Graz, 01.09.2014

Acknowledgments

It is time to thank those who have contributed in different ways to the completion of my thesis. First of all, I would like to thank my mentor Erwin Zinser for his interest demonstrated in my work and the constant support in any way over those years. The interesting discussions and enlightening conversations have always been a pleasure. I also want to thank Erwin for sharing with me a little part of his admirable knowledge, which makes him not only an inspiring model of an enthusiastic scientist but also an admirable person. I also want to thank Hubert Scharnagl and Günter Fauler for guiding me through my thesis.

A big “Thank you” goes to Bettina and Miriam, who shared with me the joy and pain of research. They deserve an honorable mention since they patiently endured long sessions of unfiltered conversations and stinky running shoes over the years.

I also want to thank my family and friends for many different reasons that would actually require an extra appendix if proper listed. Thank you for being silently present when I am lost, but encouraging when it is needed. Knowing that you are there really makes the difference.

I also want to thank Valentina Verduci for her laughter, chats, cooking skills and unconditional support. You are the best flat mate I ever had, a great friend and a constant when everything else kept fluctuating around me. I think we both are grown-ups now.

Table of Contents

Abbreviations and Definitions

8-iso-PGF2α	8-iso-Prostaglandine $F_{2\alpha}$
8-MeG	8-mercaptoguanosine
8-OHdG	8-hydroxy-2'-deoxyguanosine
AA	Arachidonic acid
ALA	α-Linolenic acid
APCI	Atmospheric pressure chemical ionization
BHT	Butylhydroxytoluene
BSTFA	N,O-Bis(trimethylsilyl)trifluoroacetamide
CAN	Acetonitrile
COX	COX Cyclooxygenase
CYP450	Cytochrome P450
DGLA	Dihomo-γ-linolenic acid
DHA	Docosahexaenoic acid
DHET	Dihydroxyeicosatrienoic acid
dMRM	Dynamic multiple reaction monitoring
DNA	Deoxyribonucleic acid
EDTA	Ethylenediaminetetraacetic acid
EETs	Epoxyeicosatrienoic acids
EPA	Eicosapentaenoic acid
ESI	Electrospray ionization
FA	Fatty acid
FDA	Food and Drug administration
FT	Freeze-thaw
GC	Gas chromatography
HETE	hydroxyeicosatetraenoic acid
HLB	Hydrophobic-lipophilic balance
HPLC	High performance liquid chromatography
IS	Internal standard
LA	Linoleic acid
LC	Liquid chromatography
LOD	Limit of detection
LOQ	Limit of quantification
LOX	Lipoxygenase
m/z	Mass to charge ratio
MOX	Monooxygenase
MRM	Multiple reaction monitoring
MS	Mass spectrometry
MS/MS	Tandem mass spectrometry
MSTFA	N-Methyl-N-(trimethylsilyl)trifluoroacetamide
NaOH	Sodium hydroxide

NMR	Nuclear magnetic resonance
PBS	Phosphate buffer saline
PCA	Principal component analysis
PG	Prostaglandin
PLS	Partial least square analysis
PUFA	Poly unsaturated fatty acid
QC	Quality Control
QQQ	Triple quadrupole
Q-TOF	Quadrupole – time of flight
R^2	Coefficient of regression
ROS	Reactive oxygen species
S/N	Signal to noise ratio
SD	Standard deviation
SPE	Solid phase extraction
TX	Thromboxane
UHPLC-ESI-MS/MS	Ultra high performance liquid chromatography electrospray tandem mass spectrometry

Zusammenfassung

Jeder aerobe Organismus ist sogenanntem oxidativen Stress ausgesetzt, worunter man jene chemischen Vorgänge versteht, die den Organismus durch Oxidationsprodukte schädigen können. Um nachhaltige Schäden zu vermeiden, haben Organismen unterschiedliche Abwehrmechanismen entwickelt. Kommt es zu einem Ungleichgewicht zwischen oxidativem Stress und diesen Abwehrmechanismen, kann das zu pathophysiologischen Veränderungen führen. Daher ist die Kenntnis über Biomarker des oxidativen Stresses und Status des Metaboloms von immenser Wichtigkeit.

Diese metabolische Prozesse und exogene Faktoren des oxidativen Stresses gelten als Mitursache für neurodegenerative Erkrankungen wie Parkinson oder Alzheimer und werden mit kardiovaskulären Krankheiten und Diabetes in Verbindung gebracht. Die Möglichkeit der simultanen Bestimmung solcher Biomarker verspricht wertvolle Hinweise darauf zu liefern, wie sich verschiedene Formen oxidativen Stresses auf molekularer Ebene auswirken und in weiterer Folge zu pathologischen Veränderungen führen können.

Die Entwicklung neuer bioanalytischer Methoden sowie die Etablierung der bestehenden Methoden an vielen Forschungs- und Diagnostikeinrichtungen eröffnen nicht nur vielversprechende Perspektiven für eine frühzeitige molekulare Diagnostik, sondern ermöglichen auch die Entwicklung neuer und effizienter Behandlungsregimes auf Basis von individuellen zielgerichteten Therapien.

Diese Arbeit zeigt die Entwicklung spezifischer und sensitiver Analyseverfahren verschiedener Biomarker aus humanen Körperflüssigkeiten. Als analytische Verfahren werden Ultrahochdruckflüssigkeitschromatographie gekoppelt mit Tandem-Massenspektrometrie für die Bestimmung von Biomarkern des oxidativen Stresses (8-iso-Prostaglandin F2α, 8-hydroxy-2'-deoxyguanosine) sowie des Status des Metaboloms (Oxilipine) entwickelt. In Kombination mit einschlägigen Methoden der Biostatistik wurde hier ein multidimensionales bioanalytisches Modellsystem für die gesicherte Identifikation der Auswirkungen von oxidativen Stressfaktoren auf den Organismus etabliert.

Abstract

Free radical-induced lipid peroxidation has been implicated in several human diseases, such as cardiovascular diseases, cancer, neurodegenerative diseases and diabetes. The physiological levels of reactive oxygen species (ROS) and other free radicals are regulated by an antioxidant defence system. However, when the rate of radical production exceeds the elimination capacity of the antioxidant defence system, cell damage occurs due to the formation of artificially transformed nucleic acids, proteins, and lipids. Isoprostanes are a unique class of prostaglandin-F_2-like compounds formed in vivo and in vitro by free radical attack on arachidonic acid as well as on other polyunsaturated long-chain fatty acids (PUFAs). Several F_2-isoprostanes have the potential to be used as specific markers for the extent of damage of biological membranes caused by reactive oxygen species. In particular, 8-iso-Prostaglandin $F_{2\alpha}$ has been established as a reliable marker of oxidative stress due to its direct correlation with lipid peroxidation as well as its low abundance under normal physiological conditions in plasma and urine. The field of redox biology serves as a basis for non-invasive markers to assess physiological regulation processes and reactive oxygen species production in vivo. An analytical platform for the simultaneous profiling of oxidative stress markers (8-iso-Prostaglandin $F_{2\alpha}$ and 8-hydroxy-2'-deoxyguanosine) and bioactive lipid mediators from polyunsaturated fatty acids in human body fluids has been developed. Using solid phase extraction and ultra-high performance liquid chromatography coupled to tandem mass spectrometry a easy to handle and less time consuming method could be accomplished. This approach represents a sensitive and versatile analytical technique for qualitative and quantitative analysis targeted markers, which can be constituted as a useful tool for the determination of oxidative stress biomarkers.

The main goal of this thesis is to establish of a high-throughput assay for ROS markers and oxylipins that could become important as a screening tool in nutritional and clinical research.

Overall, this thesis discribes a powerful analytical tool to examine ROS markers and oxylipin profiles as it provides a generic and comprehensive lipidomics approach for simultaneous identification and quantitation of lipid mediators.

1 Introduction

The field of redox biology serves as a basis for non-invasive markers to assess physiological regulation processes and reactive oxygen species (ROS) production in vivo. Metabolomics is a relatively prominent term that have emerged over the last decade. Lipodomics, as a subfield of metabolomics, describes the complex lipid composition of the lipodome, which is the complete lipid profile present in any biological fluid, cell or tissue. The spectrum of lipids covers various structures and functionalities that are divided into different classes. Whereas proteins have modular components (amino acids), lipids do not have similar units. Lipids have a high diversity, structure and large number over a wide concentration range, resulting in a challenge for nowadays-analytical method development.

Lipid associated disorders have reached epidemic proportions in industrialized nations (Scorletti and Byrne, 2013). The peroxidation of lipids is believed to contribute to several diseases include neurodegenerative disorders (Alzheimer's disease, Parkinson's disease, Creutzfeld-Jakob disease), brain aging, cardiovascular disease, multiple sclerosis, tumors, stroke, chronic inflammation and other pathogenic scenarios (Miller et al., 2014, Finkelstein et al., 2014, Engler and Engler, 2006). Aggression of ROS are a possible impairment of the blood brain barrier resulting not only in vascular or inflammatory diseases but also disrupting the circulatory system as well as the central nervous system (Enciu et al., 2013). Due to the vulnerability of the central nervous system to oxidative injury, based on its high demand of oxygen, polyunsaturated fatty acids and weak anti-oxidative defense, the risk of oxidative damage is pervasive.

1.1 Oxilipins and Isoprostanes

Oxylipins are oxidized metabolites and mainly signaling lipids that play an important role in regulation of physiological processes (Tourdot et al., 2014). The ability to measure a wide range of oxylipin levels, as well as markers of oxidative stress, helps to understand their role in health and disease while enabling the non-invasive assessment of ROS production in vivo (Balazy, 2004). Oxylipins are derived from various polyunsaturated fatty acids (PUFAs).

One distinct group of oxylipins are the eicosanoids. The metabolites of the arachidonic acid (C20:4; n-6; AA), which is released by phospholipase A2 from membrane phospholipids is currently in the focus of research. Arachidonic acid is oxygenated by various enzymatic and non-enzymatic reactions. Involving cyclooxygenase-1 (COX-1), cyclooxygenase-2 (COX-2), lipoxygenase

(LOX) and cytochrome monooxygenase (MOX), arachidonic acid is the precursor of major members like series 2-prostanoids, series 4-leukotrienes, hydroxyeicosatetraenoic acids (HETEs), prostacyclin, thromboxane and epoxides (Murphy et al., 2005, Blair et al., 1982). Those metabolites, generated by enzymatic pathways, are mediators of inflammation, fever, and specific diseases (Miller, 2006). Among other factors, oxilipins play an important role in physiological processes such as apoptosis, tissue repair, proliferation, blood clotting, immune response, inflammation and vessel permeability among others (Chan et al., 2011, Lengel, 2014, Wang et al., 2013, Park et al., 2006, Guix et al., 2005, Mungrue et al., 2003, Halliwell and Whiteman, 2004, Beckman and Ames, 1997, Enciu et al., 2013, Finkelstein et al., 2014). They are rapidly metabolized by enzymatic and non-enzymatic, in-vivo as well as in-vitro. Each of the biologically active eicosanoids are potent lipids, very unstable compounds and undergo further biochemical transformation via metabolic degradation, shown in (Haeggström et al., 2010).

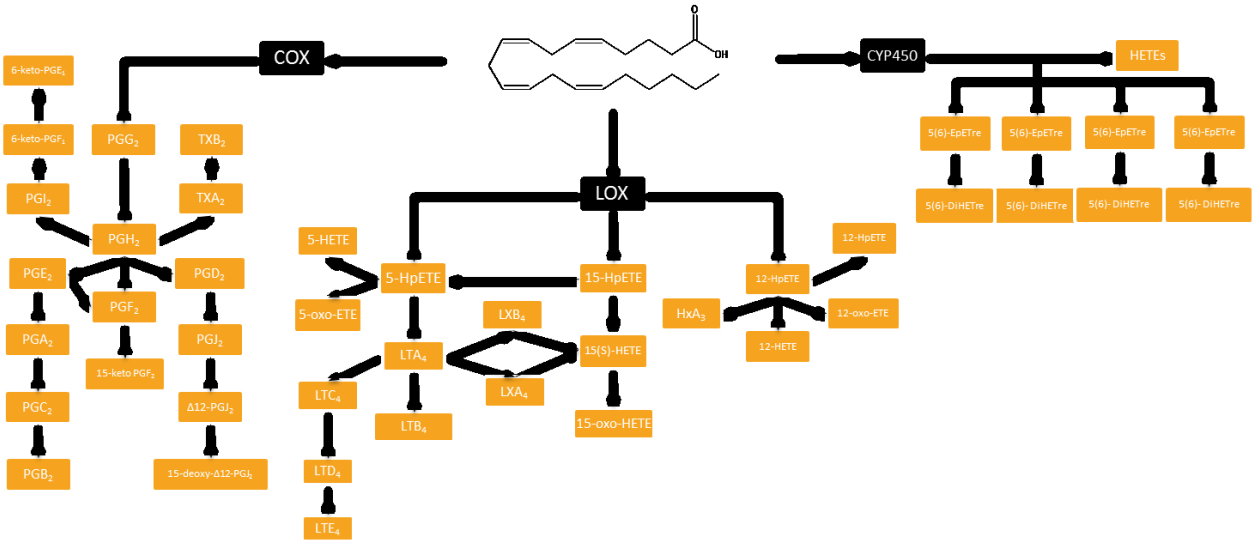

Figure 1-1 Pathway of the precursor arachidonic acid by COX, LOX and CYP450 enzyme metabolism (Strassburg et al., 2012)

Next to those enzymatic metabolites of arachidonic acid, distinct pathways lead to the generation of various hydroxy-, hydroperoxy- and epoxy-fatty acids and isoprostanes, which also involves free radical-mediated oxidations by ROS or Cytochrome P450 (CYP450) (MONTUSCHI et al., 2004). Those, non-enzymatic metabolites, are mainly generated by free radical attack of arachidonic acid esterified in phospholipids (Rokach et al., 1997a, Stafforini et al., 2006). Therefore, high levels of lipid peroxidation products are considered characteristic for damaging the cellular membrane. Isoprostanes are unique prostaglandin-like products containing a variety of prostane ring structures and are composed of various isomers (Rokach et al., 1997b). F2-

isoprostanes represent currently the gold standard of available biomarker in lipid peroxidation (Miller et al., 2014, Nikolaidis et al., 2011, Roberts and Milne, 2009, Davies, 2009).

Other PUFA precursors of the oxylipin formation are for instance the eicosapentaenoic acid (C20:5; EPA) and docosahexaenoic acid (22:6; n-3; DHA), as well as α-linoleic acid (18:3; n-3; ALA) and dihomo-γ-linolenic acid (20:3; n-6; DGLA) representing the further part of oxilipin formation (Mungrue et al., 2003, Halliwell and Whiteman, 2004). Those fatty acids undergo similar metabolic pathways by interacting with ROS and auto-oxidation as well as conversion to oxylipins by three main classes of enzymes, COX, LOX and CYP450. The LOX enzymatic pathway can be divided into 5-LOX, 12-LOX and 15-LOX. For instance leukotrienes are generated via 5-LOX pathway, 12-HETE and 9-HETE are generated via the 12- and 15-LOX pathway among others (Strassburg et al., 2012). Cytochrome P450 generates epoxides that play an important role in cardiovascular functions like vasodilatation. Those epoxides are further metabolized to diols or dihydroxy-fatty acids by hydrolases. An overview is shown in Figure 1-2.

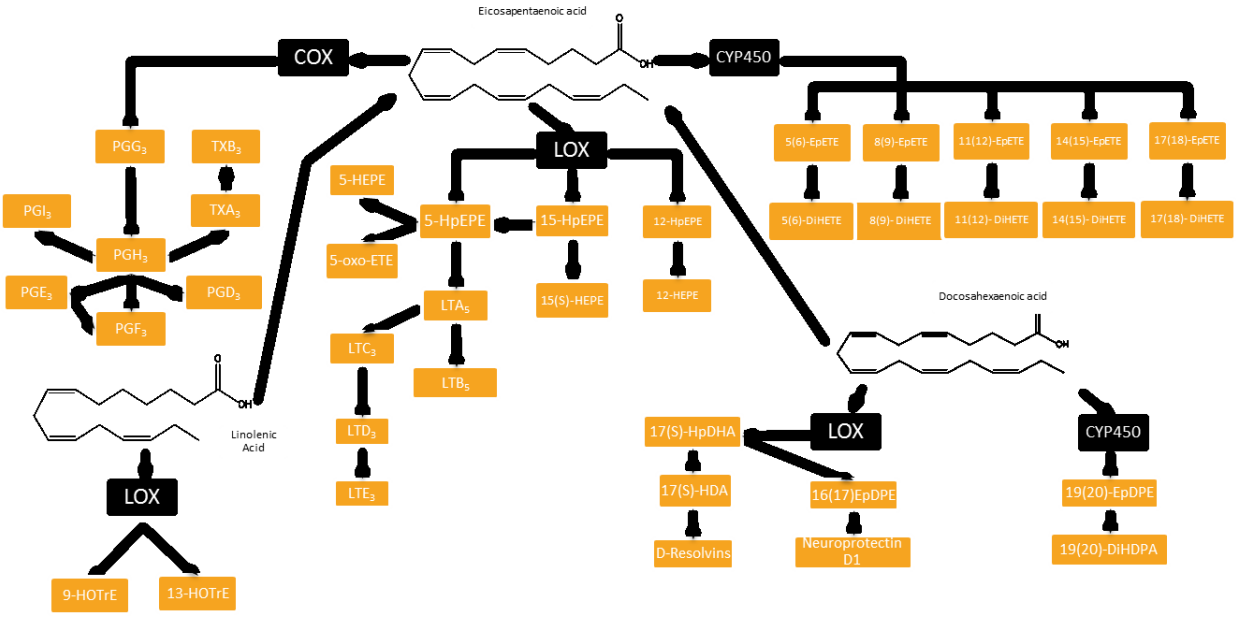

Figure 1-2 Pathway of the precursors linolenic, eicosapentaenoic and docosahexaenoic acid by COX, LOX and CYP450 enzyme metabolism (Strassburg et al., 2012)

Various pathways have already been allocated with association to different autoimmune diseases like neural degeneration, inflammatory diseases or osteoarthristis, whereas others remain unclear (Enciu et al., 2013, Mena et al., 2012, Engler and Engler, 2006, Scorletti and Byrne, 2013, Tourdot et al., 2014, Tsikas and Zoerner, 2014). Novel insights are expected in the field of oxylipin research.

The development of an accurate, specific and sensitive analytical method of these analytical metabolites is a challenging task and requires the development of advanced methods.

1.2 8-Hydroxy-2'-Deoxyguanosine

Next to lipid peroxidation, ROS interactions with DNA can result in modified deoxynucleosides and have been linked to mutation, cancer, inflammation, arteriosclerosis as well as degenerative effects (Cooke et al., 2002, Beckman and Ames, 1997). 8-Hydroxy-2'-deoxyguanosine (8-OHdG) is a resulting oxidation product of deoxyguanosine and has received attention as an indicator of oxidative DNA damage. When damaged DNA is repaired, 8-OHdG is then excreted in urine without further metabolism (Halliwell and Whiteman, 2004).

The reaction of reactive species like peroxynitrite and nitrogen oxide with soluble tyrosine or tyrosine residues in proteins results in free or protein associated 3-nitrotyrosine (Mungrue et al., 2003). The nitriative modification of tyrosine in biological samples is of interest due the very short half-life of reactive species. 3-nitrotyrosine is a very stable metabolite and may serve as a biomarker for reactive species with proteins (Guix et al., 2005).

1.3 Analytical Platform Development

Biomarkers are indicators of biologic and pathologic processes and can be measured and evaluated. Those biomarkers may be used for health examination, diagnosis and further prognosis. Endogenous metabolites are the by-products or end products of numerous complex pathways in human organisms. The concept of monitoring alterations in endogenous metabolites is a common practice. Due to the large inter- and intra-individual variation, lifestyle, endogenous and exogenous influences, the validity of one single metabolite as biomarker is very low. Therefore, a global metabolomic profiling, as the "*big picture*" of the human metabolism is the goal of contemporary "omics" approaches.

Recent advances in analytical technologies have enabled the non-hypothesis-driven non-targeted profiling of metabolites in complex biological matrices. Diversity in chemical properties and wide ranges of metabolite concentrations makes metabolomic profiling a challenge for today's available analytical instruments. High-resolution mass spectrometry coupled to liquid chromatography/gas chromatography separation are powerful tools to determine quantitatively the dynamic multiparametric metabolic response of biological systems. Due to the design of high resolution mass spectrometers, sensitivity is a general problem of those instruments compared to triple

quadruple (QQQ) mass spectrometers. When it comes to LC-MS-MS fragmentation, lower scan speeds of Q-TOF and orbitrap instruments show the limitation of high resolution instruments to detect oxilipins in LC-MS in their isomeric variety at concentrations under 1 nM. Due to their various isomeric forms, full scan high resolution mass spectrometry is not able to differentiate between the different metabolites and MS^2 fragmentation patterns. Furthermore, the higher resolution of orbitrap instruments have their limitation in even less scan rates per second than conventional Q-TOF instruments at same resolution. Hence, they lose even more sensitivity when measuring in strong matrices-background interferences. These limitations are based in the linear trap design of orbitrap instruments.

Profiling platforms, using gas chromatography mass spectrometry (GC-MS), are the methods of choice when it comes to matrix effects. Due the design of the electron ionization (EI) source, ion suppression is less prone to matrix effects (Halket et al., 2005). EI spectra for data convolution are comparable across different MS-manufactures, based on the standardized EI ionization voltage of 70 eV. Furthermore, scan rates up to 500Hz in high resolution are possible with GC-TOF instruments. Availability of standardized spectral libraries, high sensitivity, reproducibility and high resolution chromatography are advantages over LC-MS (Pasikanti et al., 2008). When it comes to oxylipins detection, the analytes are mostly derivatized prior to analysis, in order to reduce their polarity and facilitate chromatographic separation. A clear disadvantage over LC-MS are these several necessary, moisture sensitive derivatization steps to reduce polarity or increase the vapor pressure to overcome volatility problems of metabolites for GC-MS compatibility.

Overcoming the limitations of GC-MS, with needs for derivatization and long sample preparation, electrospray ionization (ESI) LC-MS is the favored technique for oxlipin analysis, due to its ability to measure polar or pre-ionized compounds. When analyzed by ESI-LC-MS-MS, oxylipins easily form deprotonated anions on higher pH in negative mode. Furthermore, LC-MS-MS can lead to the development of fast and sensitive high throughput assays for profiling and quantitative analysis. Due to their low basal levels, QQQ mass spectrometers and targeted analysis are the analytical technique of choice.

The classical analytical concept of targeted analysis/profiling is limited by a relatively small fraction of analytes of the metabolome, time consuming method development and limited sample information compared to non-targeted analysis. However, the strengths of this approach are higher sensitivity, great accuracy and precision, particularly where stable isotope labelled internal

standards are available. When it comes to biological matrices, ion suppression effects are often critical in ESI-LC-MS and have to be evaluated very carefully. Since non-targeted profiling does not include any analyte-specific checks on validity, quantitative results of those techniques should be handled with reservation (Murphy et al., 2005, Stafforini et al., 2006, Weißenbacher, 2013, Gritti and Guiochon, 2013, Theodorou et al., 2007, Gouveia-Figueira and Nording, 2013, Roux et al.).

Next to mass spectrometry NMR spectroscopy represents a rapid and nondestructive technique with advanced chemical structural information and minimal sample preparation. Multiple metabolites can be identified and quantified in one single analytical run, but sensitivity is significant lower compared to mass spectrometry. Moreover, low-abundance metabolites may be overlapped by signals from high abundance sources (Theodorou et al., 2007). Therefore, NMR is not an option for profiling oxylipins.

Depending on the analytical question, the choice of analytical techniques plays an important role due to the unique strengths and weaknesses of every platform.

The collected data of the acquired samples in "omics" approaches need a statistical processing framework (Trappe et al., 2013). Several well-established statistical methods are therefore the tools of choice to detect small differences in metabolic studies. Starting from post-processing of acquired data sets, followed by data analysis using principal component analysis (PCA) and partial least-squares discriminant analysis (PLSDA) a final validation of statistical models represents an applicable strategy for dealing with large-scale human metabolomics studies (FDA, 2001).

Classical diagnosis is based on "one variable at a time" (OVAT) approaches (Maddipati and Zhou, 2011). To this day, the diagnosis of diabetes depends on the glucose levels in blood or cholesterol levels for arteriosclerosis diagnosis. However, the high complexity and high variance of endogenous levels of humans make those OVAT- approaches struggle. Various variables with dozens of observations resulting in huge data matrices are hard to overcome with basal statistics. Therefore, chemometrics helps to reduce the dimensionality without losing the original information. PCA is a linear dimensionality reduction technique that has been widely applied in all scientific domains. It embeds data from a high dimensional space to a low dimensional space while keeping all the relevant linear structures intact (FDA, 2001). The PCA is an unsupervised technique meaning the process depends exclusively on the input variables, and does not take into account

information about the observations (grouping). Partial least square discriminant analysis (PLSDA) is a supervised feature extraction, the process takes into account the input variables as well as additional information. The PLSA has been developed over the years (Roberts and Morrow, 2000, Milne et al., 2005). One advantage of this supervised technique is the ability to work well for data with small observation sizes and large numbers of parameters (Morrow et al., 1990). In general, the PCA and PLSDA provides useful information in the original data. However, because of the reduced dimension, the interpretation of the results cannot be readily made and the extraction of meaningful information is still a challenging task.

1.4 Aim

The aim of this thesis is to develop an analytical platform, starting from pre-analytics to liquid chromatography mass spectrometry detection, to the conversation and post-processing of the acquired data using multivariate statistic techniques. This platform could serve as a powerful tool for growing interests in oxidative stress research. The main goal of this platform development is to offer sufficient fundamental knowledge about expected effects, resulting in diseases and therefore comprehensive analysis of involved metabolic pathways.

2 Material and Methods

2.1 8-iso-Prostaglandin $F_{2\alpha}$ Method Development for Online Solid Phase Extraction

Chemicals and materials used in these experiments are found in the appendix and 2.3.

For sample preparation, 1 mL of plasma was spiked with 100 ng of 8-iso-$PGF_{2\alpha}$ and 10 ng 8-iso-$PGF_{2\alpha}$–d_4 in methanol. The sample was mixed with 1 mL of water and 2 mL of hydrolyze reagent (20 mL of 25% NaOH in 20 mL, 100 mL methanol). After hydrolysis at 37°C for 1 hour, the sample was cooled at room temperature, mixed with 1 mL of 3% formic acid and adjusted to pH 3 by hydrochloric acid.

Afterwards, the solution was extracted 3 times with 5 mL of hexane. The supernatants were pooled and evaporated to dryness by a steam of nitrogen. The sample was resolved in 1 mL of 25% methanol and injected on the online-SPE-LC-MS system.

The developed online-SPE-LC-MS system was equipped with two quaternary pumps and an external Rheodyne MX Series II switching valve. The UHPLC System includes an Accela 1000 system with a surveyor quaternary pump (Thermo Electron, USA). 950 µL sample were injected on a strata-x SPE-cartridge (25µm, 20 x 2.0mm, Phenomenex, Aschaffenburg, Germany). Flow was set to 0.3 mL/min with 0.1% acetic acid/methanol 80:20, isocratic conditions. After 5 minutes, the sample loopwas washed and a linear gradient over 2 minutes to 40% methanol was induced and held for 1.5 minutes. After finishing the cartridge cleaning step, the valve was switched to the second position and targeted analytes were eluted by the second pump with an linear gradient starting from 15:85 to 5:95 over 10 minutes, 0.1% acetic acid in water : 0.1% acetic acetonitrile. Flow rate was set to 0.15 ml/min and held for 5 minutes. A Kinetex C18 (150x2.1mm, 2.6µm, Phenomenex, Aschaffenburg, Germany) was used for analytical separation after the SPE cartridge.

Mass spectrometry detection was performed with a LCQ fleet ion trap, using MS-MS negative full scan mode with the precursor ion 353.2 m/z (8-iso-$PGF_{2\alpha}$) and 357.2 m/z (8-iso-$PGF_{2\alpha}$-d_4) in negative mode.

2.2 8-iso-Prostaglandin $F_{2\alpha}$ Offline Solid Phase Extraction Method Development

The columns, solvents and gradients tested are show in Table 2-1 to Table 2-3

Table 2-1 tested columns for offline-SPE method development

Product Name	Dimension	Manufacturer
YMC Triat C18	150 x 2.0 mm; S-3 µm	YMC Europe GmbH
YMC-Pack Pro C18	150 x 2.0 mm; S-3 µm	YMC Europe GmbH
YMC-Pack C8	150 x 2.0 mm; S-3 µm	YMC Europe GmbH
Titan C18	100 x 2.1 mm; 1.9 µm	YMC Europe GmbH
Luna 3u C18(2) 100A	250 x 2.1 mm; 5 µm	Phenomenex
Kinetex 2.6u C18 100A	150 x 2.1 mm; 2.6 µm	Phenomenex
Kinetex 5u C18 100A	250 x 2.1 mm; 4.6 µm	Phenomenex
Synergi 5u Hydro RP-100A	250 x 2.1 mm; 5 µm	Phenomenex
Inertsil ODS-4 3µm	150 x 2.1 mm;3 µm	GL Sciences
Kinetex 1.7u, C18, 100A	150 x 2.1 mm;1.7 µm	Phenomenex
Kinetex 1.7u, XB-C18, 100A	150 x 2.1 mm;1.7 µm	Phenomenex
Kinetex 2,6u Phenyl-Hexyl, 100A	100 x 2.1 mm;2.6 µm	Phenomenex
Kinetex 2.6u C8, 100A	100 x 2.1 mm;2.6 µm	Phenomenex
Poroshell 120 SB-18	150 x 2.1 mm;2.7 µm	Agilent
Poroshell 120 EC-CN	100 x 2.1 mm;2.6 µm	Phenomenex
Synergi 4u Hydro RP-80A	250 x 2.1 mm; 4 µm	Phenomenex
Nucleoshell RP 18	150 x 2.1 mm; 2.7 µm	Machery-Nagel

Table 2-2 tested L solvents

Solvent A	Solvent B
0.1% acetic acid	0.1% acetic methanol
0.1% acetic acid	0.1% acetic acetonitrile
0.1% acetic acid	0.1% acetic methanol/0.1% acetic acetonitrile 75%/25% (v:v)
0.1% acetic acid	0.1% acetic acetonitrile/0.1% acetic methanol 75%/25% (v:v)
0.1% acetic acid	0.1% acetic methanol/0.1% acetic isopropanol 75%/25% (v:v)
0.1% acetic acid	0.1% acetic acetonitrile/0.1% acetic isopropanol 75%/25% (v:v)

Table 2-3 tested isocratic and gradient methods

Isocratic 30		
[min]	Solvent A [%]	Solvent B [%]
0.00	70	30
20.0	70	30
Isocratic 40		
[min]	Solvent A [%]	Solvent B [%]
0.00	60	40
20.0	60	40
Isocratic 50		
[min]	Solvent A [%]	Solvent B [%]
0.00	50	50
20.0	50	50
Isocratic 60		
[min]	Solvent A [%]	Solvent B [%]
0.00	40	60
20.0	40	60
Isocratic 70		
[min]	Solvent A [%]	Solvent B [%]
0.00	30	70
20.0	30	70
Gradient 15		
[min]	Solvent A [%]	Solvent B [%]
0.00	95	5
15	5	95
20	5	95
Gradient 10		
[min]	Solvent A [%]	Solvent B [%]
0.00	95	5
10	5	95
15	5	95

2.3 Sample Preparation Plasma/Urine

SPE columns have been tested based on the recommended manufacture protocols. Strata C18-E, Strata-X, Strata-X-AW, (Phenomenex, Aschaffenburg, Germany), Bond Elute C18, Bond Elute Certify II (Agilent, Waldbronn, Germay) and Waters HLB (Waters, Eschborn, Germany) materials were used and SPE column recovery was determined, by processing a working solution of 1 ng/mL 8-iso-$PGF_{2\alpha}$/8-iso-$PGF_{2\alpha}$-d_4 in 15% methanol (v:v). 1 mL of the solution has been analyzed directly or after the different SPE extractions.

Higher methanol starting concentrations up to 40% methanol (v:v) of the working solution have been tested to gain proper starting conditions for SPE after methanol-alkali-hydrolysis.

Matrix recovery has been tested by spiking 100 ng of 8-iso-$PGF_{2\alpha}$ and 8-iso-$PGF_{2\alpha}$-d_4 respectively in 10 mL urine and plasma. The concentration of the blank plasma and urine solutions were determined before spiking.

2.4 Validation 8-iso-Prostaglandin $F_{2\alpha}$

For the determination of 8-iso-$PGF_{2\alpha}$ in human plasma and urine, a sensitive liquid chromatography mass spectrometry (LC-MS) method was validated in the concentration range 100-3200 pg/mL. The sample preparation included SPE for der subsequent LC-MS measurement. The mass spectrometer operated, in MRM mode under negative electrospray ionization conditions. Stable isotope labeled 8-iso-$PGF_{2\alpha}$–d_4 has been used as internal standard.

2.4.1 Standards

The working standard reference compound was 8-iso-$PGF_{2\alpha}$, lot # 196633 (Cayman Chemical). The internal standard reference compound was 8-iso-$PGF_{2\alpha}$-d_4 , lot # 176634 (Cayman Chemical). Due to the inherited endogenous levels of 8-iso-$PGF_{2\alpha}$, methanol was used as a blank matrix.

2.4.2 Reagents:

Reagents used for validation are shown in Table 5-1.

2.4.3 Instruments

Instruments used for Validation are shown in Table 5-2

2.4.4 Sample Preparation Plasma:

Samples and calibration standards were thawed at room temperature. An aliquot of 1 mL was diluted with 0.5 mL water, 1 mL sodium hydroxide reagent (10 mL 50% [w/w] NaOH, 100 mL methanol and 10 mL water) was added, gently mixed, flushed with nitrogen, closed and incubated for 45 minutes in a water bath at 37°C for 60 minutes. The vials were cooled in cold water and acidified with HCl to pH 3. 10 ng 8-iso-$PGF_{2\alpha}$-d_4 were added from the internal standard working solution. Then 3 mL methanol were added to each sample, gently mixed and centrifuged, at 4000 rpm for 10 min. Then, the supernatant was diluted with 6 mL of 1% formic acid and loaded on a Strata-X SPE column (200 mg). Previous, the SPE column was conditioned with 3 mL of methanol and 3 mL of water. The samples were washed with 5 mL 10% methanol in water and 5 mL of 50%

methanol in water. Afterwards, the analytes were eluted two times with 2 mL 0.1% formic methanol. The eluate was dried under nitrogen and reconstructed in 100 µL methanol.

The vials were closed and stored at -70°C until analysis.

2.4.5 Sample Preparation Urine

Analytical samples and standards were thawed at room temperature mixed and centrifuged for 10 minutes at 4000 rpm. A 1 mL aliquot of the supernatant was diluted with 0.5 mL methanol, 1 ng 8-iso-$PGF_{2\alpha}$-d_4 was added from the internal standard working solution and mixed. Afterwards, 2 mL of 2 mM BIS-TRIS buffer was added, mixed and the pH was then adjusted with potassium hydroxide to pH 6. The sample was loaded subsequently on the SPE-X-AW-column (200 mg), previous conditioned with 3 mL of 1% formic methanol and 3 mL of water. Then, the column was washed with 3 mL water 3 mL 30% methanol and 3 mL acetonitrile. The analytes were eluted with two times of 2 mL methanol, eluates were pooled, evaporated and reconstituted in 100 µL methanol with 0.1% formic acid (v:v).

2.4.6 LC-MS Setup

A thermo Surveyor chromatography system was coupled to a TSQ Quantum discovery max QQQ mass spectrometer (Thermo Electron, USA). Column temperature was heated to 40°C. Autosampler temperature was controlled at 10 °C. For separation a 2.1 x 250 mm Luna C18(2) column (Phenomenex, Aschaffenburg, Germany) was used. The mobile phase contained 0.1% acetic acid in water (solvent A) and 0.1% acetic acid in methanol (solvent B). Gradient, MS-switching valve positions and flow rates are shown in

Table 2-4 LC parameters 8-iso-PGF$_{2\alpha}$

LC gradient				
Time [min]	Solvent A [%]	Solvent B [%]	Flow rate [µl/min]	Switching valve
0.00	70	30	400	waste
0.25	70	30	400	waste
0.75	35	65	400	waste
5.50	35	65	400	waste
5.51	35	65	200	detector
8.00	30	70	200	detector
12.00	0	100	200	detector
12.01	0	100	600	waste
14.50	0	100	600	waste
14.51	70	30	600	waste
16.5	70	30	600	waste

MS tune parameters are shown in Table 2-5.

Table 2-5 tune parameters 8-iso-PGF$_{2\alpha}$ TSQ Quantum discovery max

API	HESI
Ionization mode	Negative
Spray voltage	2500 V
Vaporizer temperature	347 °C
Sheath gas pressure	50
Aux gas pressure	15
Capillary temperature	320 °C
Collision pressure	3.0 arb
Mode	SRM
Transition 8-iso-PGF$_{2\alpha}$	353=>193 m/z
Transition 8-iso-PGF$_{2\alpha}$-d4	357=>197 m/z
Scan width	1 amu
Dwell time	500 msec
Collision Energy	35
Q1 Peak width	1.5 (FWHM)
Q3 Peak width	1.5 (FWHM)

Data acquisition and evaluation was performed using XCALIBUR 1.5 & 2.1. The calibration was obtained by weighted least squares linear regression of the peak area ratios of sample/standard versus the nominal concentration of the target analyte. The weighting factor was $1/x^2$.

$$y = kx + d$$

y ….. peak area ratio sample / standard

x ….... nominal concentration of target

k ….... slope of the regression line

d ….... y-intercept of the regression line

2.4.7 Validation procedure

2.4.7.1 Specificity

The specificity of the method was examined by the analysis of six blank water samples. The samples were worked up without addition of the internal standard. All blank water extracts must not exhibit significant interferences at the retention time of target and internal standard.

2.4.7.2 Linearity

To check the calibration model, five replicates of the calibration standards were prepared. All standards were used for calculation of the calibration curve. The linearity was checked by plotting versus the nominal concentration of:

- the peak area ratios of 8-iso-$PGF_{2\alpha}$ / 8-iso-$PGF_{2\alpha}$ $-d_4$
- the back-calculated concentrations for each calibration sample
- the percentage deviation of the back-calculated values

The regression model will be accepted if no tendency can be observed visually between the nominal standard concentrations and the back-calculated values.

2.4.7.3 Accuracy and precision

2.4.7.3.1 Intra-Day

Five replicates of QC samples at 280 and 1120 pg/mL concentration levels were prepared and chromatographed with a set of calibration standards in one single run. Accuracy was measured as

bias (percent deviation of the calculated versus the nominal values) and precision was expressed as coefficient of variation (%). Both, accuracy and precision should not exceed 15%.

2.4.7.3.2 Inter-Day

Four sets of 5 QC samples at 280 and 1120 pg/mL concentration levels were prepared and chromatographed with a set of calibration standards on four different days. Means were calculated and accuracy was measured as bias (percent deviation of the calculated versus the nominal values) and precision was expressed as coefficient of variation (%) of the means. Both, accuracy and precision should not exceed 15%.

2.4.7.4 Limit of Quantitation

2.4.7.4.1 Intra-day

Five replicates of LOQ samples at 100 pg/ml concentration level were prepared and chromatographed with a set of calibration standards in one single batch. Accuracy was measured as bias (percent deviation of the calculated versus the nominal values) and precision was expressed as coefficient of variation (%). Both, accuracy and precision should not exceed 20%.

2.4.7.4.2 Inter-Day

Four sets of five replicates of LOQ samples at 100 pg/ml concentration level were prepared and chromatographed with a set of calibration standards on four different days. Accuracy was measured as bias (percent deviation of the calculated versus the nominal values) and precision was expressed as coefficient of variation (%). Both, accuracy and precision should not exceed 20%.

2.4.7.5 Stability

Stability data were calculated over the validated range 5 samples from the blank plasma pool were analyzed to determine endogenous basal values.

Stability data were calculated over the validated range 5 samples from the blank urine pool were analyzed to determine endogenous basal values.

2.4.7.5.1 Short Term Stability in Plasma

Five spiked plasma samples at 280, 700 and 1120 pg/ml concentration levels were melted to room temperature and left to stand three hours at room temperature. Further, five spiked plasma samples of the same concentrations were melted and all samples were spiked with the IS and analyzed. The means of the concentrations were compared. Instability or decomposition is indicated by a deviation of the means of more than 15%.

2.4.7.5.2 Short Term Stability in Urine

Five spiked urine samples at 280, 700 and 1120 pg/ml concentration levels were melted to room temperature and left to stand three hours at room temperature. Further five spiked urine samples of the same concentrations were melted and all samples were spiked with the IS and analyzed. The means of the concentrations were compared. Instability or decomposition is indicated by a deviation of the means of more than 15%.

2.4.7.5.3 Long Term Stability in Plasma

Five spiked plasma samples were spiked with 280, 700 and 1120 pg/ml concentration levels and prepared for analysis. Five replicas of each concentration level were melted at room temperature and were then immediately analyzed. Five replicates of each level were analyzed on four different days and 2 month later. Additionally, five samples from the blank plasma pool were analyzed to determine endogenous basal values. Concentrations were calculated and the means were compared to the immediately analyzed samples. The means should not deviate for more than 15%.

2.4.7.5.4 Long Term Stability in Urine

Five spiked urine samples were spiked with 280, 700 and 1120 pg/ml concentration levels prepared for analysis. Five replicas of each concentration level were melted at room temperature and immediately analyzed; five replicates of each level were analyzed on four different days and 2 month later. Additionally, five samples from the blank urine pool were analyzed to determine endogenous basal values. Concentrations were calculated and the means were compared to the immediately analyzed samples. The means should not deviate for more than 15%.

2.4.7.5.5 Freeze-thaw Stability in Plasma

Three series of three spiked plasma samples at 280, 700 and 1120 pg/ml concentration levels were prepared and stored at –70°C. Three samples from each level were subjected to three freeze/thaw cycles, three samples to two, three samples to one, and three samples to none. The samples were then spiked with the internal standard and analyzed. Additionally, the means of the concentrations were compared. Instability or decomposition is indicated by a deviation of the means after freeze-thaw cycles from the means of samples not thawed of more than 15%.

2.4.7.5.6 Freeze-thaw Stability in Urine

Three series of 3 spiked urine samples at 280, 700 and 1120 pg/ml concentration levels were prepared and stored at –70°C. Three samples from each level were subjected to three freeze/thaw cycles, three samples to two, three samples to one, and three samples to none. The samples were

then spiked with the internal standard and analyzed. Additionally, the means of the concentrations was compared. Instability or decomposition is indicated by a deviation of the means after freeze-thaw cycles from the means of samples not thawed of more than 15%.

2.4.7.5.7 Autosampler Stability Plasma Samples

Five QC samples at 280, 700 and 1120 pg/mL were prepared and loaded onto the autosampler. The samples were chromatographed at once and 24 hours later. The means of the concentrations were compared. Instability or decomposition is indicated by a deviation of the means of more than 15%.

2.4.7.5.8 Autosampler Stability Urine Samples

Five QC samples at 280, 700 and 1120 pg/mL were prepared and loaded onto the autosampler. The samples were chromatographed at once and 24 hours later. The means of the concentrations were compared. Instability or decomposition is indicated by a deviation of the means of more than 15%.

2.4.7.6 Aliquot Analysis

In order to study the possible effect of dilution in case of out-of-range samples, five samples at a concentration of 3200 pg/mL were analyzed in one single run. A sample aliquot of 200 µl (dilution factor=2) was used. Analysis of 200 µl aliquots was performed as described. Concentrations were calculated against the usual standard curve (undiluted). The measured concentrations should not deviate more than 15% from the nominal concentration.

2.4.7.7 Study Design

Day 1:	Linearity test	Intra-day accuracy and precision	LOQ – day 1	F-T-stability day 0	Dilution	Specificity
Day 2:	Linearity test	Inter-day accuracy and precision	LOQ – day 2	F-T-stability day 1	Aliquot analysis	Short term stability
Day 3:	Linearity test	Inter-day accuracy and precision	LOQ – day 3	F-T-stability day 2		
Day 4:	Linearity test	Inter-day accuracy and precision	LOQ – day 4	F-T-stability day 3		
Day 5:	Linearity test	Inter-day accuracy and precision	LOQ – day 5			
Day 6:	Linearity test	Inter-day accuracy and precision	LOQ – day 5	Long term stability		

2.5 Development of analytical LC-MS method for the detection of 8-hydroxy-2'-deoxyguanosine

To achieve fast chromatography with good separation several columns, solvents and gradients have tested shown in Table 2-6 to Table 2-8.

Table 2-6 tested columns for 8-OHdG detection

Product Name	Dimension	Manufacturer
YMC Triat C18	150 x 2.0 mm; S-3 µm	YMC Europe GmbH
YMC-Pack Pro C18	150 x 2.0 mm; S-3 µm	YMC Europe GmbH
YMC-Pack C8	150 x 2.0 mm; S-3 µm	YMC Europe GmbH
Luna 3u C18(2) 100A	250 x 2.1 mm; 5 µm	Phenomenex
Kinetex 2.6u C18 100A	150 x 2.1 mm; 2.6 µm	Phenomenex
Kinetex 5u C18 100A	250 x 2.1 mm; 4.6 µm	Phenomenex
Synergi 5u Hydro RP-100A	250 x 2.1 mm; 5 µm	Phenomenex
Inertsil ODS-4 3µm	150 x 2.1 mm;3 µm	GL Sciences
Kinetex 2,6u Phenyl-Hexyl, 100A	100 x 2.1 mm;2.6 µm	Phenomenex
Kinetex 2.6u C8, 100A	100 x 2.1 mm;2.6 µm	Phenomenex
Poroshell 120 SB-18	150 x 2.1 mm;2.7 µm	Agilent
Poroshell 120 EC-CN	100 x 2.1 mm;2.6 µm	Phenomenex
Synergi 4u Hydro RP-80A	250 x 2.1 mm; 4 µm	Phenomenex
Nucleoshell RP 18	150 x 2.1 mm; 2.7 µm	Machery-Nagel

Table 2-7 tested solvents for the detection of 8-OHdG

Solvent A	Solvent B
0.1% formic acid	0.1% formic methanol
0.1% formic acid	0.1% formic acetonitrile
0.1% formic acid	0.1% formic methanol/0.1% formic acetonitrile 75%/25% (v:v)
0.1% formic acid	0.1% formic acetonitrile/0.1% formic methanol 75%/25% (v:v)
0.1% formic acid	0.1% formic methanol/0.1% formic isopropanol 75%/25% (v:v)
0.1% formic acid	0.1% formic acetonitrile/0.1% formic isopropanol 75%/25% (v:v)

Table 2-8 tested isocratic and gradient methods for 8-OHdG detection

Isocratic 30		
[min]	Solvent A [%]	Solvent B [%]
0.00	70	30
20.0	70	30
Isocratic 40		
[min]	Solvent A [%]	Solvent B [%]
0.00	60	40
20.0	60	40
Isocratic 50		
[min]	Solvent A [%]	Solvent B [%]
0.00	50	50
20.0	50	50
Isocratic 60		
[min]	Solve56766666nt A [%]	Solvent B [%]
0.00	40	60
20.0	40	60
Isocratic 70		
[min]	Solvent A [%]	Solvent B [%]
0.00	30	70
20.0	30	70
Gradient 15		
[min]	Solvent A [%]	Solvent B [%]
0.00	95	5
15	5	95
20	5	95
Gradient 10		
[min]	Solvent A [%]	Solvent B [%]
0.00	95	5
10	5	95
15	5	95

After the general testing procedure, the optimal gradient conditions were optimized for the chosen column.

The recovery was determined by preparing pooled urine. Samples were prepared as descripted in 2.6.4. 10 replicas of blank urine was measured and ten replicas of blank urine spiked with 5 ng/mL.

2.6 Validation of 8-hydroxy-2'-deoxyguanosine in Human Urine

For the determination of 8-hydroxy-2'-deoxyguanosine (8-OHdG) in human urine a sensitive liquid chromatography/mass spectrometry (LC-MS) method was validated in the concentration ranges indicated. The sample preparation contains a filtration step for der subsequent LC-MS measurement. The mass spectrometer was operated in MRM mode under positive electrospray ionization conditions. 8-mercaptoguanosine (8-MeG) was used as internal standard.

2.6.1 Standards

The working standard reference compound was 8-OHdG, lot # 031M4074V (Sigma). The internal standard reference compound was 8-MeG, lot # 011H4060 (Sigma). Due to the inherited endogenous levels of 8-OHdG, methanol was used as a blank matrix.

2.6.2 Reagents

Reagents used for validation are shown in Table 5-3

2.6.3 Instruments

Instruments used for Validation are shown in Table 5-4

2.6.4 Sample Preparation Urine

Samples and calibration standards were centrifuged at 4000 rpm for 10 minutes and 850 µL of the supernatant were spiked by adding 50 µL internal standard 8-MeG [1000 nM] and gently mixed. The resulting solution was further filtrated over a 0.45 µm nylon syringe filter into a 2 mL glass vial for LC-MS/MS analysis.

The vials were closed and stored at -70°C until analysis.

2.6.5 LC-MS Setup

A Thermo Surveyor chromatography system was coupled to a TSQ Quantum discovery max QQQ mass spectrometer (Thermo Electron, USA). Column temperature was heated to 40°C. Autosampler temperature was controlled at 10°C. For separation a 4.0 x 150 mm (5µm) Hypersil Gold aQ column (Thermo Fisher, USA) was used. The mobile phase contained 0.1% formic acid in water (solvent A) and 0.1% formic acid in methanol (solvent B). Gradient, MS-switching valve positions and flow rates are shown in Table 2-9.

Table 2-9 LC parameter 8-OHdG

Gradient program				
Time [min]	Solvent A [%]	Solvent B [%]	Flow rate [µl/min]	Switching valve
0.00	75	25	800	waste
6.30	79	21	800	waste
6.31	79	21	200	detector
10.00	67	33	200	detector
10.50	67	33	200	detector
10.51	0	100	400	waste
13.50	0	100	400	waste
13.51	100	0	400	waste
15.51	100	0	400	waste

MS tune parameters are shown in Table 2-10.

Table 2-10 tune parameters 8-OHdG TSQ Quantum discovery max

API	HESI
Ionization mode	Negative
Spray voltage	4000 V
Vaporizer temperature	100 °C
Sheath gas pressure	45
Aux gas pressure	5
Capillary temperature	330 °C
Collision pressure	3.0 arb
Mode	MRM
Transition 8-OHdG	284=>168 m/z
Transition 8-MeG	316=>184 m/z
Scan width	1 amu
Dwell time	500 msec
Collision Energy 8-OHdG	22
Collision Energy 8-MeG	23
Q1 Peak width	0.7 (FWHM)
Q3 Peak width	0.7 (FWHM)

Data acquisition and evaluation was performed using XCALIBUR 1.5 & 2.1. The calibration was obtained by weighted least squares linear regression of the peak area ratios of sample/standard versus the nominal concentration of the target analyte. The weighting factor was 1/x.

$$y = kx + d$$

y ….. peak area ratio sample / standard

x …... nominal concentration of target

k …... slope of the regression line

d …... y-intercept of the regression line

2.6.6 Validation procedure

2.6.6.1 Specificity

The specificity of the method was examined by the analysis of six blank water samples. The samples were worked up without addition of the internal standard. All blank water extracts must not exhibit significant interferences at the retention time of target and internal standard.

2.6.6.2 Linearity

To check the calibration model, five replicates of the calibration standards were measured. All standards were used for calculation of the calibration curve. The linearity was checked by plotting versus the nominal concentration of:

- the peak area ratios of 8-hydroxy-2'-deoxyguanosine/8-mercaptoguanosine
- the back-calculated concentrations for each calibration standard
- the percent deviation of the back-calculated values

The regression model will be accepted if no tendency can be observed visually between the nominal standard concentrations and the back-calculated values.

2.6.6.3 Accuracy and Precision

2.6.6.3.1 Intra-day

Five replicates of QC samples at 8.75, 35 and 70 nM concentration levels were prepared and chromatographed with a set of calibration standards in one single batch. Accuracy was measured as bias (percent deviation of the calculated versus the nominal values) and precision was expressed as coefficient of variation (%). Both, accuracy and precision should not exceed 15%.

2.6.6.3.2 Inter-Day

Four sets of 5 QC samples at 8.75, 35 and 70 nM concentration levels were prepared and chromatographed with a set of calibration standards on 3 different days. Means were calculated and accuracy was measured as bias (percent deviation of the calculated versus the nominal values)

and precision was expressed as coefficient of variation (%) of the means. Both, accuracy and precision should not exceed 15%.

2.6.6.4 Limit of Quantification

2.6.6.4.1 Intra-Day

Five replicates of LOQ samples at 3.11 nM concentration level were prepared and chromatographed with a set of calibration standards in one single run. Accuracy was measured as bias (percent deviation of the calculated versus the nominal values) and precision was expressed as coefficient of variation (%). Both, accuracy and precision should not exceed 20%.

2.6.6.4.2 Inter-Day

Four sets of five replicates of LOQ samples at 3.11 nM concentration level were prepared and chromatographed with a set of calibration standards on three different days. Accuracy was measured as bias (percent deviation of the calculated versus the nominal values) and precision was expressed as coefficient of variation (%). Both, accuracy and precision should not exceed 20%.

2.6.6.5 Stability

Five samples from the blank urine pool were analyzed to determine endogenous basal values.

2.6.6.5.1 Long Term Stability in Urine

Five spiked urine samples were spiked with 10 and 50 nM concentration levels prepared for analysis. Five replicas of each concentration level were melted at room temperature and immediately analyzed; five replicates of each level were analyzed on four different days. Additionally, five samples from the blank urine pool were analyzed to determine endogenous basal levels. Concentrations were calculated and the means were compared to the immediately analyzed samples. The means should not deviate for more than 15%.

2.6.6.5.2 Freeze-Thaw Stability

Three series of 3 spiked urine samples at 10 and 50 nM concentration levels were prepared and stored at –70°C. Three samples from each level were subjected to three freeze/thaw cycles, three samples to two, three samples to one, and three samples to none. The samples were then spiked with the internal standard and analyzed. Additionally, the means of the concentrations were compared. Instability or decomposition is indicated by a deviation of the means after freeze-thaw cycles from the means of samples not thawed of more than 15%.

2.6.6.5.3 Autosampler Stability

Five QC samples at 6 nM were prepared and loaded onto the autosampler. The samples were chromatographed at once and 24 hours later. The means of the concentrations were compared. Instability or decomposition is indicated by a deviation of the means of more than 15%.

2.6.6.5.4 Aliquot Analysis

In order to study the possible effect of dilution in case of out-of-range samples, five samples at a concentration of 100 nM were analyzed in one single run. A sample aliquot of 200 µl (dilution factor=2) was used. Analysis of 200 µl aliquots was performed as described. Concentrations were calculated against the usual standard curve (undiluted). The measured concentrations should not deviate more than 15% from the nominal concentration.

2.6.7 Study Design

Run 1:	Linearity test	Intra-day accuracy and precision	LOQ – day 1	F-T-stability day 0	Dilution	Specificity
Run 2:	Linearity test	Inter-day accuracy and precision	LOQ – day 2	F-T-stability day 1	Aliquot analysis	
Run 3:	Linearity test	Inter-day accuracy and precision	LOQ – day 3	F-T-stability day 2		
Run 4:	Linearity test	Inter-day accuracy and precision	LOQ – day 4			
Run 5:	Linearity test	Inter-day accuracy and precision	LOQ – day 5	Long term stability		

2.7 Oxylipin Detection

Due the loss of the availability of the Thermo Surveyor chromatography system coupled with a TSQ Quantum discovery max QQQ mass spectrometer at the Kinderklinik Graz, a new tandem mass spectrometry system was acquired to cover the sensitivity for mass sensitive trace analysis.

The acquired LC-MS/MS system, at the metabology lab (FH JOANNEUM, Graz, Austria), includes a 1290 UHPLC system (Agilent Technologies, Waldbronn, Germany) coupled to a sensitive 6460 triple quadruple mass spectrometer (Agilent Technologies, Santa Clara, CA, USA). UHPLC chromatography with backpressure up to 1250 bar, ensuring faster chromatography hence higher sensitivity, coupled to a more sensitive mass spectrometer enables a sensitivity increase up to 10 fold, compared to the previous system.

The ability to inject lower volume of sample extracts is an important capability to reduce matrix effects. A possible cause for matrix effects is a limited number of excess charges and space on the surface of the charged droplet. Therefore, a more efficient ionization of the target compound and an increased robustness of the analytical methods is a clear benefit compared to the methods developed previous on the TSQ Quantum discovery max triple quad mass spectrometer.

Oxilipins were purchased from Cayman Chemicals Europe, Tallin, Estonia. A list of oxylipins used for analysis is shown in Table 2-11.

Table 2-11 Oxilipin standards

Name	abbreviation	molecular formula
2,3-dinor-11β-ProstaglandineF$_{2\alpha}$	2,3-dinor-11β-PGF$_{2\alpha}$	$C_{18}H_{30}O_5$
2,3-dinor-8-iso-ProstaglandineF$_{2\alpha}$	2,3-dinor-8-iso-PGF$_{2\alpha}$	$C_{18}H_{30}O_5$
13-Hydroxyoctadecadienoic acid	13-HODE	$C_{18}H_{32}O_3$
9-Hydroxyoctadecadienoic acid	9-HODE	$C_{18}H_{32}O_3$
12-Hydroxyeicosapentaenoic acid	12-HEPE	$C_{20}H_{30}O_3$
15-Hydroxyeicosapentaenoic acid	15-HEPE	$C_{20}H_{30}O_3$
18-Hydroxyeicosapentaenoic acid	18-HEPE	$C_{20}H_{30}O_3$
5-Hydroxyeicosapentaenoic acid	5-HEPE	$C_{20}H_{30}O_3$
8-Hydroxyeicosapentaenoic acid	8-HEPE	$C_{20}H_{30}O_3$
9-Hydroxyeicosapentaenoic acid	9-HEPE	$C_{20}H_{30}O_3$
Prostaglandin D$_3$	PGD$_3$	$C_{20}H_{30}O_5$
Prostaglandin E$_3$	PGE$_3$	$C_{20}H_{30}O_5$

11(12)- Epoxy-eicosatrienoic acid	11(12) – EET	$C_{20}H_{32}O_3$
11-Hydroxyeicosatetraenoic acid	11-HETE	$C_{20}H_{32}O_3$
12-Hydroxyeicosatetraenoic acid	12-HETE	$C_{20}H_{32}O_3$
14(15)- Epoxy-eicosatrienoic acid	14(15)-EET	$C_{20}H_{32}O_3$
15-Hydroxyeicosatetraenoic acid	15-HETE	$C_{20}H_{32}O_3$
20-Hydroxyeicosatetraenoic acid	20-HETE	$C_{20}H_{32}O_3$
5-Hydroxyeicosatetraenoic acid	5-HETE	$C_{20}H_{32}O_3$
8-Hydroxyeicosatetraenoic acid	8-HETE	$C_{20}H_{32}O_3$
9-Hydroxyeicosatetraenoic acid	9-HETE	$C_{20}H_{32}O_3$
Leukotriene B_4	LTB_4	$C_{20}H_{32}O_4$
8-iso-15-keto-Prostaglandin $F_{2\alpha}$	8-iso-15-keto-$PGF_{2\alpha}$	$C_{20}H_{32}O_5$
Prostaglandin D_2	PGD_2	$C_{20}H_{32}O_5$
Prostaglandin E_2	PGE_2	$C_{20}H_{32}O_5$
Prostaglandin $F_{3\alpha}$	$PGF_{3\alpha}$	$C_{20}H_{32}O_5$
11-Dehydro-Thromboxane B_2	11-dehydro-TXB_2	$C_{20}H_{32}O_6$
Thromboxane B_3	TXB_3	$C_{20}H_{32}O_6$
11,12-Dihydroxyeicosatrienoic acid	11,12-DHET	$C_{20}H_{34}O_4$
14,15-Dihydroxyeicosatrienoic acid	14,15-DHET	$C_{20}H_{34}O_4$
5,6-Dihydroxyeicosatrienoic acid	5,6-DHET	$C_{20}H_{34}O_4$
8,9-Dihydroxyeicosatrienoic acid	8,9-DHET	$C_{20}H_{34}O_4$
8-iso-Prostaglandine$F_{2\alpha}$	8-iso-$PGF_{2\alpha}$	$C_{20}H_{34}O_5$
Prostaglandin D_1	PGD_1	$C_{20}H_{34}O_5$
Prostaglandin E_1 / PGE_1	PGE_1	$C_{20}H_{34}O_5$
Prostaglandin $F_{2\alpha}$	$PGF_{2\alpha}$	$C_{20}H_{34}O_5$
6-keto-Prostaglandin $F_{1\alpha}$	6-keto-$PGF_{1\alpha}$	$C_{20}H_{34}O_6$
Thromboxane B_2	TXB_2	$C_{20}H_{34}O_6$
Prostaglandin $F_{1\alpha}$	$PGF_{1\alpha}$	$C_{20}H_{36}O_5$
10-Hydroxydocosahexaenoic acid	10-HDoHE	$C_{22}H_{32}O_3$
11-Hydroxydocosahexaenoic acid	11-HDoHE	$C_{22}H_{32}O_3$
13-Hydroxydocosahexaenoic acid	13-HDoHE	$C_{22}H_{32}O_3$
14-Hydroxydocosahexaenoic acid	14-HDoHE	$C_{22}H_{32}O_3$
16-Hydroxydocosahexaenoic acid	16-HDoHE	$C_{22}H_{32}O_3$
17-Hydroxydocosahexaenoic acid	17-HDoHE	$C_{22}H_{32}O_3$
20-Hydroxydocosahexaenoic acid	20-HDoHE	$C_{22}H_{32}O_3$
4-Hydroxydocosahexaenoic acid	4-HDoHE	$C_{22}H_{32}O_3$

7-Hydroxydocosahexaenoic acid	7-HDoHE	$C_{22}H_{32}O_3$
8-Hydroxydocosahexaenoic acid	8-HDoHE	$C_{22}H_{32}O_3$

For quantitative detection, internal standards were purchased from Cayman Chemicals Europe, Tallin, Estonia. A list of isotope marked standards used for analysis is shown in Table 2-12.

Table 2-12 internal standards used for oxilipin detection

Name	abbreviation	molecular formula
14(15)-Epoxy-eicosatrienoic acid-d_{11}	14(15)-EET-d_{11}	$C_{20}H_{21}D_{11}O_3$
11,12-Dihydroxy-eicosatrienoic acid-d_{11}	11,12-DHET-d_{11}	$C_{20}H_{23}D_{11}O_4$
14,15-Dihydroxyeicosatrienoic acid-d_{11}	14(15)-DHET-d_{11}	$C_{20}H_{23}D_{11}O_4$
12,S-Hydroxyeicosatetraenoic acid-d_8	12-HETE-d_8	$C_{20}H_{24}D_8O_3$
Prostaglandin B_2-d_4	PGB_2-d_4	$C_{20}H2_6D_4O_4$
Leukotriene B_4-d_4	LTB_4-d_4	$C_{20}H_{28}D_4O_4$
Prostaglandin E_2-d_4	PGE_2-d_4	$C_{20}H_{28}D_4O_5$
8-iso-Prostaglandin F_2-d_4	8-iso-PGF_2-d_4	$C_{20}H_{30}D_4O_5$

All oxylipin standards were prepared in separated methanol-working solutions with a final concentration of 100 ng/mL each. They were infused into the ESI source of the 6460 triple quadruple mass spectrometer in negative mode using Masshunter B.06.00 acquisition software. The precursor ions were identified based on the $[M-H]^-$ negative ionization and analyte transitions were measured using product ion scan based on their specific precursor ions. The most intense transitions, from the precursor ion to the product ions, were identified and cell acceleration voltage, collision energy and fragmentor voltage was optimized to gain optimal sensitivity for the detection. All specific transitions were stored, the highest abundant ion transitions were taken into account as quantifier, and the rest was used for qualifier by triggered MRM (tMRM) measurement.

Due to increased instrumental capability, a method for the detection of multiple oxylipins had to be developed. Using instruments suitable for higher backpressures, sub 2µm column materials were tested to enhance the potential of UHPLC separation.

The columns, solvents and gradients tested are shown in Table 2-13, Table 2-14, and

Table 2-15.

Table 2-13 tested columns for oxylipin method development

Product Name	Dimension	Manufacturer
YMC Triat C18	150 x 2.0 mm; S-3 µm	YMC Europe GmbH
YMC-Pack Pro C18	150 x 2.0 mm; S-3 µm	YMC Europe GmbH
YMC-Pack C8	150 x 2.0 mm; S-3 µm	YMC Europe GmbH
Titan C18	100 x 2.1 mm; 1.9 µm	YMC Europe GmbH
Luna 3u C18(2) 100A	250 x 2.1 mm; 5 µm	Phenomenex
Kinetex 2.6u C18 100A	150 x 2.1 mm; 2.6 µm	Phenomenex
Kinetex 5u C18 100A	250 x 2.1 mm; 4.6 µm	Phenomenex
Synergi 5u Hydro RP-100A	250 x 2.1 mm; 5 µm	Phenomenex
Inertsil ODS-4 3µm	150 x 2.1 mm;3 µm	GL Sciences
Kinetex 1.7u, C18, 100A	150 x 2.1 mm;1.7 µm	Phenomenex
Kinetex 1.7u, XB-C18, 100A	150 x 2.1 mm;1.7 µm	Phenomenex
Kinetex 2,6u Phenyl-Hexyl, 100A	100 x 2.1 mm;2.6 µm	Phenomenex
Kinetex 2.6u C8, 100A	100 x 2.1 mm;2.6 µm	Phenomenex
Poroshell 120 SB-18	150 x 2.1 mm;2.7 µm	Agilent
Poroshell 120 EC-CN	100 x 2.1 mm;2.6 µm	Phenomenex
Synergi 4u Hydro RP-80A	250 x 2.1 mm; 4 µm	Phenomenex
Nucleoshell RP 18	150 x 2.1 mm; 2.7 µm	Machery-Nagel

Table 2-14 tested L solvents

Solvent A	Solvent B
0.1% acetic acid	0.1% acetic methanol
0.1% acetic acid	0.1% acetic acetonitrile
0.1% acetic acid	0.1% acetic methanol/0.1% acetic acetonitrile 50%/50% (v:v)
0.1% acetic acid	0.1% acetic acetonitrile/0.1% acetic methanol 75%/25% (v:v)
0.1% acetic acid	0.1% acetic methanol/0.1% acetic isopropanol 50%/50% (v:v)
0.1% acetic acid	0.1% acetic acetonitrile/0.1% acetic isopropanol 75%/25% (v:v)

Table 2-15 tested isocratic and gradient methods

Isocratic 30		
[min]	Solvent A [%]	Solvent B [%]
0.00	70	30
10	70	30
Isocratic 40		
[min]	Solvent A [%]	Solvent B [%]
0.00	60	40
10	60	40
Isocratic 50		
[min]	Solvent A [%]	Solvent B [%]
0.00	50	50
10	50	50
Isocratic 60		
[min]	Solvent A [%]	Solvent B [%]
0.00	40	60
10	40	60
Isocratic 70		
[min]	Solvent A [%]	Solvent B [%]
0.00	30	70
10	30	70
Gradient 15		
[min]	Solvent A [%]	Solvent B [%]
0.00	95	5
15	5	95
20	5	95
Gradient 10		
[min]	Solvent A [%]	Solvent B [%]
0.00	95	5
10	5	95
15	5	95

After the first testing, columns with possible capability for the separation of oxylipins were customized optimized to achieve optimal chromatographic resolution.

After finalizing chromatographic method development, gas temperature, gas flow, nebulizer pressure, sheath gas heater, sheath gas flow, capillary voltage and nozzle voltage were optimized to ensure maximal ionization efficiency and ion transfer.

2.7.1 Sample Extraction Procedure

The work was done with, next to, built on and continued on the work of B. Weißenbacher (Weißenbacher, 2013). The stock solutions of every analyte, shown in Table 2-11 and in Table 2-12, diluted with ethanol to a concentration of 12.5 µg/mL, were prepared and stored at - 30°C. Every mixture was prepared fresh each day. Two mixtures of all analytes in 50% methanol were prepared with a concentration of 500 and 5 ng/mL each. A mixture with internal standards in a concentration of 2.5 µg/mL diluted in methanol:water 50%:50% was prepared.

500µL of the solution were spiked with 5 ng internal standards and tested on different SPE approaches.

Strata C18-E, was purchased and tested based on the manufacture recommended SPE protocols and methods reported by Weißenbacher et al. (Weißenbacher, 2013). All protocols and calibration sets were performed in triplicates.

For hydrolysis, an in-house developed method was used to precipitate proteins and release esterified oxlipins. Therefore, 500 µl of biological sample was diluted with 1 mL of H_2O and 1 mL of sodium hydroxide solution (10 g NaOH in 20 mL H_2O and 100 mL methanol). Followed by an incubation time of 1 hour at 37°C. Samples were cooled on ice and pH was adjusted with hydrochloric acid to pH 3. Afterwards 1 mL methanol was added and incubated for 15 minutes. After centrifugation at 4000 rpm for 10 minutes, the supernatant was transferred into a vial and 8 mL of 1% formic acid was added to lower the absolute concentration of methanol to 15% for the following SPE cleanup.

All SPE preparation steps are reported in Weißenbacher at al. (Weißenbacher, 2013).

2.8 Data Analysis

Acquired sample data was processed using MassHunter QQQ Quantitative Analysis Software B.06.00. Acquired dynamic MRM data were de-convoluted, peaks integrated and data automatically identified using retention time, MRM and triggered MRM transitions verified by library matching with a matching score higher than 95%. The library was custom build for target oxilipins by using Mass Hunter Optimizer Software, generating triggered MRM transitions acquired from separately injected standards. The library includes retention times and up to eight qualitative MRM transitions for each analyte. Normalization of each sample was completed using

internal standard correction followed by quantitation of the measured set of standard in the concentration range indicated.

After Mass Hunter data processing, the results were exported to Microsoft Excel 2013 .xlsx format. Data was converted to a N x M – matrix, whereas N are the samples in rows and analytes in columns.

The following chemometric data analysis is based on the protocol of Chang et al. (Chan et al., 2011).

For chemometric data analysis the normalized data matrix was imported into SIMCA P 13.0.3 software (Umetrix, Umeå, Sweden) and primary and secondary observations and variable IDs were defined. The Primary ID was set as sample name (unique) and class information were set with secondary ID. For reducing dimensions and modeling, class information is not necessary for principal component analysis (PCA) but partial least square analysis (PLSA) build up on this information.

2.8.1 Principal Component Analysis (PCA)

PCA is a statistical data reduction technique, which results in reduced dimensions of multidimensional data sets by keeping the characteristic information with the highest variance in the measured samples.

Scaling was set to unit variance and the scaled data was used to build a PCA model using "autofit" function of the software. "Autofit" calculates up to 3 principal components by default, but more principal components can be calculated if needed. After unit variance scaling and mean centering the results are shown in the score-scatter plot. A Summary window was used to evaluate contribution of each component to model performance statistics. If the contribution of some compounds to the Q^2 were not significant, they have been deleted.

Hottelling's T2 ellipse and DModX tools were used to identify outliners. Observations outside the Hotteling's T2 ellipse critical value were treated as outliers. Observations that are more than two times the DModXcritical value were considered as outliers. Both types of outliers were evaluated and then excluded from further analysis. The PCA Model Overview shows the principal components necessary to describe the model with a variance R_2X (>> 0.98; good model accuracy).

2.8.2 Partial Least Square Analysis (PLS)

For PLS data analysis the Model Type was changed to the function "PLS discriminant analysis" The "autofit" function calculates the principal components to build the variance of the PLS-model. Pareto scaling is a recommended scaling option to reduce the relative importance of large values, but keeps data structure partially intact. Model evaluation was done as described in the PCA evaluation. Furthermore VIP statics are used to evaluate the importance of the different x-variables when they reach a value over 0.8.

Due to no multi-parametric data of samples in clinical studies were generated, up to the point of thesis finalization, only artificial data sets could be used to adopt the statistical tool.

3 Results and Findings

3.1 8-iso-Prostaglandin $F_{2\alpha}$ Online Solid Phase Extraction and Sample Preparation

Low basal levels of 8-iso-Pprostaglandin $F_{2\alpha}$ (8-iso-$PGF_{2\alpha}$) in human liquids is an analytical challenge. An online sample solid phase extraction (SPE) approach is a convenient way to enrich analyte concentration on column, clean up the injected sample matrix and therefore, reducing matrix effects before detection. Due to 8-iso-$PGF_{2\alpha}$ precursor arachidonic acid is esterified in phospholipids, the main part of the generated 8-iso-$PGF_{2\alpha}$ amount is bonded to phospholipids before released into its free form. To detect the total amount of 8-iso-$PGF_{2\alpha}$, a sample hydrolysis is recommended to achieve detectable amounts of analyte. High quantities of methanol, as well as high pH levels are necessary to release fatty acids by hydrolysis (Theodorou et al., 2007). Both factors are very critical for SPE when it comes to sufficient binding abilities of polar to moderate polar substances. Therefore, sample dilution and pH modification is an essential subsequent step to make the hydrolyzed sample ready for SPE extraction.

Based on the hydrolysis procedure of Taylor et al. (Taylor et al., 2006), hydrolysis was optimized and performed with slight modification. Several experiments were conducted to optimize 8-iso-$PGF_{2\alpha}$ SPE enrichment, injection volume sample cleaning and elution-separation gradient.

Several standards, urine and plasma samples were measured to evaluated specificity and sensitivity of the of the online-SPE system. Figure 3-1 shows the measurement of 100 ng/mL 8-iso-$PGF_{2\alpha}$ eluted with the final 10 minute gradient.

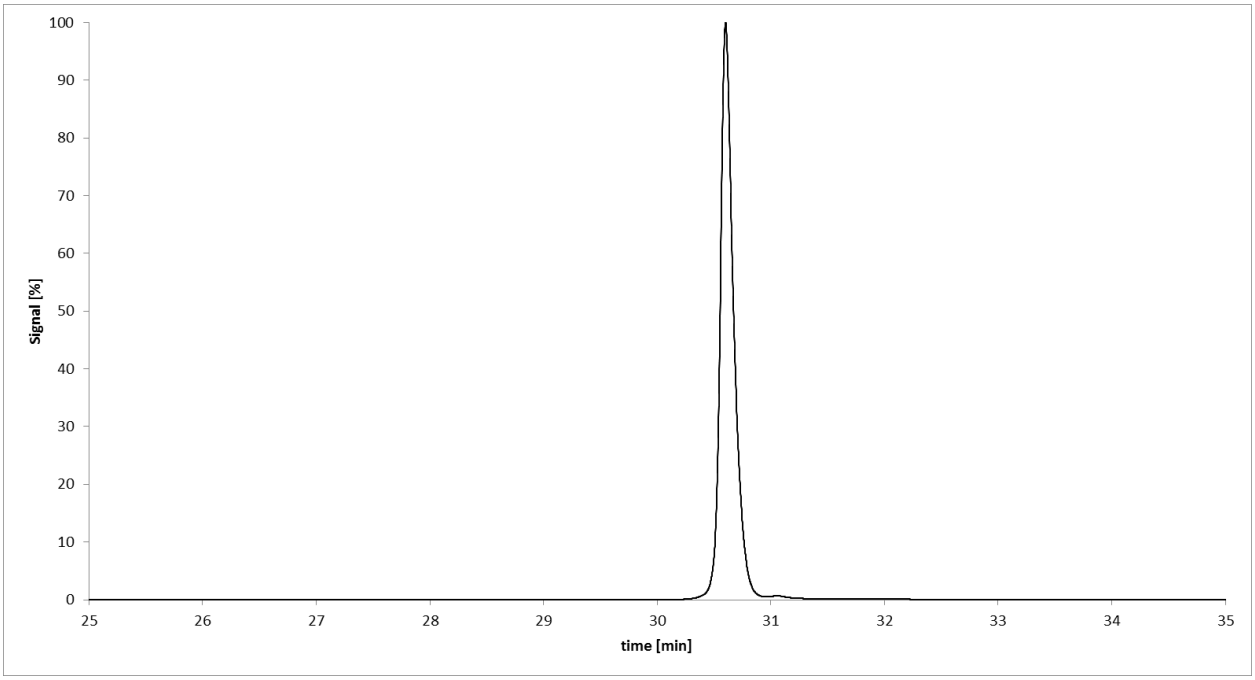

Figure 3-1 injection of 8-iso-$PGF_{2\alpha}$ standard on the online-SPE LC-MS-system

The strata-x cartridge reached 92.3 ± 8.1 % of recovery from spiked urine and 89.7± 7.4 % of recovery from spiked plasma samples. It should be noticed that the spiked amount of 8-iso-$PGF_{2\alpha}$ was around 500 times higher than basal plasma levels and 100-200 times higher than expected in human urine. Higher spike concentration were necessary to compensate the lack sensitivity due the design of the LCQ Fleet mass spectrometer.

The binding capacity of the SPE cartridge was near to the maximum using spiked plasma samples. A method upscale to 150 % for the testing of 1500 µL of spiked plasma sample resulted in a breakthrough of the SPE cartridge shown by a decrease in recovery to 72 ± 14.4% and a significant decrease in precision. Further experiments with higher sample volume were not performed.

The high binding strength capacity of the Strata-X resulted in high organic ratio of elution solvents to elute 8-iso-$PGF_{2\alpha}$ from the cartridge. The high amount of organic solvent for elution is critical to the following analytical separation before MS detection. Injection of 8-iso-$PGF_{2\alpha}$ and $PGF_{2\alpha}$ mixture resulted in a low resolution separation using 0.1% acetic acid / 0.1% acetic acetonitrile gradient over 10 minutes from 60% organic to 95% organic, shown in Figure 3-2.

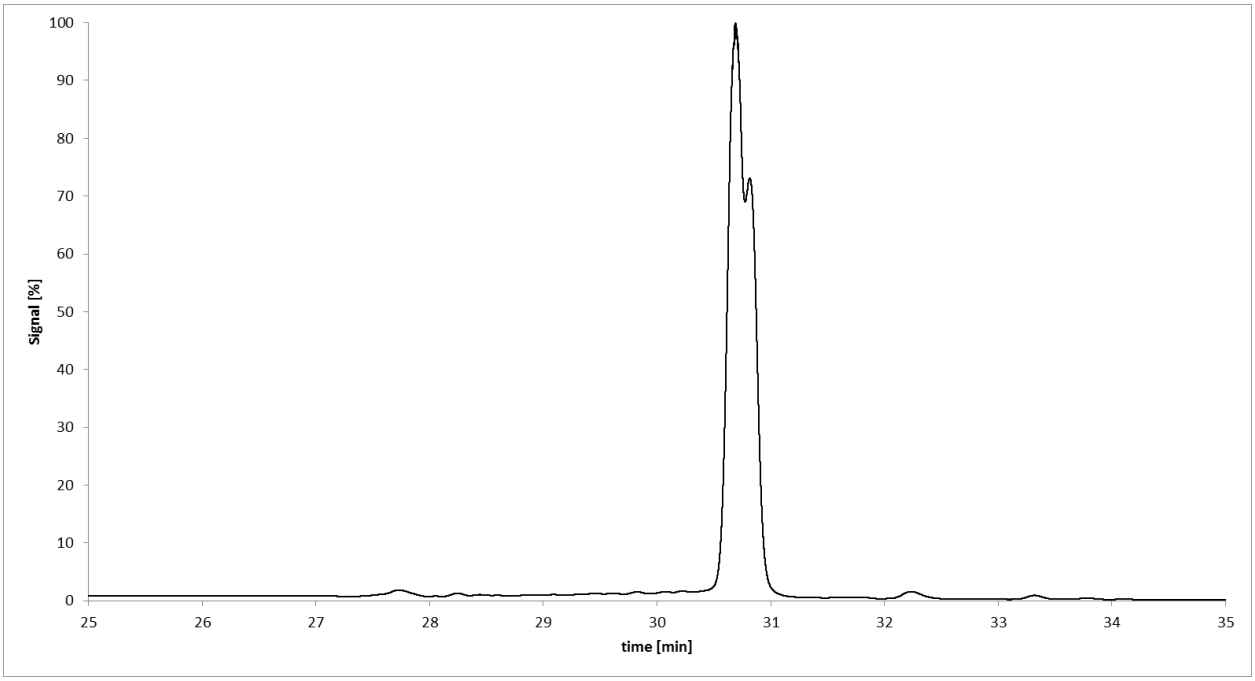

Figure 3-2 low resolution in the separation of 8-iso-PGF$_{2\alpha}$ and PGF$_{2\alpha}$ using the online-SPE-LC-MS-system

Increasing gradient time for better peak resolution to 15 and 20 minutes, and hence lowering the slope of the gradient, resulted in a strong tailing and increased peak width shown in Figure 3-3. No baseline separation could be achieved due to the tailing. Methanol as an alternative to acetonitrile showed less effective elution and even more tailing.

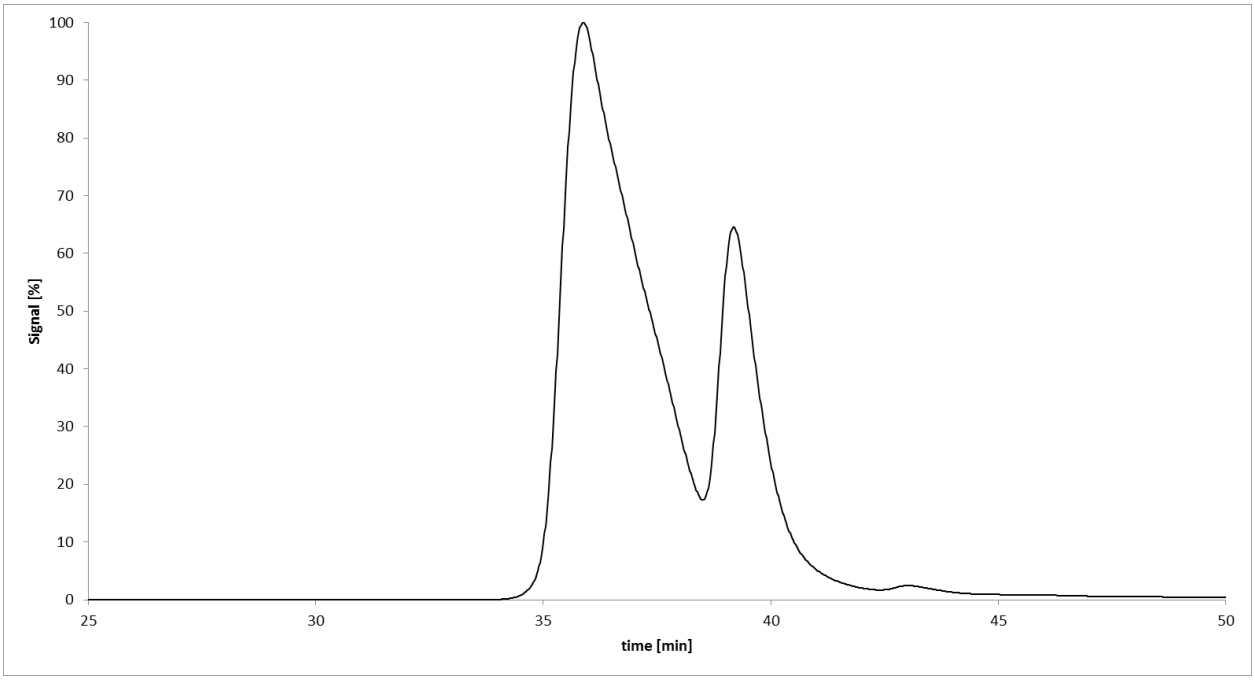

Figure 3-3 extended gradient 15 min

Compared to the offline SPE method, several isomers are not resolved, based on high organic solvent ratio, when the analyte reaches the analytical column, due to the low chromatographic resolution.

Using a further pump to decrease the organic solvent ratio by continuously infusing water in-between the SPE cartridge and the analytical column lead to an increase of backpressure in the chromatographic system. Due to the limitation of the strata-x cartridge to 270 bar isopropanol or methanol could not be used with a 150 mm column without losing chromatographic resolution based on flow rates under 100µL/min, described in the van-Deemter equation (Gritti and Guiochon, 2013). Using acetonitrile as organic elution solvent, flow rates were limited to 150 µL/min and resulted in total run time over 30 minutes. Run times over 20 minutes are inappropriate when it comes to high sample throughput in routine. Nevertheless, the chromatographic separation efficiency increased, but not all peaks of the offline-SPE approach could be reproduced in the enhanced in-between infusion online-SPE method, due to the lack of resolution. The separation of 8-iso-$PGF_{2\alpha}$ and $PGF_{2\alpha}$ is shown in Figure 3-4 .

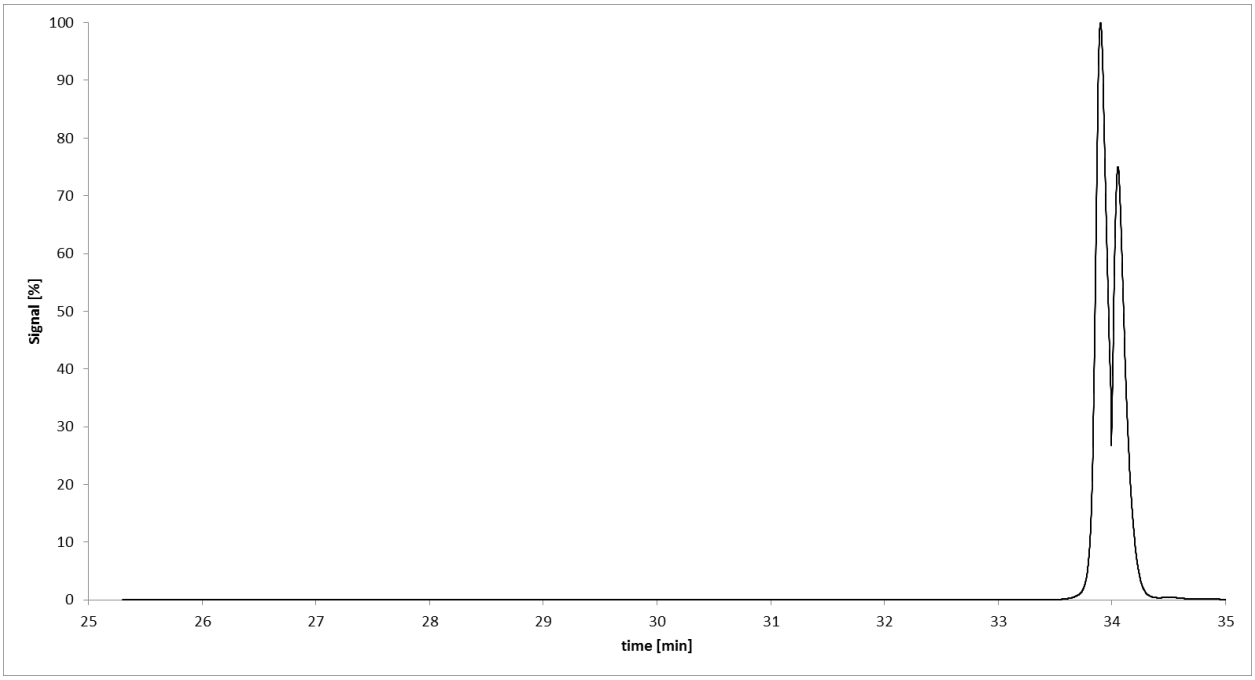

Figure 3-4 separation of 8-iso-$PGF_{2\alpha}$ and $PGF_{2\alpha}$ using SPE-column in-between water dilution

A comparison of a sample measured with a modified online-SPE LC-MS System versus an offline-SPE approach showed an increase of 8-iso-$PGF_{2\alpha}$ over 2 times while the difference between 8-iso-$PGF_{2\alpha}$-d_4 did not vary more than 15%. Hence, online-SPE could not resolve isomers of 8-iso-$PGF_{2\alpha}$

and similar substances and is therefore not suitable for the detection of 8-iso-$PGF_{2\alpha}$ in biological matrices.

3.2 8-iso-Prostaglandin $F_{2\alpha}$ Offline Solid Phase Extraction Method Development

Several analytical methods are published for the detection of 8-iso-$PGF_{2\alpha}$ (Medina et al., 2012, Taylor and Traber, 2010, Cavalca et al., 2010, Korecka et al., 2010, Mesaros et al., 2009, Winnik and Kitchin, 2008, Sicilia et al., 2008, Taylor et al., 2008, Haschke et al., 2007). Nevertheless, when it comes to the separation of isomeric forms of isoprostanes or analytes with the same 353 to 193 *m/z* transition in biological matrices, different gradient conditions or isocratic separation showed not only a shift of retention time, or a change in chromatographic resolution of 8-iso-$PGF_{2\alpha}$,. It seems like several publications tent to present gradient conditions resulting in an overlay of several matrix interferences. By modifying the published gradient conditions on their reported columns, several additional peaks showed up of the original detected 8-iso-$PGF_{2\alpha}$ peak, resulting in poor resolved peaks, nearly co-eluting with resolution <0.75. Therefore, it was necessary to test different gradients, solvent mixtures, additives and columns to find optimal conditions for the separations of those isomers and interferences for a sensitive and reproducible mass spectrometry detection.

Based on the online-SPE approach, solvents, gradients and columns were tested to verify, that co-elution of 8-iso-$PGF_{2\alpha}$ and similar substances is avoided by varying chromatographic conditions.

The Luna C18(2) column (Phenomenex, Aschaffenburg, Germany) with a dimension of 2.1 x 250 mm showed baseline separation of 8-iso-$PGF_{2\alpha}$ under different isocratic and gradient conditions. Hence its wide particle diameter of 5 µm, the column was suitable for HPLC instruments with a backpressure under 400 bar by using methanol as organic HPLC solvent. Switching valve and separation of the chromatographic run into different time segments, with different flow rates before and after the elution time window of 8-iso-PGF2α, reduce runtime without sacrificing significant chromatographic resolution. By bypassing the flow post column from start to minute 5.50 and again from minute 12 till 16, a reduced contamination of the mass spectrometer source and housing results in higher uptime, productivity and lower maintenance rates of the LC-MS system. The full method description is shown in 2.4.6.

Separation of 8-iso-$PGF_{2\alpha}$ in human fluids are shown in Figure 3-5 to Figure 3-8.

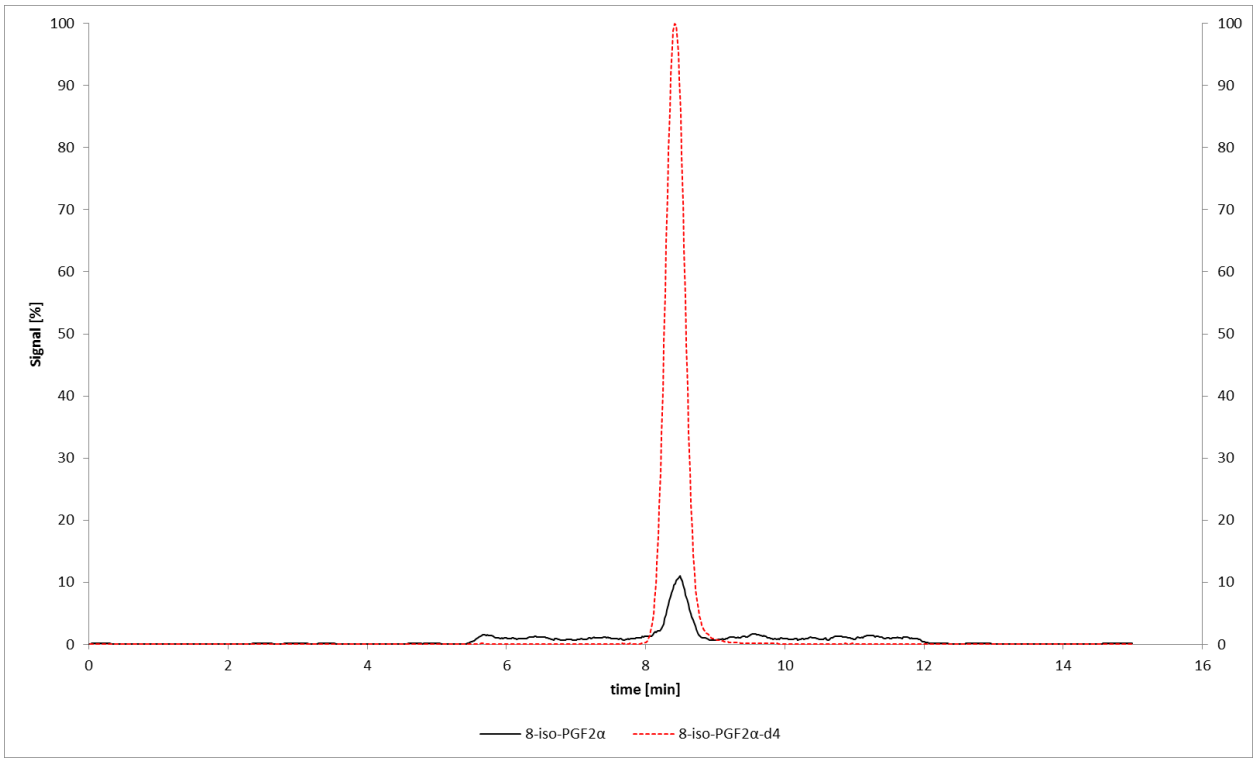

Figure 3-5 standard 150 pg/mL of 8-iso-PGF$_{2\alpha}$ (normalized to spiked plasma in Figure 3-6)

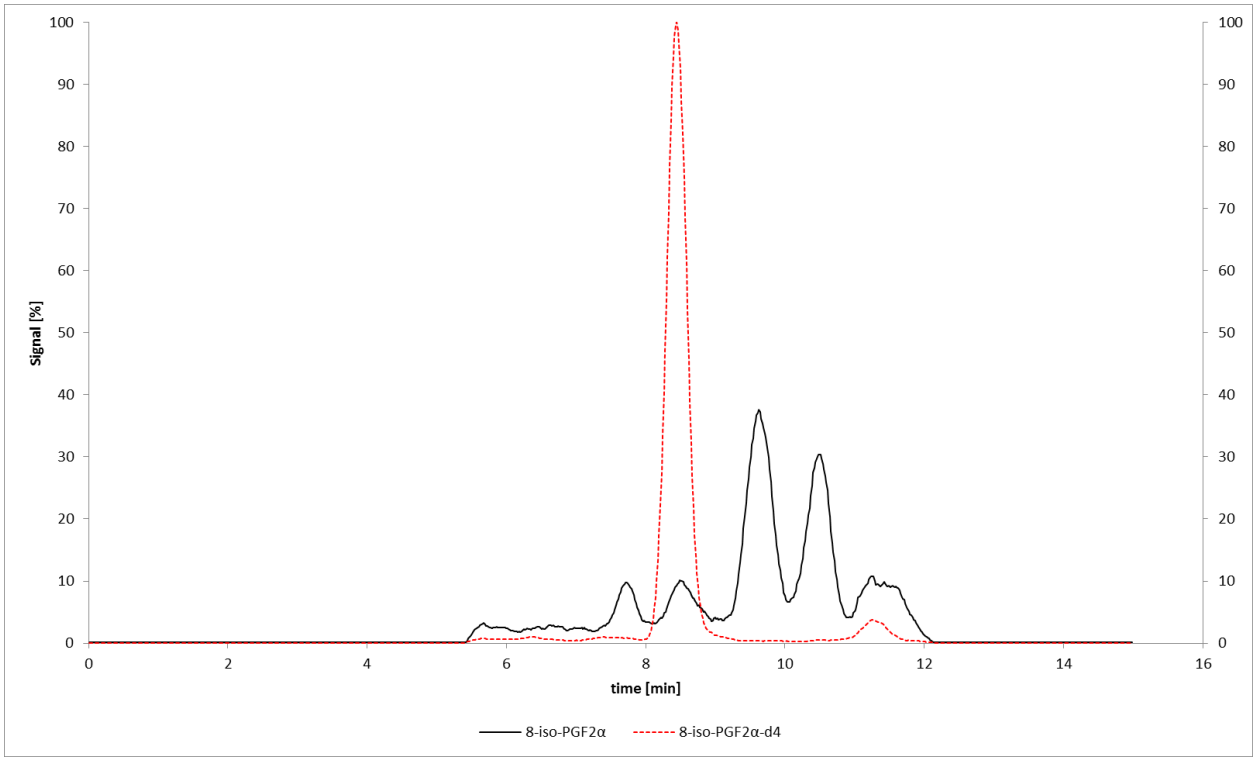

Figure 3-plasma blank of 8-iso-PGF$_{2\alpha}$ (normalized to spiked plasma in Figure 3-6)

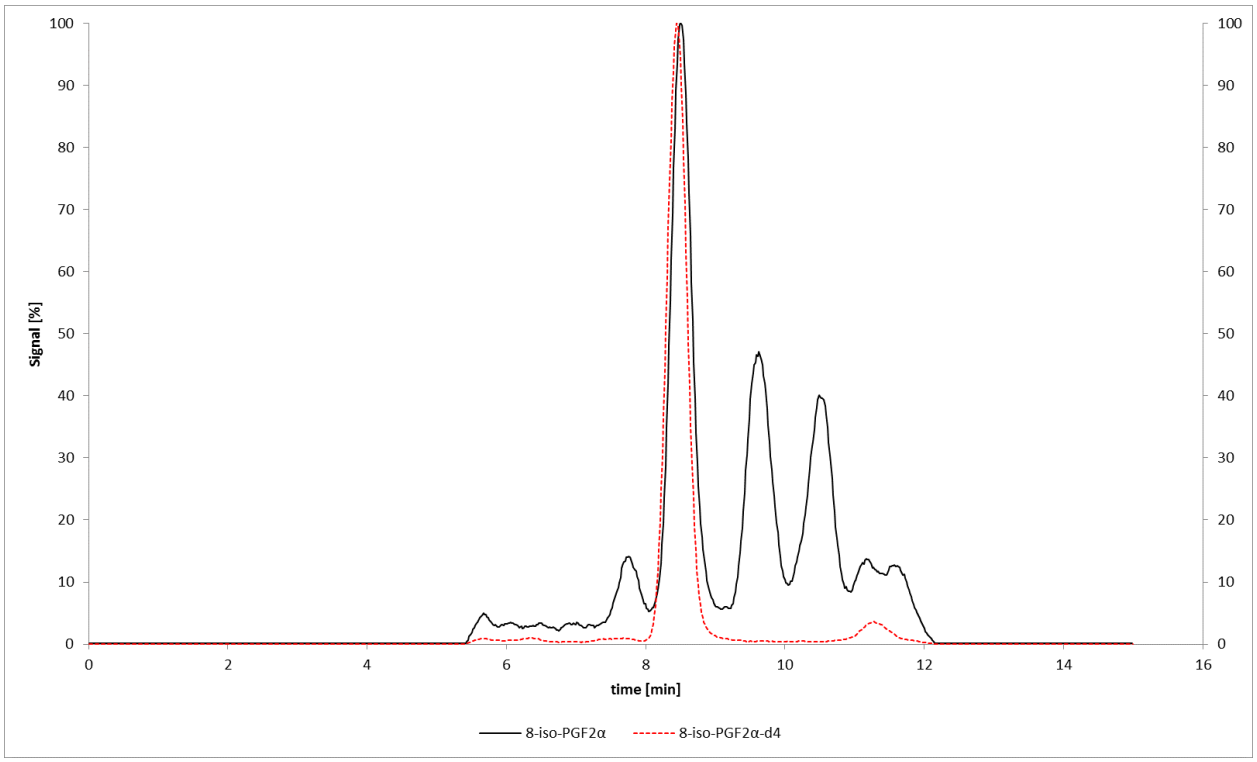

Figure 3-6 plasma spiked with 1ng/mL 8-iso-PGF$_{2\alpha}$

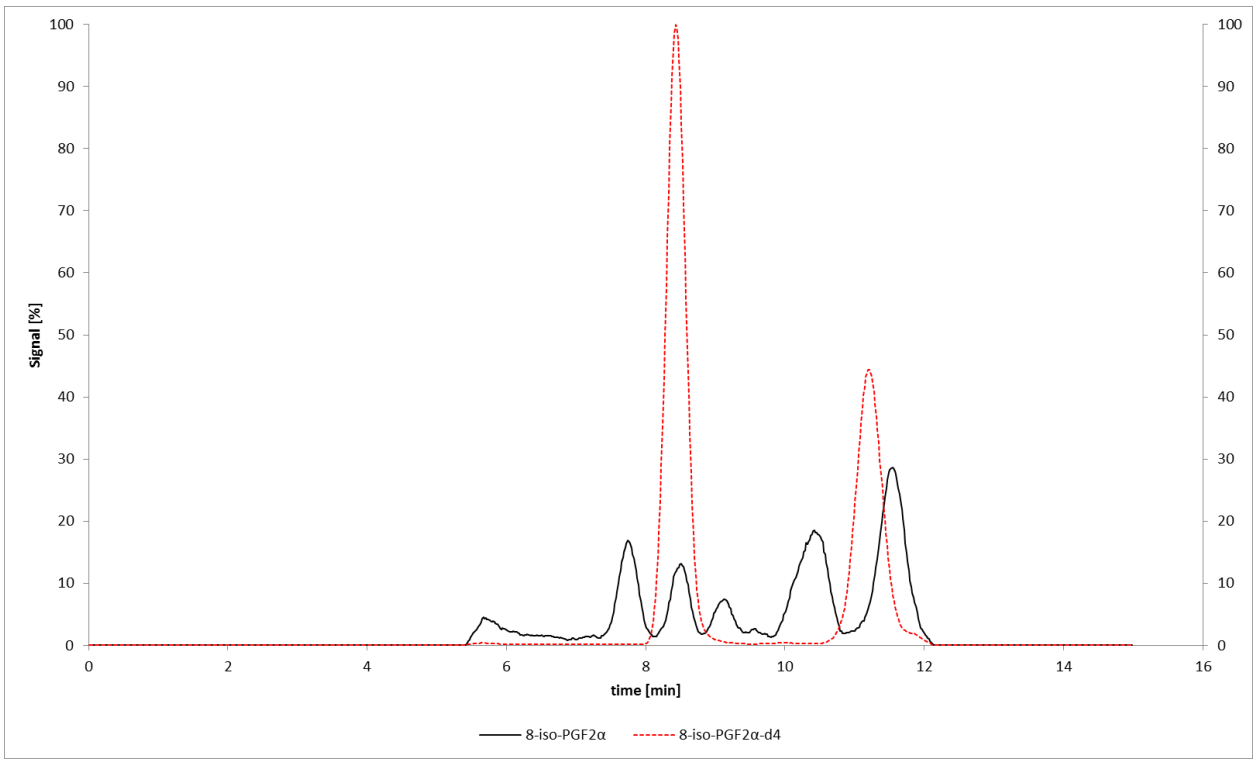

Figure 3-7 urine blank (normalized to spiked plasma in Figure 3-8)

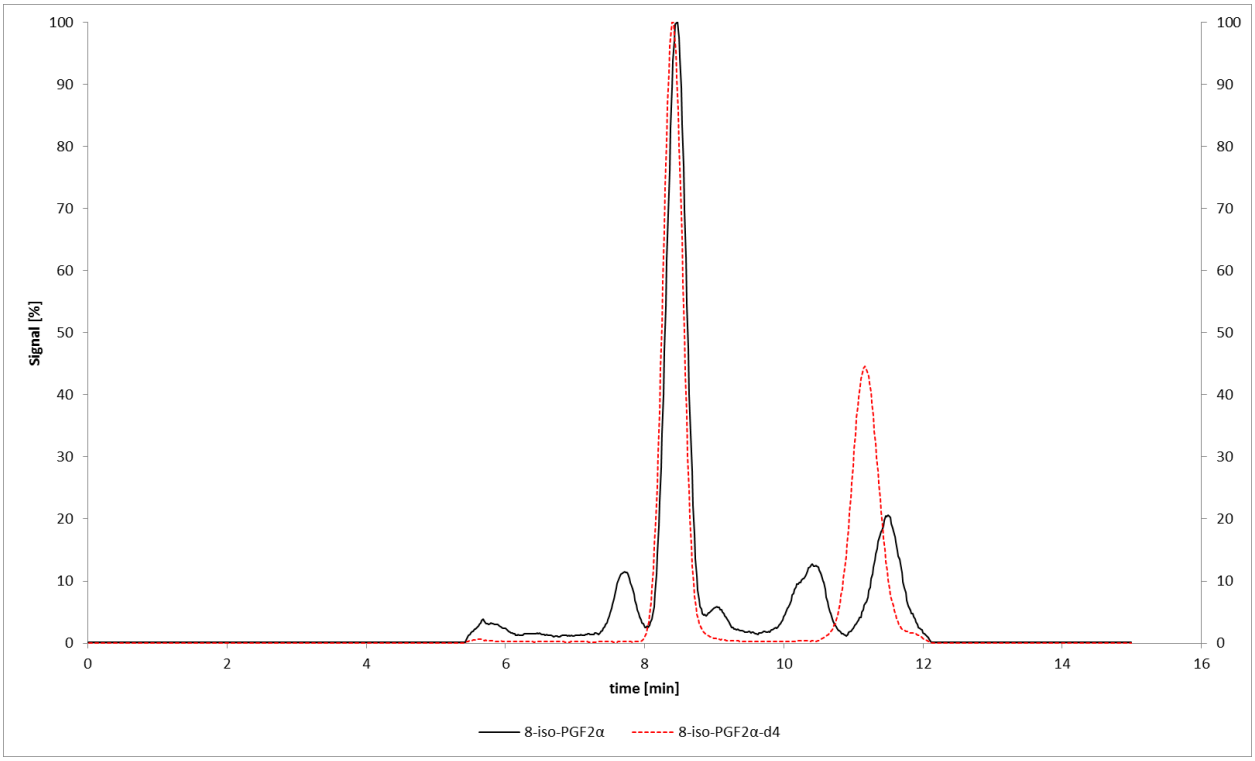

Figure 3-8 urine spiked with 1 ng/mL 8-iso-PGF$_{2\alpha}$

3.3 Validation 8-iso-Prostaglandin F$_{2\alpha}$

Validation was performed according to the FDA guidelines (FDA, 2001)

The following parameters were investigated during validation: selectivity, linearity, accuracy and precision, limit of quantitation, sample dilution, lower limit of detection, and stability. The stability tests consisted of long-term stability, freeze-thaw stability, short-term stability, and autosampler stability.

All the inter-day and intra-day accuracy and precision data of QC samples have fallen into the ±15% range at each concentration level. The plasma samples stored below –70 °C proved to be stable up to five days. No degradation occurred during freeze/thaw testing. Samples can be reliably measured after 1:1 dilution.

3.3.1 Specificity

In none of the six blank samples were any significant interference at the retention times of target and internal standard.

3.3.2 Linearity

The linearity was visually examined by plotting the nominal concentration versus

- the peak area ratios of 8-iso-$PGF_{2\alpha}$ and 8-iso-$PGF_{2\alpha}$–d_4 standard,
- the back-calculated concentrations for each calibration sample
- the percent deviation of the back-calculated values

According to the graphs below, no tendency could be observed between the nominal concentration and the residuals. The coefficient of regression was 0.9987 for plasma and 0.9976 for urine shown in Figure 3-9, Figure 3-10, Figure 3-11 and Figure 3-12, indicating similar instrument response at different days of analysis.

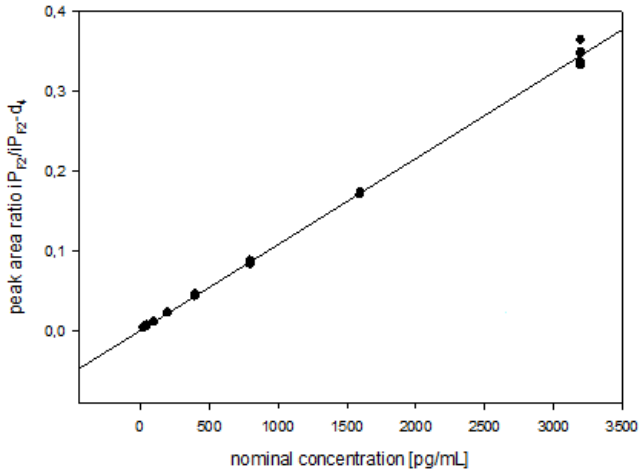

Figure 3-9 8-iso-$PGF_{2\alpha}$ linearity check calibration graph (plasma)

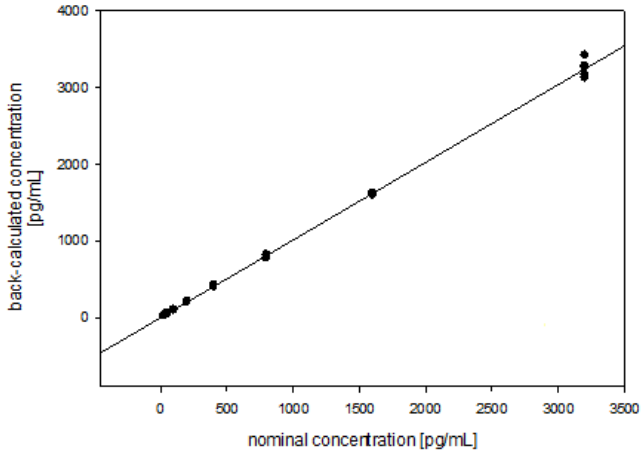

Figure 3-10 8-iso-$PGF_{2\alpha}$ linearity check back calculated values (plasma)

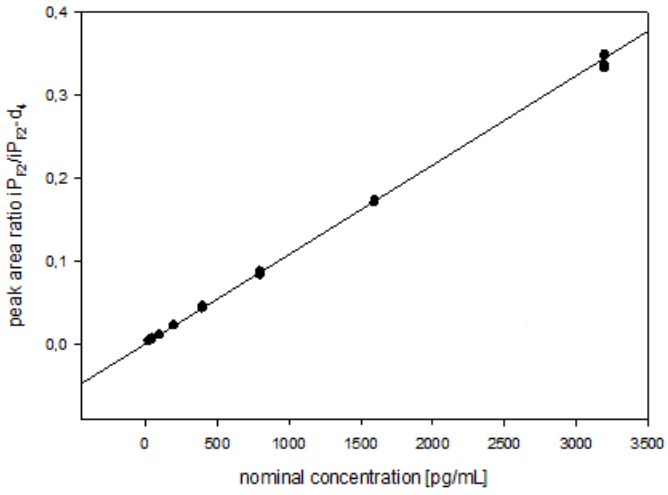

Figure 3-11 8-iso-PGF$_{2\alpha}$ linearity check calibration graph (urine)

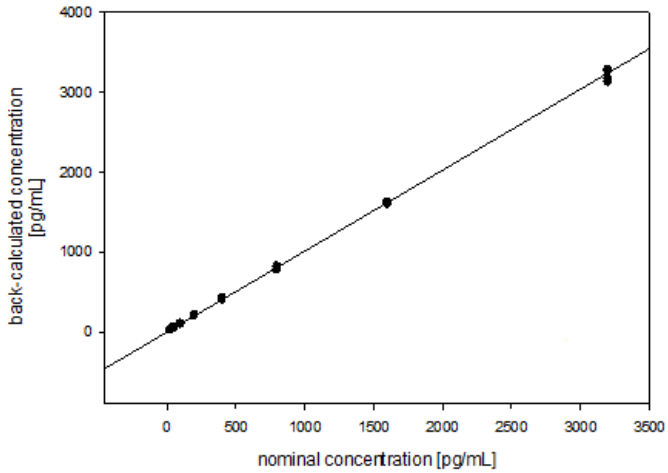

Figure 3-12 8-iso-PGF$_{2\alpha}$ linearity check back calculated values (urine)

3.3.3 Accuracy and Precision

3.3.3.1 Intra-day

The accuracy and precision data fulfilled the acceptance criteria at every concentration level for the QC plasma extraction. The accuracy (expressed as bias%) ranged from 4.2% to 5.4%. The

precision (expressed as CV%) was 6.5%. Data is shown in Table 3-1.

Table 3-1 intra-day QC plasma extraction

	nominal concentration [pg/mL]	
	280	1120
	concentration found [pg/mL]	
#1	305	1162
#2	283	1182
#3	300	1167
#4	300	1178
#5	292	1160
mean	296	1170
s.d.	7,74	8,55
CV [%]	2,6	0,7
accuracy [%]	-5,4	-4,2

The accuracy and precision data fulfilled the acceptance criteria at every concentration level for the QC urine extraction. The accuracy (expressed as bias%) ranged from -6.8% to -3.4%. The precision (expressed as CV%) was 4.6%. Data is shown in Table 3-2.

Table 3-2 intra-day QC urine extraction

replicate	nominal concentration [pg/mL]	
	280	1120
	concentration found [pg/mL]	
#1	289	1130
#2	303	1122
#3	301	1197
#4	302	1163
#5	299	1153
mean	296,2	1170
s.d.	7,740	27.0
CV [%]	1.7	2.3
accuracy [%]	-6;8	-3.4

3.3.3.2 Inter-Day

The accuracy and precision data fulfilled the acceptance criteria at every concentration level for the QC plasma extraction. The accuracy (expressed as bias%) ranged from –14.3% to 9.9%. The precision (expressed as CV%) was 12.0%. Data is shown in Table 3-3.

Table 3-3 inter day accuracy QC samples with plasma extraction

	1st inter day		2nd inter day		3rd inter day		4rd inter day	
replicate	nominal concentration [pg/mL]							
	280	1120	280	1120	280	1120	280	1120
	concentration found [pg/mL]							
#1	239	1179	294	1085	213	1215	286	1121
#2	243	1183	266	1135	262	1142	289	1143
#3	274	1160	332	1175	218	1159	234	1163
#4	242	1110	353	1079	274	1151	232	1125
#5	263	1133	356	1207	235	1090	313	1195
mean	252	1153	320	1136	240	1151	271	1149
s.d.	13.8	27.8	35.1	49.8	24.1	39.8	32.4	27.3
CV [%]	5.5	2.4	11.0	4.4	10.0	3.5	12.0	2.4
accuracy [%]	9.9	-3.0	-14.3	-1.4	14.2	-2.8	3.3	-2.6

The accuracy and precision data fulfilled the acceptance criteria at every concentration level for the QC urine extraction. The accuracy (expressed as bias%) ranged from -1.5% to 4.1%. The precision (expressed as CV%) was 12.3%. Data is shown in Table 3-4.

Table 3-4 inter day accuracy QC samples with urine extraaction

	1st inter day		2nd inter day		3rd inter day		4rd inter day	
replicate	nominal concentration [pg/mL]							
	280	1120	280	1120	280	1120	280	1120
	concentration found [pg/mL]							
#1	325	1114	280	1141	227	1096	233	1084
#2	257	1181	306	1037	291	1028	303	1183
#3	280	1164	285	1214	309	1054	244	1144
#4	232	1142	242	1154	243	1036	301	1187
#5	305	1048	262	1109	308	1158	257	1084
mean	280	1130	275	1131	276	1075	268	1136
s.d.	32.9	46.7	21.8	58.1	33.9	48.0	29.0	45.3
CV [%]	11.8	4.1	7.9	5.1	12.3	4.5	10.8	4.0
accuracy [%]	0.1	-0.9	1.8	-1.0	1.5	4.1	4.4	-1.5

3.3.4 Limit of Quantification

3.3.4.1 Intra-Day

At concentration level 100 pg/mL the accuracy of the method was 4.5% (plasma extraction) and -2.9 (urine extraction). The precision was 15.7% and 9.7% and fulfilled the acceptance criteria. Data is shown in Table 3-5.

Table 3-5 inter-day LOQ plasma extraction

	plasma extraction	urine extraction
replicate	nominal concentration [pg/mL]	
	100	100
	concentration found [pg/mL]	
#1	121	87
#2	88	107
#3	93	103
#4	76	117
#5	100	100
mean	96	103
s.d.	15.0	10.0
CV [%]	15.7	9.7
accuracy [%]	4.5	-2.9

3.3.4.2 Inter-Day

At concentration level 100 pg/mL the accuracy of the method was from -8.2% to 7.2% for the plasma extraction method. The precision was 17.0 %.and fulfilled the acceptance criteria. Data is shown in Table 3-6.

Table 3-6 inter-day LOQ plasma extraction

	1st inter-day	2nd inter-day	3rd inter-day	4rd inter-day
replicate		nominal concentration [pg/mL]		
	100	100	100	100
		concentration found [pg/mL]		
#1	117	78	90	94
#2	114	122	107	84
#3	107	106	125	86
#4	99	92	79	91
#5	104	114	86	109
mean	108	102	97	93
s.d.	6.5	15.5	16.6	8.7
CV [%]	6.0	15.2	17.0	9.4
accuracy [%]	-8.2	-2.2	2.6	7.2

At concentration level 100 pg/mL the accuracy of the method was from –4.8% to 7.7% for the urine extraction method. The precision was 17.7 %.and fulfilled the acceptance criteria. Data is shown in Table 3-7.

Table 3-7 inter-day LOQ urine extraction

replicate	1st inter-day	2nd inter-day	3rd inter-day	4rd inter-day
	nominal concentration [pg/mL]			
	100	100	100	100
	concentration found [pg/mL]			
#1	80	122	92	91
#2	94	83	104	98
#3	91	121	113	110
#4	83	79	120	88
#5	113	104	94	78
mean	92	102	105	93
s.d.	11.6	18.0	11.0	10.6
CV [%]	12.6	17.7	10.5	11.4
accuracy [%]	7.7	-1.9	-4.8	7.0

3.3.5 Stability

Prepared plasma and urine samples were analyzed immediately or stored below –70 °C at four different days. The concentrations of the stored and immediately analyzed samples differed less than the critical 15 %. Therefore the samples are considered stable within 5 days. Eight replicas of the plasma blank showed a concentration of 156 ± 21.4pg/mL. Eight urine blank replicas showed a concentration of 183 ± 18.8 pg/mL. Data is shown in Table 3-8 to Table 3-11.

Table 3-8 plasma blank concentration

	plasma blank
replicate	concentration found [pg/mL]
#1	165
#2	180
#3	148
#4	128
#5	177
#6	146
#7	179
#8	123
mean	156
s.d.	21.4
CV [%]	13.8

Table 3-9 plasma stability

	1st inter day			2nd inter day			3rd inter day			4rd inter day		
replicate	nominal concentration [pg/mL]											
	436	856	1276	436	856	1276	436	856	1276	436	856	1276
	concentration found [pg/mL]											
#1	422	809	1162	372	882	1192	433	809	1158	384	815	1402
#2	428	911	1468	445	924	1273	458	841	1455	433	743	1188
#3	383	774	1415	390	753	1292	505	953	1202	422	894	1323
#4	417	755	1263	489	832	1079	461	890	1129	475	808	1167
#5	489	909	1155	453	857	1106	445	782	1373	397	761	1288
mean	428	831	1293	430	850	1189	460	855	1263	422	804	1273
s.d.	34.4	66.1	128.6	43.0	56.9	85.6	24.3	60.8	127.6	31.6	52.4	87.2
deviation [%]	0	0	0	0.5	2.3	-8.0	7.5	2.9	-2.3	.1,4	-3.2	-1.5

Table 3-10 urine blank concentration

	urine blank
replicate	concentration found [pg/mL]
#1	200
#2	192
#3	161
#4	160
#5	205
#6	168
#7	209
#8	173
mean	183
s.d.	18.8
CV [%]	10.3

Table 3-11 urine stability

	1st inter day			2nd inter day			3rd inter day			4rd inter day		
replicate	nominal concentration [pg/mL]											
	463	883	1303	463	883	1303	463	883	1303	463	883	1303
	concentration found [pg/mL]											
#1	452	891	1307	483	975	1418	440	941	1280	500	883	1291
#2	430	905	1353	508	853	1294	393	809	1457	465	842	1134
#3	501	861	1354	414	925	1486	416	797	1193	462	952	1360
#4	404	832	1386	505	899	1314	398	813	1409	506	913	1115
#5	468	941	1496	402	841	1471	449	960	1354	422	954	1236
mean	451	886	1379	462	899	1397	419	864	1339	471	909	1227
s.d.	33.2	37.2	63.5	45.6	48.8	79.2	22.3	71.1	93.9	30.3	42.4	92.7
deviation [%]	0	0	0	2.4	1.5	1.3	-7,1	.2,5	.2,9	4,4	2,6	-11,0

3.3.6 Freeze-Thaw Stability

The deviation between the concentrations obtained for QC samples subjected to the extraction immediately after thawing and those kept at room temperature for 3 hours before extraction ranged from 5.0% to 14.1% (plasma) and 5.3% to 10.8% (urine). Data are shown in Table 3-12 and Table 3-13.

Table 3-12 freeze thaw stability plasma

	FT-cycle 0			FT-cycle 1			FT-cycle 2		
replicate	nominal concentration [pg/mL]								
	436	856	1276	436	856	1276	436	856	1276
	concentration found [pg/mL]								
#1	474	780	1414	389	964	1252	408	845	1297
#2	452	874	1337	516	841	1343	459	894	1345
#3	540	777	1271	435	870	1335	424	907	1145
#4	447	884	1272	412	865	1230	491	893	1473
#5	456	902	1423	509	979	1239	405	845	1234
mean	474	843	1343	452	904	1280	437	877	1299
s.d.	34.3	53.6	65.9	51.3	56.2	48.9	33.1	26.5	109.9
deviation [%]	0	0	0	-4.6	7.2	-4.7	-7.8	4.0	-3.3

Table 3-13 freeze thaw stability urine

	FT-cycle 0			FT-cycle 1			FT-cycle 2		
replicate	nominal concentration [pg/mL]								
	463.0	883.0	1303.0	463.0	883.0	1303.0	463.0	883.0	1303.0
	concentration found [pg/mL]								
#1	445.1	927.4	1391.0	407.5	783.3	1476.7	428.8	829.3	1390.3
#2	437.0	774.1	1105.3	444.4	887.9	1196.8	433.5	823.8	1116.4
#3	415.0	827.8	1262.5	438.4	811.0	1114.9	438.3	781.9	1240.5
#4	423.3	856.5	1190.4	394.6	981.4	1193.9	444.9	927.6	1131.8
#5	440.3	834.6	1173.9	532.3	827.5	1094.5	525.8	874.9	1093.7
mean	432.1	844.1	1224.6	443.5	858.2	1215.4	454.3	847.5	1194.5
s.d.	11.2	49.7	97.0	48.2	70.5	137.0	36.2	49.7	110.1
deviation [%]	0.0	0.0	0.0	2.6	1.7	-0.8	5.1	0.4	-2.5

3.3.7 Autosampler Stability

The mean concentrations of samples chromatographed immediately after sample preparation and 24 hours later differed between -4.9% and 13.7%. This indicates that 8-iso-$PGF_{2\alpha}$ is stable to repeated analysis conditions. Data is shown in Table 3-14.

Table 3-14 autosampler stability

	immediately			24h hours later		
replicate	nominal concentration [pg/mL]					
	280	700	1120	280	700	1120
	concentration found [pg/mL]					
#1	250	645	1082	251	739	1063
#2	266	726	1132	349	789	924
#3	272	659	1188	274	623	1218
#4	266	648	1043	315	620	1024
#5	302	746	1111	350	772	1058
mean	271	685	1111	308	708	1057
s.d.	17.1	42.6	48.6	39.6	72.9	94.6
deviation [%]	0	0	0	13.7	3.4	-4.9

3.3.8 Aliquot Analysis

The deviation is less than 15%, which shows that samples containing 8-iso-$PGF_{2\alpha}$ may be measured with sufficient reliability in 200 µl sample aliquots (1:1 dilution). Data is shown in Table 3-15.

Table 3-15 aliquot analysis

aliquote analysis	
replicate	nominal concentration [pg/mL]
	3200
	concentration found [pg/mL]
#1	3021
#2	3047
#3	3224
#4	3020
#5	3002
mean	3063
s.d.	82.0
CV [%]	2.7

3.3.9 Sample Chromatograms Plasma and Urine

Figure 3-13 shows a typical plasma blank sample with the calculated concentration indicated.

Plasma blank

Sample Chromatogram: day01-Plasma_blank_01

8-iso-$PGF_{2\alpha}$ *m/z* 393=>193

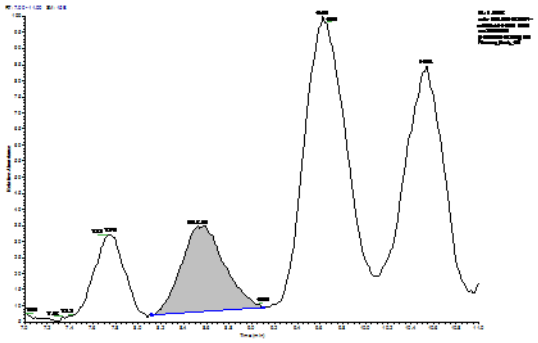

Calculated Amount [pg/mL]:	165.3
Actual RT:	8.56
Area:	7951
Area ratio:	0.019

8-iso-$PGF_{2\alpha}$-d_4 *m/z* 397=>197

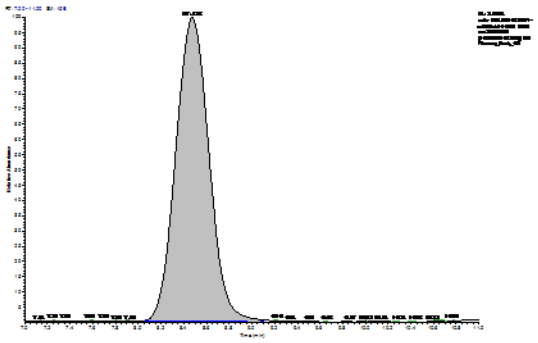

Actual RT:	8.48
Area:	415897

Figure 3-13 typical plasma blank sample of the validation procedure

Figure 3-14 shows a typical plasma spike sample with the calculated concentration indicated.

436 pg/mL Plasma Spike

Sample Chromatogram: day01-IPQC4_01

8-iso-$PGF_{2\alpha}$ m/z 393=>193

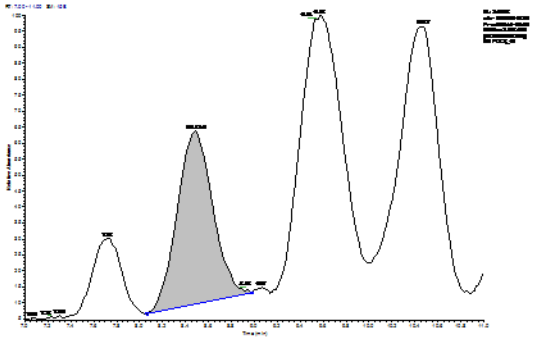

Calculated Amount [pg/mL]:	417.1
Actual RT:	8.47
Area:	21793
Area ratio:	0.048

Internal Standard: 8-iso-$PGF_{2\alpha}$ -d_4 *m/z* 397=>197

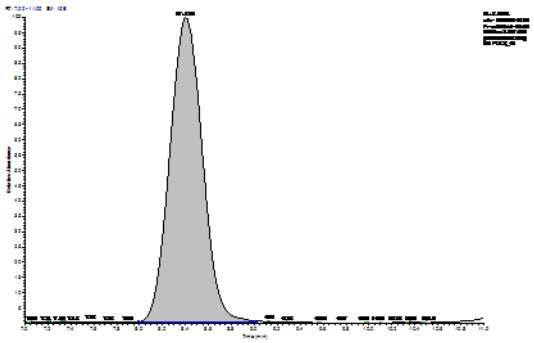

Actual RT:	8.40
Area:	454021

Figure 3-14 plasma spike sample of the validation procedure

Figure 3-15 shows a typical urine blank sample with the calculated concentration indicated.

Urine blank

Sample Chromatogram: day01-Urine_blank_01

8-iso-$PGF_{2\alpha}$ *m/z* 393=>193

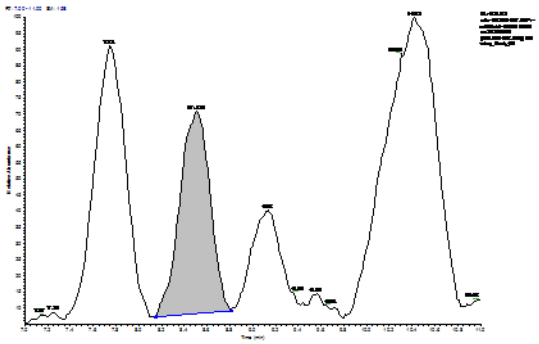

Calculated Amount [pg/mL]:	200.4
Actual RT:	8.51
Area:	10934
Area ratio:	0.023

Internal Standard: 8-iso-$PGF_{2\alpha}$ -d_4 *m/z* 397=>197

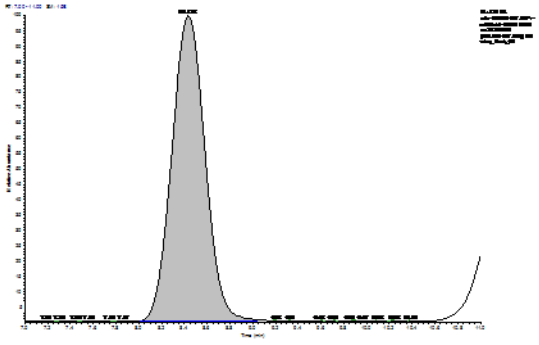

Actual RT:	8.43
Area:	475391

Figure 3-15 typical urine blank sample of the validation procedure

Figure 3-16 shows a typical urine spike sample with the calculated concentration indicated.

463 pg/mL Urine

Sample Chromatogram: day01-IUQC3_01

8-iso-$PGF_{2\alpha}$ *m/z* 393=>193

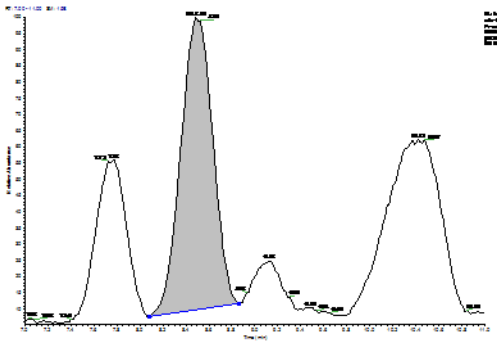

Calculated Amount [pg/mL]: 452

Actual RT: 8.49

Area: 18339

Area ratio: 0.052

Internal Standard: 8-iso-$PGF_{2\alpha}$ -d_4 *m/z* 397=>197

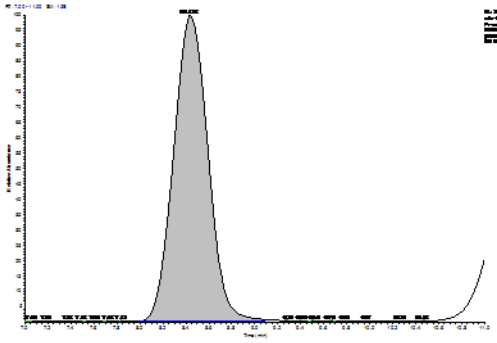

Actual RT: 8.43

Area: 352673

Figure 3-16 urine spike sample of the validation procedure

3.4 Development of analytical LC-MS Method for the Detection of 8-Hydroxy-2'-deoxyguanosine

Based on the relatively high basal amounts, no further sample enrichment was necessary to achieve measureable results, when it comes to the detection of 8-hydroxy-2'-deoxyguanosine (8-OHdG) in human urine by LC-MS detection. Nevertheless, the risk of ion suppression caused by the urine matrix can lead to falsification and has to be tested to verify this less time-consuming procedure as functional. A simple way to compensate ion suppression effects is the use of isotope marked analogue substances. Due to the high price of C_{13} or N_{15} marked internal standards, 8-mercaptoguanosine was chosen as external standard, described in Crow et al. 2008 (Crow et al., 2008b). Therefore, good chromatography is necessary to achieve well-resolved peaks and reduce ion suppression.

The Hypersil Gold aQ (Thermo Fisher, USA) with a dimension of 4.0 x 150 mm showed baseline separation of 8-OHdG under different isocratic and gradient conditions. Next to separation, wide particle diameter of 5 µm makes the column suitable for HPLC instruments with a backpressure under 400 bar, using methanol as organic HPLC solvent. Switching valve and separation of the chromatographic run into different time segments, with different flow rates before and after the elution time window of 8-OHdG, reduces runtime without sacrificing significant chromatographic resolution. By bypassing the flow post column from start to minute 6.30 and again from minute 10.51 till 15.50, a reduced contamination of the mass spectrometer source and housing results in higher uptime, productivity and lower maintenance rates of the LC-MS system.

Due to less matrix interferences, very short analytical runtimes under 5 minutes are possible to achieve. By reducing runtimes to a minimum, sensitivity and precision were sacrificed on a not acceptable level. The precision was increased up to 20% over a wide linear range starting from 2 to 100 nM samples. Strong matrix influence near the elution death volume generated strong ion suppression effects. Isotope marked internal standards would solve the problems by compensating the suppression effect due to physical and chemical properties. The lack of isotope marked internal standards lead to stretch chromatography to solve this problem. Therefore, the analytical method was developed with a run time of near 16 minutes. Stretching the gradient and increasing the separation effectiveness and chromatographic resolution led to a precision under 5% and was therefore suited for the quantitative detection. The final method is described in 2.6.5. This method reached 98.9 ± 3.7 % of recovery of 8-OHdG from spiked urine samples. Figure 3-17 to Figure

3-20 shows the chromatographic baseline separation of 8-OHdG with internal standard 8-MeG with spike experiments in human urine.

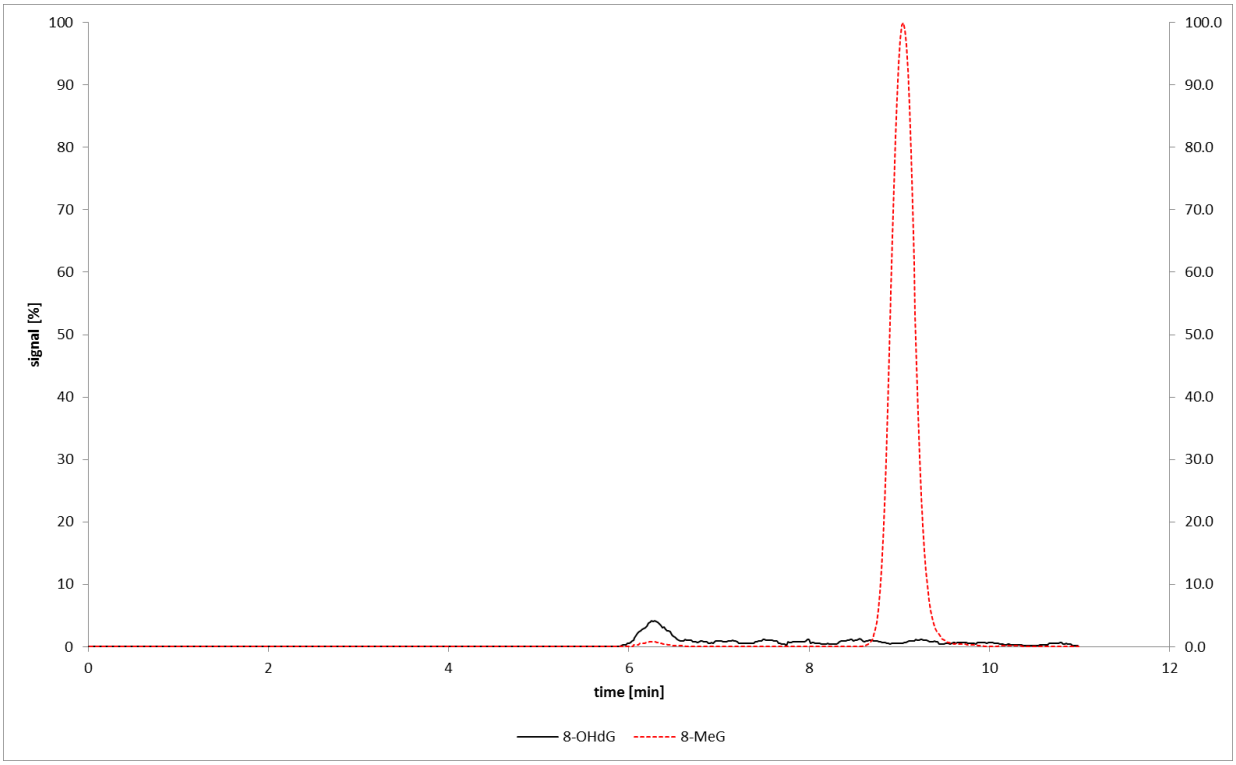

Figure 3-17 water blank (normalized to spiked urine 8-OHdG level in Figure 3-20)

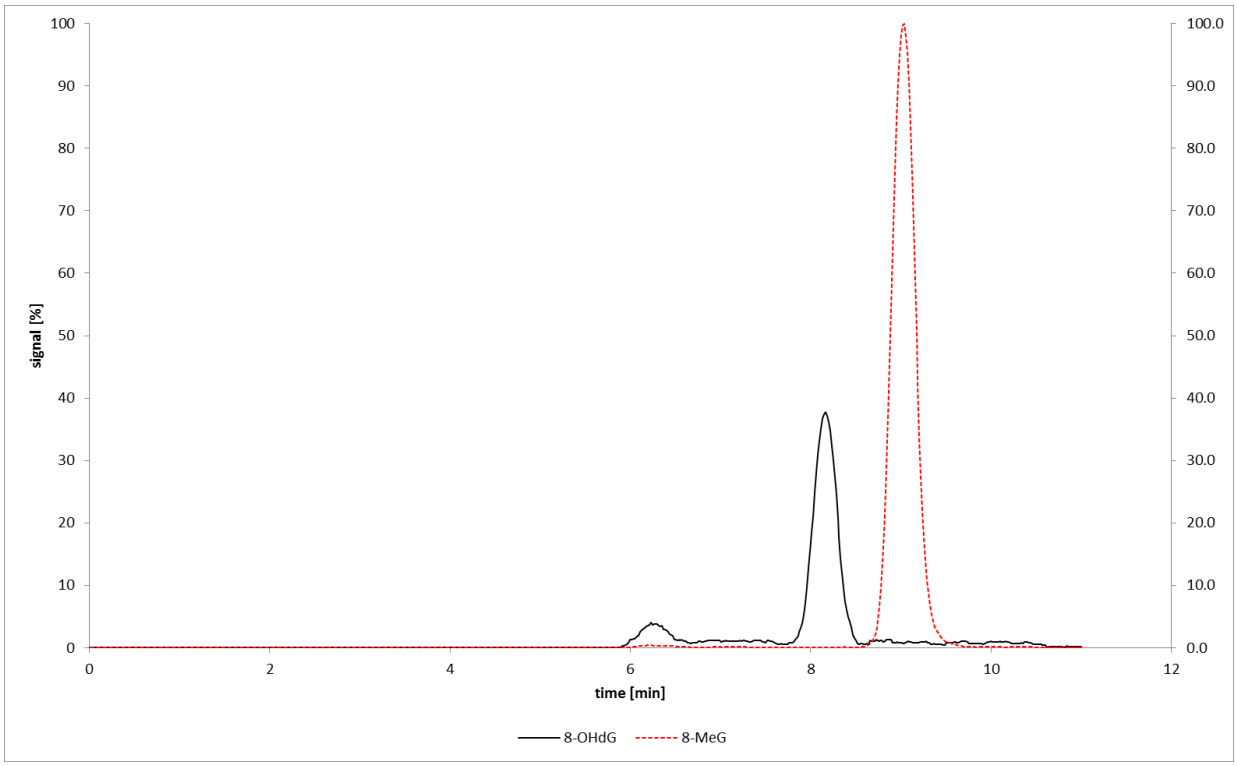

Figure 3-18 8-OHdG standard solution (normalized to spiked urine8-OHdG level in Figure 3-20)

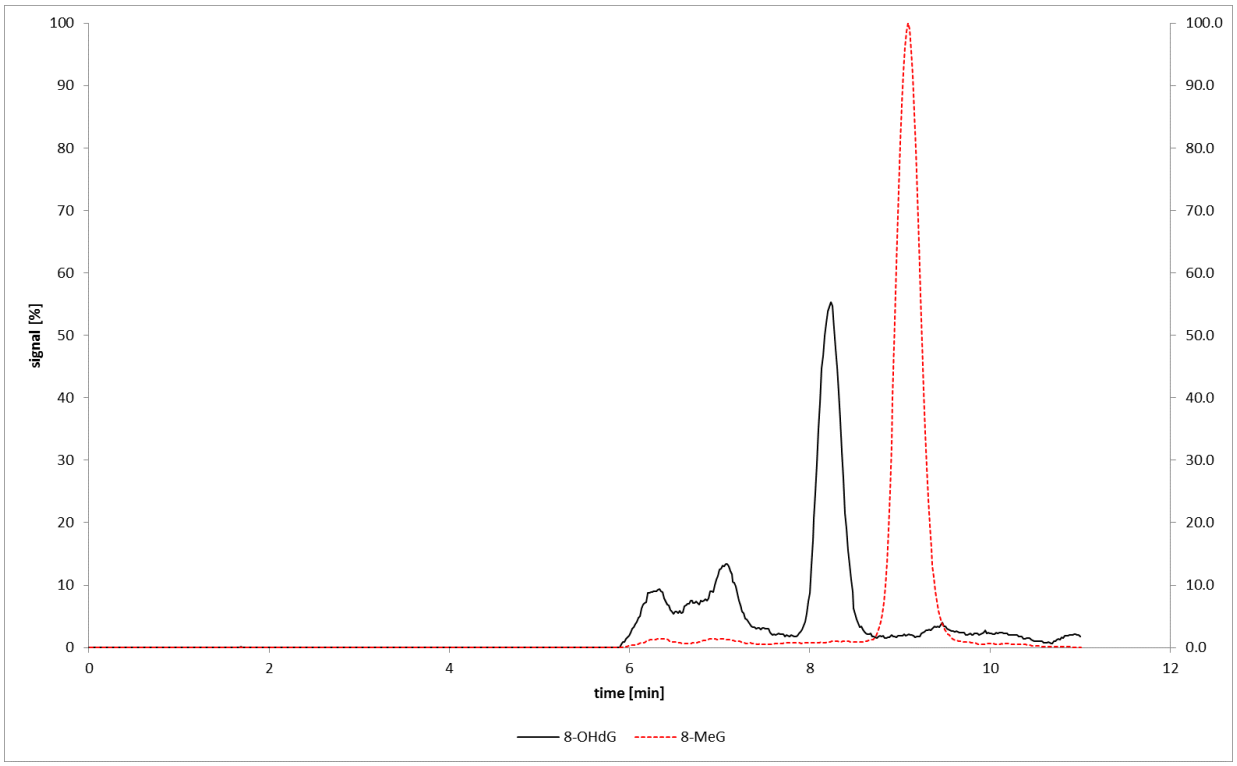

Figure 3-19 urnine blank (normalized to spiked urine 8-OHdG level in Figure 3-20)

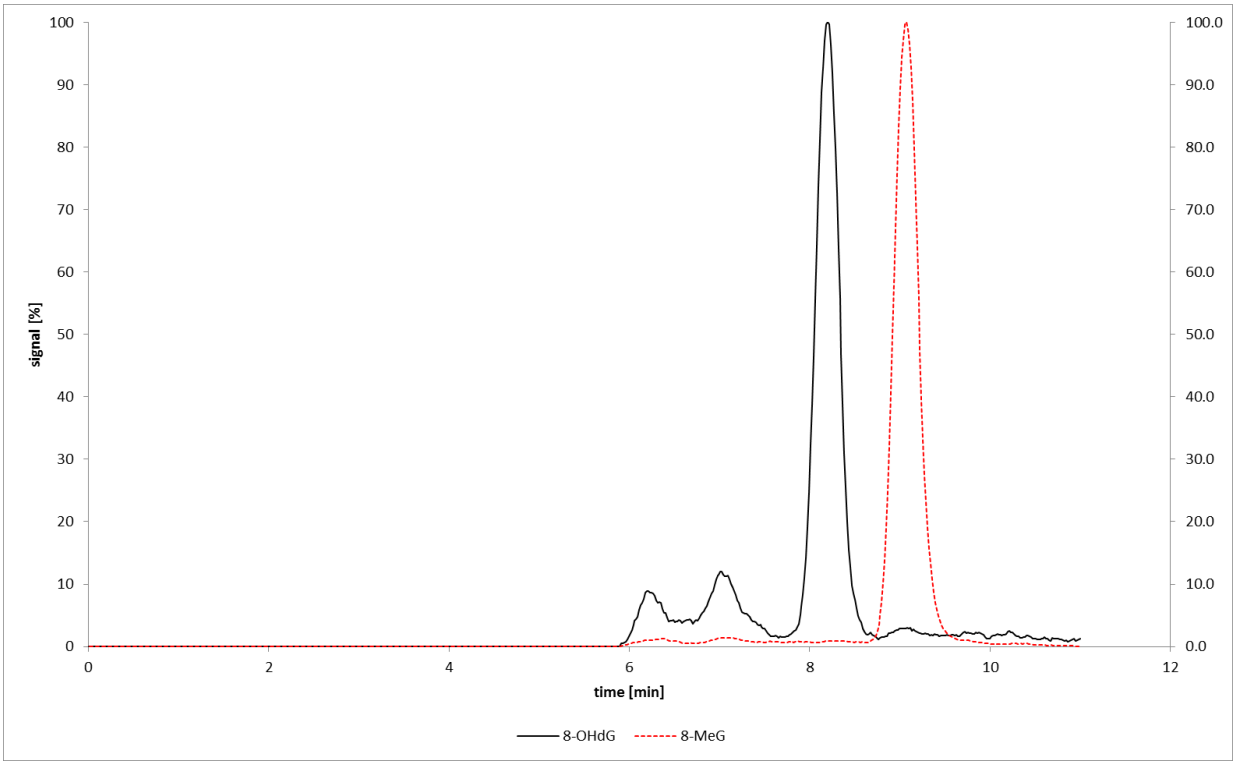

Figure 3-20 spiked urine sample

3.5 Validation of 8-Hydroxy-2'-deoxyguanosine in Human Urine

Validation was performed according to the FDA guidelines (FDA, 2001)

For the determination of 8-hydroxy-2'-deoxyguanosine (8-OHdG) in human urine a sensitive liquid chromatography/mass spectrometry (LC-MS) method was validated in the concentration ranges from 3.11 – 99.56 nM. The sample preparation contains a filtration step for der subsequent LC-MS measurement. The mass spectrometer was operated in multiple reaction monitoring mode under positive electrospray ionization conditions. 8-mercaptoguanosine (8-MeG) was used as internal standard.

3.5.1 Specificity

None of the six blank samples showed significant interference at the retention times of target and internal standard.

3.5.2 Linearity

The linearity was visually examined by plotting the nominal concentration versus

- the peak area ratios of 8-OHdG/8-MeG standard,

- the back-calculated concentrations for each calibration standard
- the percent deviation of the back-calculated values

According to the graphs below no tendency could be observed between the nominal concentration and the residuals. The coefficient of regression was 0.9988, indicating identical instrument response at different days of analysis, shown in Figure 3-21 and Figure 3-22.

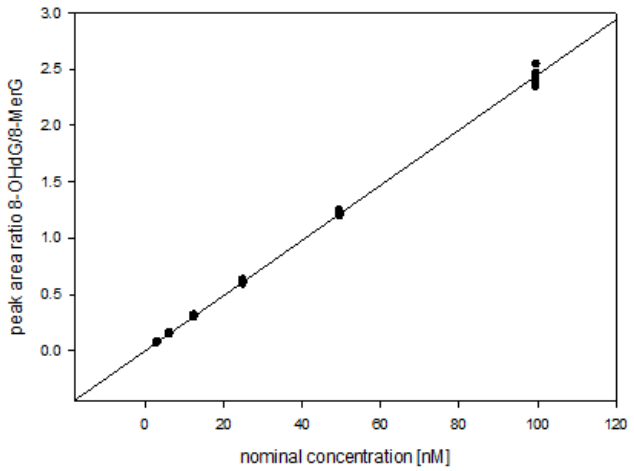

Figure 3-21 linearity check calibration graph

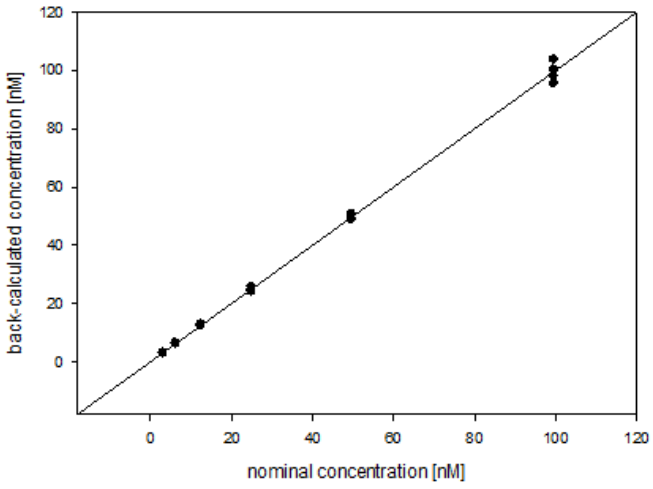

Figure 3-22 linearity check calibration back calculated values

3.5.3 Accuracy and Precision

3.5.3.1 Intra-Day

The accuracy and precision data fulfilled the acceptance criteria at every concentration level. The accuracy (expressed as bias%) ranged from -2.0% to -1.3%. The precision (expressed as CV%) was -2.0%. Data is shown in Table 3-16.

Table 3-16 intra-day accuracy and precision

intra-day			
replicate	nominal concentration [nM]		
	2.5	35	70
	concentration found [nM]		
#1	8.265	34.4	66
#2	8.824	35.4	70
#3	8.533	34.7	70
#4	8.479	33.8	71
#5	8.801	33.9	69
mean	8.6	34.4	69.2
s.d.	0.21	0.58	1.50
CV [%]	2.4	1.7	2.2
accuracy [%]	-2.0	-1.7	-1.3

3.5.3.2 Inter-Day

At concentration level 3.11 mM, the accuracy of the method was from 2.3% to 4.4%. The precision was 5.1 %.and fulfilled the acceptance criteria shown in the following tables. Data is shown in Table 3-17.

Table 3-17 inter-day accuracy and precision

				inter-day					
	day 1	day 2	day 3	day 1	day 2	day 3	day 1	day 2	day 3
replicate	nominal concentration [nM]								
	2.5	2.5	2.5	35	35	35	70	70	70
	concentration found [nM]								
#1	9	9.45	8.88	36.3	37.2	37	69.4	69.7	69
#2	8.91	8.6	9.15	36.1	34.7	36.6	70.5	67.9	70.7
#3	8.61	9.24	8.82	37.3	37	37	69.9	68.4	71.6
#4	8.55	9.11	8.96	34.3	41.1	36.1	70	70.7	72.3
#5	9.1	9.14	2.5	35.2	38.6	37	69.9	70.8	67.2
mean	8.83	9.11	8.91	35.8	36.9	36.7	69.9	69.5	70.2
s.d.	0.216	0.283	0.139	1.01	1.41	0.37	0.33	1.16	1.85
CV [%]	2.4	3.1	1.6	2.8	3.8	1	0.5	1.7	2.6
accuracy [%]	0.9	3.8	1.8	2.2	4.9	4.7	-0.1	-0.7	0.2

3.5.4 Limit of Quantification

3.5.4.1 Intra-Day & Inter-Day

At concentration level 3.11 mM, the accuracy of the method was from 2.3% to 4.4% (intra-day) and 2.3 to 4.4 (inter-day). The precision (expressed as CV%) was 8.5% (intra-day) and 5.% (inter-day).and fulfilled the acceptance. Data is shown in Table 3-18.

Table 3-18 limit of quantification

	intra-day	inter-day		
	day 1	day 2	day 3	day 4
replicate	nominal concentration [nM]			
	3.11	3.11	3.11	3.11
	concentration found [nM]			
#1	2.65	3.21	2.98	3.30
#2	3.07	3.44	3.18	3.19
#3	3.13	3.27	3.42	3.07
#4	3.24	2.97	3.20	3.36
#5	3.45	3.41	3.17	3.37
mean	3.11	3.26	3.19	3.26
s.d.	0.263	0.167	0.142	0.112
CV [%]	8.5	5.1	4.4	3.4
deviation [%]	-0.8	4.3	2.3	4.4

3.5.5 Stability

Five replicas of urine sample resulted in an 8-OHdG concentration of 6.24 ±0.45 nM. Data is shown inTable 3-19.

Table 3-19 8-OHdG concentration blank urine

replicate	concentration found [nM]
#1	6.57
#2	6.58
#3	5.68
#4	5.70
#5	6.68
mean	6.24
s.d.	0.45
CV [%]	7.2

Prepared urine samples were analyzed immediately and being stored below –70 °C and analyzed on four different days. The concentrations of the stored and immediately analyzed samples differed less than the critical 15 %. Therefore, the samples are considered stable within four days. Data is shown in Table 3-20 and Table 3-21.

Table 3-20 intra-day stability urine

	intra-day	
replicate	concentration found [nM]	
#1	15.3	60.0
#2	16.1	53.6
#3	15.3	53.2
#4	15.5	58.8
#5	17.1	60.0
mean	15.8	57.1
s.d.	0.7	3.1
CV [%]	4.3	5.4

Table 3-21 inter-day stability urine

replicate	1st inter-day		2nd inter-day		3rd inter-day		4rd inter-day	
	nominal concentration [nM]							
	16.2	56.2	16.2	56.2	16.2	56.2	16.2	56.2
	concentration found [nM]							
#1	16.9	58.8	17.3	52.4	17.3	52.8	16.9	52.6
#2	16.7	52.3	15.9	53.3	17.2	52.7	15.1	60.1
#3	15.6	56.3	15.6	55.7	15.1	53.9	17.1	55.5
#4	16.5	54.7	15.1	59.5	15.3	60.1	17.4	55.4
#5	15.7	59.4	17.1	56.5	15.8	59.2	15.3	58.1
mean	16.3	56.3	16.2	55.5	16.1	55.7	16.4	56.4
s.d.	0.5	2.6	0.8	2.5	0.9	3.3	0.9	2.6
CV [%]	3.3	4.7	5.2	4.5	5.9	5.8	5.7	4.5
deviation [%]	3.2	-1.4	2.5	-2.8	1.9	-2.5	3.8	-1.2

3.5.6 Freeze-Thaw Stability

QC samples were subjected to three, two and one freeze/thaw cycles. Mean concentrations of samples underwent the freeze/thaw cycles did not differ from that of the reference samples more than the critical 15%. Data is shown in Table 3-22.

Table 3-22 freeze thaw stability

replicate	FT-cycle 0		FT-cycle 1		FT-cycle 2	
	nominal concentration [nM]					
	16.2	56.2	16.2	56.2	16.2	56.2
	concentration found [nM]					
#1	15.3	60.2	15.1	53.3	15.4	54.0
#2	15.2	53.5	15.5	57.9	16.1	54.1
#3	15.1	53.4	15.1	54.8	15.4	53.2
#4	15.2	54.7	16.1	59.2	16.2	57.9
#5	15.3	54.5	17.1	55.5	16.3	53.8
mean	15.2	55.3	15.8	56.1	15.9	54.6
s.d.	0.1	2.5	0.8	2.1	0.4	1.7
deviation [%]			3.9	1.4	4.6	-1.3

3.5.7 Autosampler Stability

The mean concentrations of samples chromatographed immediately after sample preparation and 24 hours later differed up to -3.8%. This indicates that 8-OHdG is stable to repeated analysis conditions. Data is shown in Table 3-23.

Table 3-23 autosampler stability

	immidiate		1 day later	
replicate	nominal concentration [nM]			
	16.2	56.2	16.2	56.2
	concentration found [nM]			
#1	16.8	56.5	17.0	55.2
#2	17.1	55.4	15.5	53.0
#3	15.1	57.5	15.1	52.6
#4	16.8	54.2	15.0	57.5
#5	15.8	59.0	16.2	58.6
mean	16.3	56.5	15.7	55.4
s.d.	0.8	1.7	0.7	2.4
deviation [%]	0	0	-3.8	-2.4

3.5.8 Aliquot Analysis

The deviation is -2.2%, which shows that samples containing 8-OHdG may be measured with sufficient reliability in 200 µl sample aliquots (1:1 dilution). Data is shown in Table 3-24.

Table 3-24 aliquot analysis

	aliquot analysis
replicate	nominal concentration [nM]
	100
	concentration found [nM]
#1	99.9
#2	97.7
#3	98.7
#4	94.5
#5	98.2
mean	97.8
s.d.	1.8
deviation [%]	-2.2

3.5.9 Sample Chromatograms Urine

Figure 3-23 shows a typical urine blank during validation.

Urine blank

Sample Chromatogram: Urine_blank_01

8-OHdG *m/z* 284 =>168

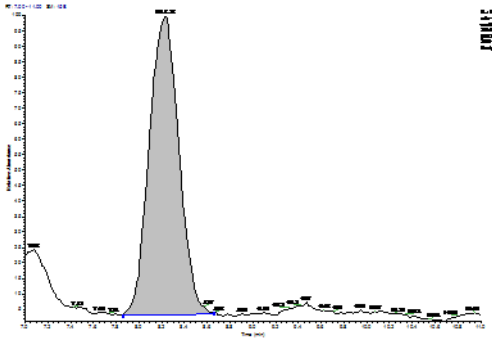

Calculated Amount [nM]: 6.57

Actual RT: 8.23

Area: 310056

Area ratio: 0.122

Internal Standard: 8-MeG *m/z* 316=>184

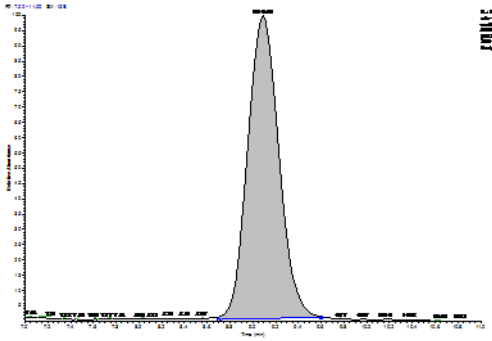

Actual RT: 9.09

Area: 2541443

Figure 3-23 sample chromatogram of urine blank of 8-OHdG

Figure 3-24 shows a typical urine spike during validation.

15.3 nM Urine

Sample Chromatogram:	day01-UQC1_01	
8-OHdG	*m/z* 284 =>168	
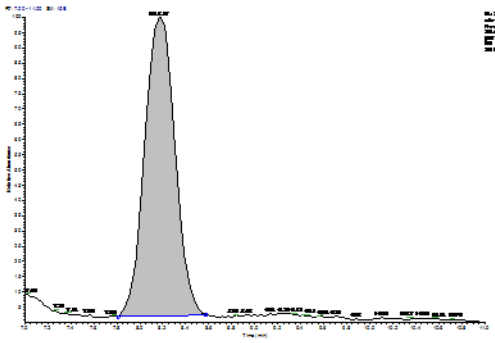	Calculated Amount [nM]:	15.3
	Actual RT:	8.17
	Area:	361459
	Area ratio:	0.284
	Signal to noise:	444
Internal Standard: 8-MeG	*m/z* 316=>184	
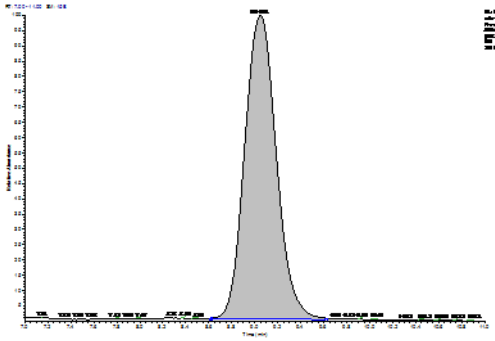	Actual RT:	9.04
	Area:	1272742

Figure 3-24 sample chromatogram of urine spike of 8-OHdG

3.6 Oxilipin Method Development

Solvents, gradients and columns were tested to verify, that co-elution of targeted oxilipins were avoided by testing chromatographic conditions.

Best chromatographic performance was found with a YMC-Triart C18 1.9 µm column (YMC Europe, Dinslaken, Germany) with a dimension of 2.0 x 100 mm. The bioactive lipids were separated using a linear mobile phase gradient (A, 0.1% acetic acid in water; B 0.1% acetic acid in acetonitrile/isopropanol 50:50 v:v) at 0.6 mL/min. The starting conditions consisted 35 % solvent B and were maintained over 0.75 min. The gradient was then increased to 53% solvent B over 6 minutes followed by an increase to 95% over 4.5 min and hold for 2 minutes. A post run equilibration returned to the initial conditions maintaining for 2 minutes. Injection volume was set to 10 µL. The analysis of the 6460 triple quadruple was performed using jet-stream ESI ionization with gas and sheath gas flows of at 9 and 10, respectively. The gas and sheath gas heater were set to 250 and 325 respectively. The negative capillary and nozzle voltage was adjusted to 3600 V and 500 V, respectively. Nebulizer pressure was set to 45 psi. Ion width was set to wide. Triggered MRM was activated to achieve optimal dwell times and qualitative information. Cycle time was set to 250 ms. MRM transitions optimized are shown in Table 3-25. Several other qualifier MRM transitions were optimized for qualitative tMRM detection but are not shown in this thesis.

Table 3-25 oxilipin MRM transition

analyte	precursor Ion	product ion	Fragmentor	collision energy
9-HODE	295.2	171.1	64	8
	295.2	277.2	146	14
13-HODE	295.2	113.1	118	23
	295.2	195.1	149	9
	295.2	277.2	99	24
18-HEPE	317.2	71.1	162	29
	317.2	133.2	97	10
	317.2	149.1	79	30
15-HEPE	317.2	248.1	129	16
	317.2	255.2	98	20
	317.2	273.1	90	29
12-HEPE	317.2	109.1	161	15
	317.2	135	136	19
	317.2	163.1	114	27
9-HEPE	317.2	177.2	85	13
	317.2	201.1	172	12

	317.2	219.1	127	27
8-HEPE	317.2	109.1	74	16
	317.2	111.1	173	24
	317.2	121.1	133	9
5-HEPE	317.2	163.1	64	17
	317.2	201.1	71	7
14(15)-EET	319.2	59	122	16
	319.2	113.1	166	13
	319.2	121.2	147	13
11(12) - EET	319.2	59	115	25
	319.2	149.1	86	23
	319.2	163	162	27
20-HETE	319.2	245.2	178	18
	319.2	257.2	62	8
	319.2	273.2	90	25
15-HETE	319.2	275.2	102	14
	319.2	203.1	95	17
12-HETE	319.2	275.2	137	18
	319.2	139.1	125	17
	319.2	163.1	119	10
11-HETE	319.2	59	130	28
	319.2	149.1	160	14
9-HETE	319.2	257.2	81	15
	319.2	275.1	99	25
	319.2	301.2	163	17
8-HETE	319.2	127	77	30
	319.2	275.2	169	28
	319.2	203.1	87	24
5-HETE	319.2	59	71	21
	319.2	203.1	99	6
	319.2	257.2	156	8
2,3-dinor-11-beta-$PGF_{2\alpha}$	325.2	153.1	63	9
	325.2	173.1	142	9
	325.2	263.2	151	11
2,3-dinor-8-iso-$PGF_{2\alpha}$	325.2	82.9	147	26
	325.2	99	142	9
	325.2	111	72	29
LTB4	335.2	109	158	18
	335.2	135.1	128	21
	335.2	203.2	123	10
14,15-DHET	337.2	59	152	15
	337.2	219.1	172	10

	337.2	257.1	162	18
11,12-DHET	337.2	197	162	16
	337.2	163	91	9
8.9-DHET	337.2	111	118	21
	337.2	141.1	158	22
5,6-DHET	337.2	191	144	15
	337.2	115	128	21
	337.2	99	65	10
20-HDoHE	343.2	71.1	175	9
	343.2	121.1	95	25
	343.2	187	129	10
17-HDoHE	343.2	59	157	7
	343.2	111	124	29
	343.2	121.1	88	10
16-HDoHE	343.2	261	158	6
	343.2	59	83	14
	343.2	135.2	76	29
14-HDoHE	343.2	189.1	73	27
	343.2	299.1	106	26
	343.2	109	77	6
13-HDoHE	343.2	299.1	120	5
	343.2	149.1	177	16
11-HDoHE	343.2	299.1	179	19
	343.2	59	127	27
10-HDoHE	343.2	137.2	113	18
	343.2	227	156	13
	343.2	135.2	91	7
8-HDoHE	343.2	243.2	150	27
	343.2	281.2	72	21
	343.2	299.1	123	16
7-HDoHE	343.2	189.1	140	12
	343.2	299.1	62	19
4-HDoHE	343.2	71.1	138	21
	343.2	115.1	72	22
	343.2	133	86	14
PGE_3	349.2	175.2	174	8
	349.2	262.1	96	15
PGD_2	351.2	251.1	160	17
	351.2	233	95	7
PGE_2	351.2	175	125	10
PG_{F3}	351.2	59	70	5
	351.2	181.1	82	28

	351.2	315.1	101	23
8-iso-15-keto-$PGF_{2\alpha}$	351.2	59	156	21
	351.2	119.1	84	28
	351.2	307.1	173	16
8-iso-$PGF_{2\alpha}$	353.2	193.1	103	21
	353.2	255.1	103	7
	353.2	273.2	78	5
PGE_1	353.2	235.1	95	15
	353.2	335.2	110	28
PGD_1	353.2	123.1	148	28
	353.2	205.1	103	10
$PGF_{2\alpha}$	353.3	193	131	22
	353.3	171	68	7
	353.3	165	88	7
$PGF_{1\alpha}$	355.2	167.3	90	10
	355.2	211.1	112	7
	355.2	237.2	82	23
TXB_3	367.2	125	117	14
	367.2	151.1	92	8
	367.2	169	149	30
	367.2	177	164	28
11-dehydro-TXB_2	367.2	135.1	81	22
	367.2	161.1	138	16
	367.2	163.1	140	18
TXB_2	369.3	351.1	147	11
	369.3	333.1	113	25
	369.3	125	121	10
6-keto-$PGF_{1\alpha}$	369.3	143	110	11
	369.3	121	161	23
	369.3	307.1	116	9

Triggered MRM windows were set to peak retention time plus four times the peak width for automatic peak recognition.

3.6.1 Chromatographic Separation of Oxilipins

Figure 3-25 shows a chromatogram of measured oxilipins in a typical standard sample.

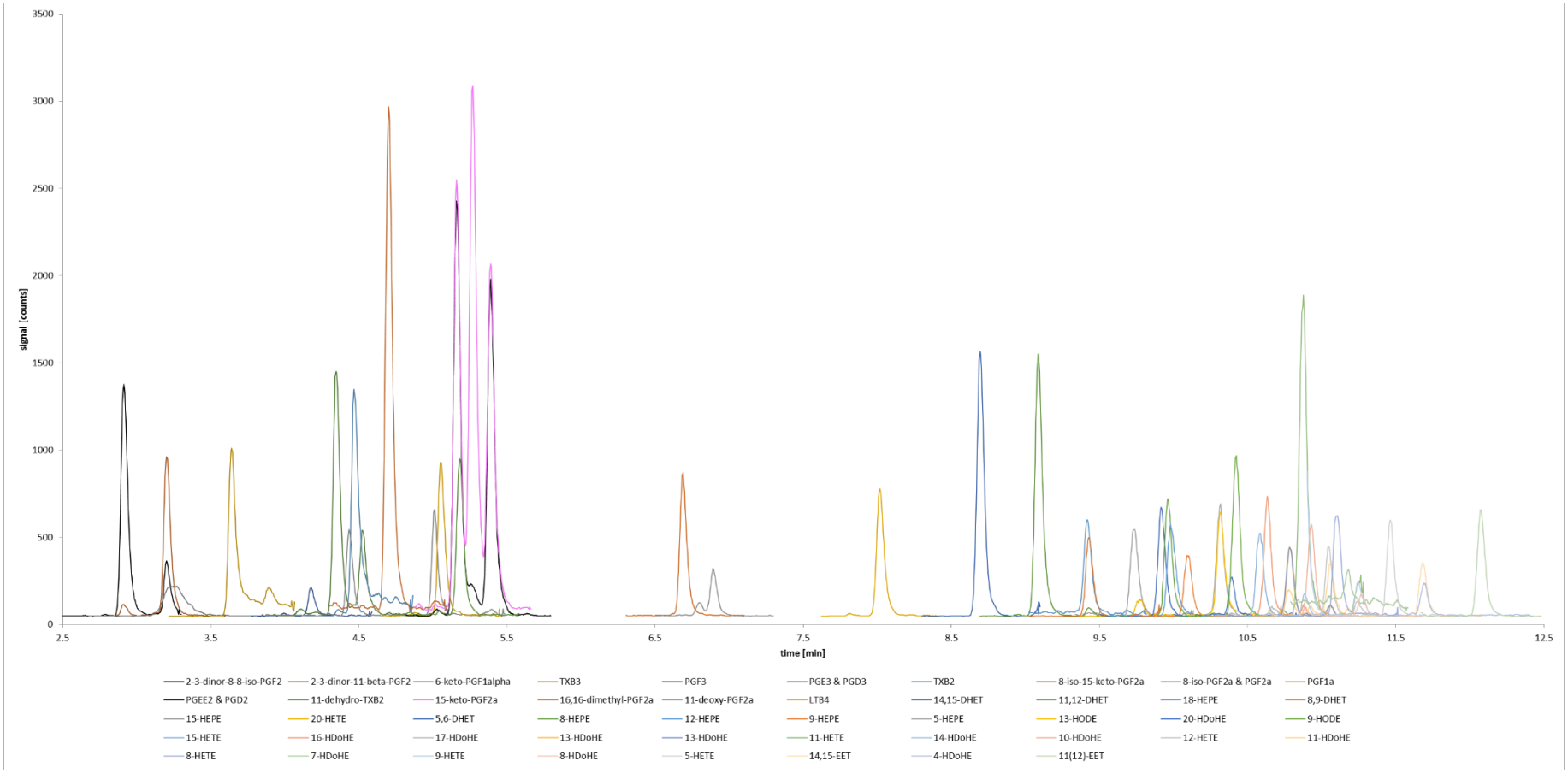

Figure 3-25 chromatogram of 1 ng/mL oxilipin standards using dynamic MRM detection

3.6.2 Chromatographic Evaluation

Evaluation of the chromatographic capacity was tested using different biological matrices. Plasma, follicular fluid and semen plasma were chosen for evaluation due to their diversity of analytes with high variety in concentration.

Due to great variety between each human sample, the showing signal intensity of following chromatograms can vary very strong between different samples. Nevertheless, those chromatograms give a good overview about the chromatographic performance and instrument sensitivity. Chromatograms represent the measured signal intensity on the left chromatogram and the same data scaled to 100% each, to deliver comparable peaks and resolution for every concentration level.

The validation procedure was not finished while composing this work. Nevertheless, the results, showed in the following pages, present well detectable basal concentrations in body fluids indicating a good outlook to perform quantitative data acquisition for several oxilipins.

3.6.2.1 2,3-dinor-8-iso-Prostaglandin $F_{2\alpha}$

Figure 5-1 shows 2,3-dinor-8-iso-$PGF_{2\alpha}$ well resolved next to its similar compound 2,3-dinor-11-beta-$PGF_{2\alpha}$ at minute 3.2. No trace of 2,3-dinor-8-iso-$PGF_{2\alpha}$ could be found in this plasma and follicular fluid samples. High amounts of in semen plasma recommends further dilution steps or less injection amounts of the sample to lower matrix interferences and increase resolution of the analyte peak with a small tailing over a assumed co-eluting peak at the end.

3.6.2.2 2,3-dinor-11-beta-Prostaglandin $F_{2\alpha}$

Figure 5-2 shows 2,3-dinor-11-beta-$PGF_{2\alpha}$ well resolved, next to its compounds with similar MRM transition. No trace of 2,3-dinor-11-beta-$PGF_{2\alpha}$ could be found in this plasma and follicular fluid samples. High amounts of in semen plasma recommends further dilution steps or less injection amounts of the sample to lower matrix interferences and increase resolution. No assumed co-eluting peak could be detected.

3.6.2.3 6-keto-Prostaglandin $F1_{\alpha}$

Figure 5-3 shows no peak assuming 6-keto-$PGF_{1\alpha}$ in all three body fluids. By a further dilution of the prepared semen plasma sample, an increase in chromatography could maybe lead to a well resolved peak of 6-keto-$PGF_{1\alpha}$.

3.6.2.4 Thromboxane B_3

Figure 5-4 shows low levels of Thromboxane B_3 in the human plasma sample. Compared to low to samples the 1 ng/mL standard mixture sample shows a huge tailing over 1 minute (data not shown). Therefore, it is recommended to carefully evaluate peak integration and quantitation over high and low Thromboxane B_3 amounts.

3.6.2.5 Prostaglandin $F_{3\alpha}$

Figure 5-5 shows high amounts of PGF_3 in semen plasma sample. A small shift in retention times recommends diluting the semen plasma sample for higher chromatographic resolution. It is recommended to undergo further spike experiments to verify the elution of PGF_3.

3.6.2.6 Prostaglandin D_3 and E_3

Figure 5-6 shows no significant peaks of PGD_2 in all three biological samples. Next to the high amounts of matrix interference, coeluting substances with similar MRM transition, a poor resolved peak of PGE_2 (earlier eluting peak of the two peaks in the 1 ng/mL standard chromatogram) has been found in semen plasma sample. A further sample dilution is recommended to reduce peak width resulting in baseline separating of these three coeluting peaks. Reducing peak tailing with dilution steps could result in a possible detectable peak of PGD_3 in semen plasma sample.

3.6.2.7 Thromboxane B_2

Figure 5-7 shows detectable amounts of Thromboxane B_2 in all samples. Similar to Thromboxane B_3, all peaks show a significant tailing over a large time scale. Hence, tailing has to be considered to perform reproducible quantification.

3.6.2.8 8-iso-15-keto-Prostaglandin $F_{2\alpha}$

Figure 5-8 shows poor resolved peaks due to the high amount of co-eluting peaks in semen plasma sample. Further dilution and spike experiments will possible show, if one of these poor resolved peaks is 8-iso-15-keto-$PGF_{2\alpha}$.

3.6.2.9 8-iso-Prostaglandin $F_{2\alpha}$ and Prostaglandin $F_{2\alpha}$

Figure 5-9 shows 8-iso-$PGF_{2\alpha}$ and $PGF_{2\alpha}$ eluting in this order showed the 1 ng/mL standard measurement. Semen plasma and follicular fluid sample should be diluted further to achieve good baseline separation, even though quantification should be possible with this peak resolution. $PGF_{2\alpha}$ resulted in even better chromatographic resolution found in every sample measured.

3.6.2.10 Prostaglandin $F_{1\alpha}$

Figure 5-10 showed very low amounts of $PGF_{1\alpha}$ in plasma and follicular fluids near the LOD. Semen plasma instead resulted in very high amounts with good chromatographic separation efficiency.

3.6.2.11 Prostaglandin E_2 and D_2

Next to 8-iso-$PGF_{2\alpha}$, the separation of PGE_2 and PGD_2 is very critical when it comes to matrix co-eluting interferences. Figure 5-11 shows the need for dilution steps to achieve chromatographic separation. Nevertheless, dilution steps have to be considered with care due the thin line between separation and LOQ. Especially when it comes to the detection of PGD_2 next to the higher amount of PGE_2 and the resulting tailing of the earlier elution.

3.6.2.12 11-dehydro-Thromboxane B_2

Figure 5-12 showed no detectable amount of 11-dehydro-TXB_2 in all three biological samples.

3.6.2.13 15-keto- Prostaglandin $F_{2\alpha}$

Figure 5-13 shows 15-keto- $PGF_{2\alpha}$ not baseline separated between PGE_2 (front) and PGD_2 (tail) based on their similar MRM transition in 1 ng/mL standard.

3.6.2.14 16,16-dimethyl-Prostaglandin $F_{2\alpha}$

Figure 5-14 shows no detectable amounts of 16,16-dimethyl- $PGF_{2\alpha}$ in all three biological samples.

3.6.2.15 11-deoxy-Prostaglandin $F_{2\alpha}$

Figure 5-15 shows two peaks in the 1 ng/mL standard mixture solution resulting in an unclear identification of the retention time of 11-deoxy-$PGF_{2\alpha}$. Standard single injection and further spike experiments are necessary to identify 11-deoxy-$PGF_{2\alpha}$.

3.6.2.16 Leukotriene B_4

Figure 5-16 shows the detection of LTB_4 in plasma and follicular fluid samples. Semen plasma samples points on a co-eluting substance with similar MRM transition, which could be an interference in follicular fluid measurement.

3.6.2.17 14,15-Dihydroxy Eicosatrienoic Acid

Figure 5-17 shows baseline separated peaks of 14,15-DHET in all measured samples in detectable amounts.

3.6.2.18 11,12-Dihydroxy Eicosatrienoic Acid

Figure 5-18 shows baseline separated peaks of 11,12-DHET in all measured samples in detectable amounts.

3.6.2.19 18-Hydroxy Eicosapentaenoic Acid

Figure 5-19 represents baseline separation of 18-HEPE. Detectable amounts were found in plasma and follicular liquid samples.

3.6.2.20 8,9-Dihydroxy Eicosatrienoic Acid

Figure 5-20 shows detectable amounts of 8,9-DHET in plasma and follicular fluid sample with baseline separated chromatography.

3.6.2.21 15-Hydroxy Eicosapentaenoic Acid

Figure 5-21 shows detectable amounts of 15-HEPE in every biological sample with peak baseline separation.

3.6.2.22 20-Hydroxy Eicosatetraenoic Acid

Figure 5-22 shows detectable amounts of 20-HETE in every biological sample with good separation.

3.6.2.23 5,6-Dihydroxy Eicosatrienoic Acid

Figure 5-23 shows good separated peaks of 5,6-DHET in detectable amounts of every biological sample. Even though concentration in semen plasma is critical to the LOD.

3.6.2.24 8-Hydroxy Eicosapentaenoic Acid

Figure 5-24 shows detectable amounts of 8-HEPE in plasma a follicular fluid samples.

3.6.2.25 12-Hydroxy Eicosapentaenoic acid

Figure 5-25 shows detectable amounts of 12-HEPE in plasma and follicular fluid samples.

3.6.2.26 9-Hydroxy Eicosapentaenoic Acid

Figure 5-26 shows detectable amounts of 9-HEPE in plasma and follicular fluid samples. 9-HEPE was baseline separated to other matrix interferences.

3.6.2.27 5-Hydroxy Eicosapentaenoic Acid

Figure 5-27 shows detectable amounts of 5-HEPE in every biological fluid. Semen plasma samples amounts are critical near to LOD.

3.6.2.28 13-Hydroxy Octadecadienoic Acid

Figure 5-28 shows high amounts of 13-HODE in every biological sample. Co-elution of an unknown matrix interference at the tail side of the 13-HODE peaks results in critical chromatography. Resolution will not increase significant due to the comparison with lower amount of 1 ng/mL and similar peak width. Therefore samples should be evaluated carefully when it comes to automated peak detection.

3.6.2.29 20-Hydroxy Docosahexaenoic Acid

Figure 5-29 shows 20-HDoHE detectable in every biological sample over a wide concentration range.

3.6.2.30 9-Hydroxy Octadecadienoic Acid

High amounts of 9-HODE are shown in Figure 5-30. Good separation of matrix interferences is achieved in all samples. Follicular fluid sample may need a further dilution to increase chromatographic resolution in the front.

3.6.2.31 15-Hydroxy Eicosatetraenoic Acid

15-HETE is baseline separated detected in all three biological samples. High concentrations do not influence peak resolution as shown in Figure 5-31.

3.6.2.32 16-Hydroxy Docosahexaenoic Acid

Figure 5-32 shows good separation of 16-HDoHE with good peak separation efficiency over the whole concentration range. Semen plasma sample shows low amount of 16-HDoHE.near to LOQ.

3.6.2.33 17-Hydroxy Docosahexaenoic Acid

Baseline separation of 17-HDoHE is shown every biological sample in Figure 5-33. Detectable amounts higher than the 1 ng/mL standard could be measured.

3.6.2.34 13-Hydroxy Docosahexaenoic Acid

Except of plasma sample high amounts of 13-HDoHE can be found in follicular fluid and semen plasma sample. Good separation could be achieved shown in Figure 5-34.

3.6.2.35 11-Hydroxy Eicosatetraenoic Acid

Baseline separation over all samples on a wide concentration range was achieved, shown in Figure 5-35.

3.6.2.36 14-Hydroxy Docosahexaenoic Acid

Baseline separation of 14-HDoHE could be achieved over all biological samples, shown in Figure 5-36. Semen plasma levels are near the LOQ.

3.6.2.37 10-Hydroxy Docosahexaenoic Acid

Baseline separation of 14-HDoHE could be achieved over all biological samples, shown in Figure 5-37. Semen plasma levels are near the LOQ.

3.6.2.38 12-Hydroxy Eicosatetraenoic Acid

12-HETE could be detected in all biological samples without any interferences shown in Figure 5-38.

3.6.2.39 11-Hydroxy Docosahexaenoic Acid

Amount of 11-HDoHE is very low near to the LOQ. Good separation could be achieved over all biological samples shown in Figure 5-39.

3.6.2.40 8-Hydroxy Eicosatetraenoic Acid

8-HETE could be detected in all biological samples shown in Figure 5-40. Good chromatographic resolution is achieved except for plasma sample. A small fronting in the beginning of the peak could be the reason for a possible co-elution.

3.6.2.41 7-Hydroxy Docosahexaenoic Acid

Only low amounts of 7-HDoHE are detected in those three biological samples, shown in Figure 5-41.

3.6.2.42 9-Hydroxy Eicosatetraenoic Acid

The detection of 9-HETE is critical when it comes to biological matrices. Baseline separation could not be achieved which is very critical at low concentration levels, shown in Figure 5-42. Therefore manual peak integration should be the method of choice.

3.6.2.43 8-Hydroxy Docosahexaenoic Acid

8-HDoHE is detected in low amounts in these biological samples. Only follicular fluid had detectable amounts over the LOQ, shown in Figure 5-43.

3.6.2.44 5-Hydroxy Eicosatetraenoic Acid

Figure 5-44 shows baseline separation in all biological samples. All detected amounts of 5-HETE were higher than the LOQ.

3.6.2.45 14(15)-Epoxy Eicosatrienoic Acid

Only follicular fluid sample showed detectable amounts of 14(15)-EET shown in Figure 5-45.

3.6.2.46 4- Hydroxy Docosahexaenoic Acid

Plasma and follicular fluid samples resulted detectable amounts of 4-HDoHE, shown in Figure 5-46.

3.6.2.47 11(12)- Epoxy Eicosatrienoic Acid

Figure 5-47 showed detectable amounts of 11(12)-EET, but only follicular fluid sample was higher than the LOQ.

4 Discussion

This thesis focused on the development of an analytical platform for the detection of substances generated by ROS as well as bioactive lipid signal mediators in various biological matrices. These includes urine, plasma as well as semen plasma and follicular fluid. By using generic, as well as in house developed extraction SPE methods (Weißenbacher, 2013, Taylor et al., 2008, Taylor and Traber, 2010, Masoodi and Nicolaou, 2006, Masoodi et al., 2008), the work demonstrated that different matrices showed a wide range of detectable analytes with the LC-MS instruments employed. It also utilized chromatographic separation of all analytes in a total runtime less than 16 minutes. The objective of this work was to develop this platform capable of identifying, confirming and quantifying targeted analytes at basal levels. Method validations were successfully completed for 8-iso-$PGF_{2\alpha}$ and 8-OHdG. The calculations of all relevant validation characteristics were performed during validation. Those two validation studies showed, that the developed methods meet the accuracy and precision of each analyte within ranges required.

4.1 8-iso-Prostaglandin $F_{2\alpha}$

Morrow et al. (Morrow et al., 1990) reported the occurrence of free 8-iso-$PGF_{2\alpha}$ in human plasma and urine with concentration between 4-50 pg/mL and 500 to 4000 pg/mg of creatinine. In rats, they reported an increase up to 200-fold of 8-iso-$PGF_{2\alpha}$ by free radical-catalyzed lipid peroxidation induced by administration of chemokine CCl_4. For the quantitative detection, GC-MS technique was used. Several concentration of free 8-iso-$PGF_{2\alpha}$ in plasma were reported over the years (Battistini et al., 1998, Davies, 2009, Janssen, 2001, Kadiiska et al., 2005, Li et al., 1999, Liu et al., 2009, Masoodi and Nicolaou, 2006, Medina et al., 2012, Milne et al., 2005, Morrow and Roberts, 1996, Schwedhelm et al., 2007, Sircar and Subbaiah, 2007, Taylor and Traber, 2010, Yin et al., 2005). Due to the high variation of reported free 8-iso-$PGF_{2\alpha}$ levels, and the fact that 8-iso-$PGF_{2\alpha}$ is an extreme potent renal vasoconstrictor in its free form (Morrow et al., 1992, Kromer and Tippins, 1996), a further metabolism and therefore low stability in plasma is critical for the assessment of a reliable biomarker. Higher stability as well as higher concentrations of bonded 8-iso-$PGF_{2\alpha}$ are reported in phospholipids (Morrow et al., 1992). The release of 8-iso-$PGF_{2\alpha}$ by phospholipase A_2 from phospholipids is reason of appearance of its free form. Therefore, a total 8-iso-$PGF_{2\alpha}$ analysis was established using methanol alkaline hydrolysis as the best way to release 8-iso-$PGF_{2\alpha}$ in sample preparation.

The tandem mass spectrometer used for the quantification of 8-iso-$PGF_{2\alpha}$ and 8-OHdG was a triple quadrupole mass analyzer that provided an average sensitivity of its class. For the sensitive detection in human plasma, standard chromatography conditions recommended from column manufactures are a limiting factor for sample loading. Therefore, an enhanced method development was necessary to achieve detectable levels of 8-iso-$PGF_{2\alpha}$ in human plasma and urine (Taylor et al., 2008, Taylor et al., 2006). Hence, sample availability is limited in clinical studies; a limit of 1 mL plasma for sample preparation was set. Using short columns with small diameter, typically 2.1 mm, is the best way to get an increase in sensitivity (Medina et al., 2012). In fact, using smaller diameter columns is always limited to injection volume. The length of those columns are a disadvantage for resolution. Of course, higher resolution is possible using sub 2 µm packing material, but the analytical HPLC used, is limited to a maximum pressure of 400 and is not capable for this type of UHPLC columns. Using 4.6 mm HPLC columns was not an option, as the LOQ/LOD would have had to be increased.

In order to overcome the lack of chromatographic resolution using higher injection volumes, a new strategy was developed. A column head enrichment after injection is the best way to improve the downside of increased injection volume. For the enrichment of the injected sample, analyte-catching conditions were set using only 30% methanol for 0.25 minutes. After the enrichment of 8-iso-$PGF_{2\alpha}$ on the column head, the gradient jumped to 60% methanol to start with the chromatographic separation. Still, using a 100 mm column resulted in a loss of resolution. Therefore, column length was increased to 250 mm, resulting in no loss of chromatographic resolution. Increasing injection volume is often accompanied with matrix effects and suppression effects. An increase in column length to the 250 mm is a pleasant way to overcome these problems effectively enough.

From the method development, the sample clean-up was the second most critical step in the analysis method. Especially the clean-up procedure proved to be a critical factor for obtaining reproducible chromatographic resolution. The reconstitution of 100 µL from originally 1 mL of plasma is a critical step in solubility, as well as matrix effects. Furthermore, the previous plasma hydrolysis is critical to sample loading before SPE. Several conditions were tested to gain optimal recovery to lower the limit of quantification. The use of deuterated internal standards is a very helpful tool since, quiet diverse results in ion suppression, depending on the plasma sample deployed, were found.

Urine preparation was less critical, due to higher basal levels, as well as much lower matrix interferences. The measurement of urinary 8-iso-$PGF_{2\alpha}$ is a noninvasive way to assess lipid peroxidation damage in vivo. In this analytical approach, 8-iso-$PGF_{2\alpha}$ is measured in its free form. Since many eicosanoids are excreted as urine glucuronide conjugates (Rivera et al., 2004, Prakash et al., 1992), the report of glucuronic acid conjugates of 8-iso-$PGF_{2\alpha}$ should be adopted using β-glucuronidase enzymes, to enhance the free form with the assessment of total amount 8-iso-$PGF_{2\alpha}$ levels of free and conjugate form (Yan et al., 2010).

Online-SPE detection has to be critically evaluated, due to the unknown amount of isomers in human plasma. Taylor et al. reported good separation efficiency to several forms of F_2-prostanes (Taylor et al., 2006). Without the knowledge of those isomers, online-SPE can be a pitfall when it comes to quantitation. On one hand, there is a need for a SPE-cartridge with good binding capacity and binding efficiency. Otherwise, targeted analytes will break through the trapping capacity of the online SPE. On the other hand, elution of targeted analytes from the SPE cartridge often leads to a strong organic influx into the analytical column due to the high organic amount of SPE cartridge elution phase. This influx reduces following chromatographic separation on the analytical column. Isomeric separation of F_2-prostaglandins is not possible under these conditions. A way to undergo this problem is a second pump, between the SPE cartridge and the analytical column. The 2^{nd} pump reduces the organic amount by infusing water for organic phase dilution. However, this approach is limited <300 bar pressure. At least 9 times the flow of SPE elution is necessary from the 2^{nd} pump to allow a column head enrichment. Several washing steps of the loaded SPE cartridge are necessary to reduce ion suppression effects before elution. Furthermore, reversed flow SPE column equilibration is unavoidable to prevent the SPE cartridge from clogging effects. All these necessary steps are limitations when more than 40 samples need to be taken in 24 hours.

4.2 3-Nitrotyrosine

The development of a method for the quantification of 3-nitrotyrosine was discarded after long literature studies. Carbon dioxide (CO_2) is physiologically present and has effects on tyrosine-nitration (Tsikas, 2010a). It increases the extent of tyrosine-nitration due to the intermediate formation of nitrosoperoxycarbonate. Assessing those challenges in sample preparation is a critical step. Especially the clean-up procedure is reported to be a critical factor in the appearance of 3-nitrotyrosine formation (Schwedhelm et al., 1999, Tsikas et al., 2003, Tsikas et al., 2005, Ryberg and Caidahl, 2007, Rabbani and Thornalley, 2008, Radabaugh et al., 2008, Tsikas, 2010c, Tsikas,

2010b). Since hydrolysis is necessary to access the whole spectra of ROS damage on proteins, releasing 3-nitrotyrosine as well as tyrosine, the risk of artificial enhancing 3-nitrotyrosine levels is very critical, due to a mean 3-nitrotyrosine : tyrosine ratio of around $1:1*10^6$ (Shigenaga et al., 1997). Even nitration less than 0.1% of protein-bonded tyrosine would falsify the results of the analytical approach significantly. This method would influence multivariate statistics very strong based on high variation due to sample preparation. Therefore, the decision was clear to exclude this biomarker from further investigations and development steps.

4.3 8-Hydroxy-2'-deoxyguanosine

Since the report of Floyd et al. of 8-OHdG detection using HPLC-ECD with high sensitivity, several improvements have been made to access DNA damage caused by oxidative stress (Floyd et al., 1986, Kadiiska et al., 2005, Hu et al., 2010, Mangal et al., 2009, Woo et al., 2009, Caliskan-Can et al., 2008, Vaya, 2008, Crow et al., 2008a). Using mass spectrometry enhances the capability to measure samples in high through put over a short time span. Less requirements in sample preparation where the main goal to assess this biomarker. Using fast elution gradients, as well as balancing measurement time and ion suppression effects, were the main steps in method development. A simple filtering step and adding of internal standard was enough to make this analytical approach work.

4.4 Oxilipins

Oxilipin detection is very demanding on analytical instruments available today. Due to their functional groups, positive ionization is not an option. The acid group tents to emit its hydrogen atom. Therefore, good ionization conditions are 2-3 values over the characteristic pka-value oft targeted analytes. This would be perfectly suited for volatile HPLC buffers with a pH of 7 or higher. Ammonium acetate would result in in very good ionization conditions. Nevertheless, the bottleneck comes in chromatography. A deprotonated carboxylate group suppresses the interaction of the C18 stationary phase material. Hugh tailing effects makes baseline separation on C18 nearly impossible measuring isomers. Even post-column injection of ammonia into acidic, resulting in a buffer with pH around seven, showed no increase in signal intensity. Even more, an intensity breakdown was determined by using this online infusion technique. Therefore, acetic acid was used as additive to control protonation of the targeted analytes during chromatographic separation. Quantifying 48 substances at the same time have some disadvantages when it comes to chromatography. 6-keto-$PGF_{1\alpha}$ shows an increase over two times in peak width over more than two times using water,

acetonitrile and isopropanol with acetic acid. This peak broadening lowers the limit of quantification significant compared to the use of water, acetonitrile with acetic acid alone. However, the use of isopropanol allows to increase peak shape for dihydroxyeicosatrienoic acids enhancing signal up to 5 times over the use of acetonitrile only. Still, thromboxanes show the typical broad peak shape owing to its inter-conversion between its two hemiacetal isomers. This could not be solved using different acidic C18 reversed phase conditions. Nevertheless, this analytical approach is capable of sensitively identifying and quantifying targeted oxilipins in various biological fluids. Nevertheless, the development was a balancing act of not losing accuracy and specificity due to complex matrix composition and suppression effects.

To measure major lipid influences in the inflammatory cascade, the following part will describe the targeted oxilipins and how their monitoring will help to measure inflammatory effects, which possibly play an important role in cardiovascular disease, obesity and other metabolic disorders. For pro-inflammatory effects, arachidonic acid is the most prominent omega-6 fatty acid. It gets stored into phospholipids from intake or from deconstruction of dihomo-γ-linolenic acid. Under diet conditions, linolenic acid is de-saturated over δ-6-desaturase and converts to γ-linolenic acid, followed to dihomo-γ-linolenic acid by elongase, and finally converts by δ-5-desaturase in arachidonic acid (Rago and Fu, 2013, Le Faouder et al., 2013). This is especially important to people suffering with obesity, due to the dependency of δ-6-desaturase to the fatty acid ratio 20:3/18:3 and the dependency of δ-5-desaturase to 20:4/20:3 fatty acid ratio (Shaik et al., 2014, Pedro Mena 1email, 2012). COX-1 acts then with dihomo-γ-linolenic acid and forms the thromboxane 1-series, prostaglandin 1-series and thromboxane 1-series, which leads to proinflamatoric reactions (Wang et al., 2013). Next to COX-1 formation, COX-2 forms the prostaglandin 2-series and thromboxane 2-series over arachidonic acid and are called prostanoids.

Lipooxygenase on the other hand forms leukotrienes 4-series by hydroperoxidation of arachidonic acid. The action of 5-LOX converts arachidonic acid to its intermediate 5-hydroxyperoxy eicosatetraenoic acid (5-HpETE) that immediately reduces to 5-hydroxy eicosatetraenoic acid (5-HETE and/or Leukotriene A_4 (LTA_4), both interconvertible. LTA_4 converts to LTB_4. 5-, 12, and 15-LOX converts arachidonic acid to their products 5-12- and 15- hydroxy eicosatetraenoic acids (HETE). CYP450 products of arachidonic acid are covered by this method measuring HETEs as well as epoxy-eicosatrienoic acids (EET) and further dihydroxy eicosatetraenoic acids (DHET).

Omega-3 fatty acids belong to the category of fatty acids, which provide anti-inflamatory mediators by enzymatic conversions. Eicosapentaenoic acid acts to γ-linolenic acid via competitive inhibition, displacement or being counteractive (Maldini et al., 2012). Eicosapentaenoic acid, as well as docosahexaenoic acid, are found in fish oils and supporting the treatment inflammatory or chronic diseases (Hong and Lu, 2013). Under diet conditions, α-linolenic acid is de-saturated and elongated with an extra double bond and converts to eicosapentaenoic acid. Furthermore, this product also converts to docosahexaenoic acid by furthered de-saturation, elongation and β-oxidation (Chan et al., 2011, Lengel, 2014). COX activity results in the generation of prostanoids 3-series by converting eicosapentaenoic acid (Mena et al., 2012). LOX deoxygenates the fatty acid to its leukotrienes 5-series and hydroxy eicosapentaenoic acids (HEPE) (Strassburg et al., 2012). Docosahexaenoic acid is not converted by COX (Miller et al., 2014) but is measured as hydroxy docosahexaenoic acid (HDoHE) after LOX and CYP450 conversation. Finally α-linolenic acid converts to 9- and 13- hydroxyl octadecadienoic acid (HODE) over the LOX pathway (Strassburg et al., 2012).

5 Conclusion

Overall, the developed platform represents a rapid and sensitive approach to analyse ROS and lipid mediators simultaneous. Several enrichment strategies were accomplished to overcome sensitivity limitations due to analytical resources. The analytical platform was tested on different biological fluids to validate the specificity and sensitivity. Furthermore, even more oxilipins can be adopted to expand this method. Due to a water/acetonitrile/isopropanol gradient, the adoption of fatty acid precursors into this method should possible, due to comprehensive SPE method development. Longer dwell times, higher sample loads as well as optimized chromatography helps to achieve sensitivity, necessary for endogenous basal level detection.

This platform allows examining oxilipin profiles within the signaling cascade in cells, tissue, whole blood, plasma, semen, follicular semen and other biological fluids. It represents a powerful tool for the investigation of new hypothesis in cardiovascular diseases, obesity, metabolic disorders and influences in the inflammatory cascade.

Bibliography

BALAZY, M. 2004. Eicosanomics: targeted lipidomics of eicosanoids in biological systems. *Prostaglandins & Other Lipid Mediators,* 73**,** 173-180.

BATTISTINI, B., PICARD, S., BORGEAT, P. & SIROIS, P. 1998. Measurements of Prostanoids, Leukotrienes, and Isoprostanes by Enzyme Immunoassays.

BECKMAN, K. B. & AMES, B. N. 1997. Oxidative decay of DNA. *J Biol Chem,* 272**,** 19633-6.

BLAIR, I. A., BARROW, S. E., WADDELL, K. A., LEWIS, P. J. & DOLLERY, C. T. 1982. Prostacyclin is not a circulating hormone in man. *Prostaglandins,* 23**,** 579-589.

CALISKAN-CAN, E., FIRAT, H., ARDIC, S., SIMSEK, B., TORUN, M. & YARDIM-AKAYDIN, S. 2008. Increased levels of 8-hydroxydeoxyguanosine and its relationship with lipid peroxidation and antioxidant vitamins in lung cancer. *Clin Chem Lab Med,* 46**,** 107-12.

CAVALCA, V., MINARDI, F., SCURATI, S., GUIDUGLI, F., SQUELLERIO, I., VEGLIA, F., DAINESE, L., GUARINO, A., TREMOLI, E. & CARUSO, D. 2010. Simultaneous quantification of 8-iso-prostaglandin-F2[alpha] and 11-dehydro thromboxane B2 in human urine by liquid chromatography-tandem mass spectrometry. *Analytical Biochemistry,* 397**,** 168-174.

CHAN, E. C., PASIKANTI, K. K. & NICHOLSON, J. K. 2011. Global urinary metabolic profiling procedures using gas chromatography-mass spectrometry. *Nat Protoc,* 6**,** 1483-99.

COOKE, M. S., EVANS, M. D. & LUNEC, J. 2002. DNA repair: insights from urinary lesion analysis. *Free Radic Res,* 36**,** 929-32.

CROW, B., BISHOP, M., KOVALCIK, K., NORTON, D., GEORGE, J. & BRALLEY, J. A. 2008a. A simple and cost effective method for the quantification of 8-hydroxy-2′-deoxyguanosine from urine using liquid chromatography tandem mass spectrometry. *Biomedical Chromatography,* 22**,** 394-401.

CROW, B., BISHOP, M., KOVALCIK, K., NORTON, D., GEORGE, J. & BRALLEY, J. A. 2008b. A simple and cost effective method for the quantification of 8-hydroxy-2prime-deoxyguanosine from urine using liquid chromatography tandem mass spectrometry. *Biomedical Chromatography,* 22**,** 394-401.

DAVIES, S. S. 2009. Lipidomic approaches to measuring isoprostanes and other markers of oxidative stress. *European Journal of Lipid Science and Technology,* 111**,** 64-74.

ENCIU, A. M., GHERGHICEANU, M. & POPESCU, B. O. 2013. Triggers and effectors of oxidative stress at blood-brain barrier level: relevance for brain ageing and neurodegeneration. *Oxid Med Cell Longev,* 2013**,** 297512.

ENGLER, M. M. & ENGLER, M. B. 2006. Omega-3 fatty acids: role in cardiovascular health and disease. *J Cardiovasc Nurs,* 21**,** 17-24, quiz 25-6.

FDA, U. D. O. H. A. H. S. 2001. Guidance for Industry. Bioanalytical Method Validation.

FINKELSTEIN, J., HEEMELS, M. T., SHADAN, S. & WEISS, U. 2014. Lipids in health and disease. *Nature,* 510**,** 47.

FLOYD, R. A., WATSON, J. J., WONG, P. K., ALTMILLER, D. H. & RICKARD, R. C. 1986. Hydroxyl free radical adduct of deoxyguanosine: sensitive detection and mechanisms of formation. *Free Radic Res Commun,* 1**,** 163-72.

GOUVEIA-FIGUEIRA, S. & NORDING, M. L. 2013. Development and Validation of a Sensitive UPLC-ESI-MS/MS Method for the Simultaneous Quantification of 15 Endocannabinoids and Related Compounds in Milk and Other Biofluids. *Analytical Chemistry,* 86**,** 1186-1195.

GRITTI, F. & GUIOCHON, G. 2013. The van Deemter equation: Assumptions, limits, and adjustment to modern high performance liquid chromatography. *Journal of Chromatography A,* 1302**,** 1-13.

GUIX, F. X., URIBESALGO, I., COMA, M. & MUNOZ, F. J. 2005. The physiology and pathophysiology of nitric oxide in the brain. *Prog Neurobiol,* 76**,** 126-52.

HAEGGSTRÖM, J. Z., RINALDO-MATTHIS, A., WHEELOCK, C. E. & WETTERHOLM, A. 2010. Advances in eicosanoid research, novel therapeutic implications. *Biochemical and Biophysical Research Communications,* 396**,** 135-139.

HALKET, J. M., WATERMAN, D., PRZYBOROWSKA, A. M., PATEL, R. K. P., FRASER, P. D. & BRAMLEY, P. M. 2005. Chemical derivatization and mass spectral libraries in metabolic profiling by GC/MS and LC/MS/MS. *Journal of Experimental Botany,* 56**,** 219-243.

HALLIWELL, B. & WHITEMAN, M. 2004. Measuring reactive species and oxidative damage in vivo and in cell culture: how should you do it and what do the results mean? *Br J Pharmacol,* 142**,** 231-55.

HASCHKE, M., ZHANG, Y. L., KAHLE, C., KLAWITTER, J., KORECKA, M., SHAW, L. M. & CHRISTIANS, U. 2007. HPLC-Atmospheric Pressure Chemical Ionization MS/MS for Quantification of 15-F2t-Isoprostane in Human Urine and Plasma. *Clin Chem,* 53**,** 489-497.

HONG, S. & LU, Y. 2013. Omega-3 fatty acid-derived resolvins and protectins in inflammation resolution and leukocyte functions: targeting novel lipid mediator pathways in mitigation of acute kidney injury. *Front Immunol,* 4**,** 13.

HU, C.-W., CHAO, M.-R. & SIE, C.-H. 2010. Urinary analysis of 8-oxo-7,8-dihydroguanine and 8-oxo-7,8-dihydro-2'-deoxyguanosine by isotope-dilution LC-MS/MS with automated solid-phase extraction: Study of 8-oxo-7,8-dihydroguanine stability. *Free Radical Biology and Medicine,* 48**,** 89-97.

JANSSEN, L. J. 2001. Isoprostanes: an overview and putative roles in pulmonary pathophysiology. *Am J Physiol Lung Cell Mol Physiol,* 280**,** L1067-1082.

KADIISKA, M. B., GLADEN, B. C., BAIRD, D. D., GERMOLEC, D., GRAHAM, L. B., PARKER, C. E., NYSKA, A., WACHSMAN, J. T., AMES, B. N., BASU, S., BROT, N., FITZGERALD, G. A., FLOYD, R. A., GEORGE, M., HEINECKE, J. W., HATCH, G. E., HENSLEY, K., LAWSON, J. A., MARNETT, L. J., MORROW, J. D., MURRAY, D. M., PLASTARAS, J., ROBERTS II, L. J., ROKACH, J., SHIGENAGA, M. K., SOHAL, R. S., SUN, J., TICE, R. R., VAN THIEL, D. H., WELLNER, D., WALTER, P. B., TOMER, K. B., MASON, R. P. & BARRETT, J. C. 2005. Biomarkers of Oxidative Stress Study II: Are oxidation products of lipids, proteins, and DNA markers of CCl4 poisoning? *Free Radical Biology and Medicine,* 38**,** 698-710.

KORECKA, M., CLARK, C. M., LEE, V. M. Y., TROJANOWSKI, J. Q. & SHAW, L. M. 2010. Simultaneous HPLC-MS-MS quantification of 8-iso-PGF2[alpha] and 8,12-iso-iPF2[alpha] in CSF and brain tissue samples with on-line cleanup. *Journal of Chromatography B,* 878**,** 2209-2216.

KROMER, B. M. & TIPPINS, J. R. 1996. Coronary artery constriction by the isoprostane 8-epi prostaglandin F2 alpha. *Br J Pharmacol,* 119**,** 1276-80.

LE FAOUDER, P., BAILLIF, V., SPREADBURY, I., MOTTA, J.-P., ROUSSET, P., CHÊNE, G., GUIGNÉ, C., TERCÉ, F., VANNER, S., VERGNOLLE, N., BERTRAND-MICHEL, J., DUBOURDEAU, M. & CENAC, N. 2013. LC–MS/MS method for rapid and concomitant quantification of pro-inflammatory and pro-resolving polyunsaturated fatty acid metabolites. *Journal of Chromatography B,* 932**,** 123-133.

LENGEL, R. 2014. Software gestützte Interpretation von quantitativen Metabolitenprofildaten – Dimensionsreduktion über das Hauptkomponentenanalysemodell.

LI, H., LAWSON, J. A., REILLY, M., ADIYAMAN, M., HWANG, S.-W., ROKACH, J. & FITZGERALD, G. A. 1999. Quantitative high performance liquid chromatography/tandem mass spectrometric analysis of the four classes of F2-isoprostanes in human urine. *Proceedings of the National Academy of Sciences of the United States of America,* 96**,** 13381-13386.

LIU, W., MORROW, J. D. & YIN, H. 2009. Quantification of F2-isoprostanes as a reliable index of oxidative stress in vivo using gas chromatography-mass spectrometry (GC-MS) method. *Free Radical Biology and Medicine,* 47**,** 1101-1107.

MADDIPATI, K. R. & ZHOU, S. L. 2011. Stability and analysis of eicosanoids and docosanoids in tissue culture media. *Prostaglandins Other Lipid Mediat,* 94**,** 59-72.

MALDINI, M., BAIMA, S., MORELLI, G., SCACCINI, C. & NATELLA, F. 2012. A liquid chromatography-mass spectrometry approach to study "glucosinoloma" in broccoli sprouts. *J Mass Spectrom,* 47**,** 1198-206.

MANGAL, D., VUDATHALA, D., PARK, J. H., LEE, S. H., PENNING, T. M. & BLAIR, I. A. 2009. Analysis of 7,8-dihydro-8-oxo-2'-deoxyguanosine in cellular DNA during oxidative stress. *Chem Res Toxicol,* 22**,** 788-97.

MASOODI, M., MIR, A. A., PETASIS, N. A., SERHAN, C. N. & NICOLAOU, A. 2008. Simultaneous lipidomic analysis of three families of bioactive lipid mediators leukotrienes, resolvins, protectins and related hydroxy-fatty acids by liquid chromatography/electrospray ionisation tandem mass spectrometry. *Rapid Commun Mass Spectrom,* 22**,** 75-83.

MASOODI, M. & NICOLAOU, A. 2006. Lipidomic analysis of twenty-seven prostanoids and isoprostanes by liquid chromatography/electrospray tandem mass spectrometry. *Rapid Commun Mass Spectrom,* 20**,** 3023-9.

MEDINA, S., DOMÍNGUEZ-PERLES, R., GIL, J. I., FERRERES, F., GARCÍA-VIGUERA, C., MARTÍNEZ-SANZ, J. M. & GIL-IZQUIERDO, A. 2012. A ultra-pressure liquid chromatography/triple quadrupole tandem mass spectrometry method for the analysis of 13 eicosanoids in human urine and quantitative 24 hour values in healthy volunteers in a controlled constant diet. *Rapid Communications in Mass Spectrometry,* 26**,** 1249-1257.

MENA, P., CALANI, L., DALL'ASTA, C., GALAVERNA, G., GARCIA-VIGUERA, C., BRUNI, R., CROZIER, A. & DEL RIO, D. 2012. Rapid and comprehensive evaluation of (poly)phenolic compounds in pomegranate (Punica granatum L.) juice by UHPLC-MSn. *Molecules,* 17**,** 14821-40.

MESAROS, C., LEE, S. H. & BLAIR, I. A. 2009. Targeted quantitative analysis of eicosanoid lipids in biological samples using liquid chromatography-tandem mass spectrometry. *Journal of Chromatography B,* 877**,** 2736-2745.

MILLER, E., #X17C, BIETA, MOREL, A., SASO, L. & SALUK, J. 2014. Isoprostanes and Neuroprostanes as Biomarkers of Oxidative Stress in Neurodegenerative Diseases. *Oxidative Medicine and Cellular Longevity,* 2014**,** 10.

MILLER, S. B. 2006. Prostaglandins in Health and Disease: An Overview. *Seminars in Arthritis and Rheumatism,* 36**,** 37-49.

MILNE, G. L., MUSIEK, E. S. & MORROW, J. D. 2005. F2-isoprostanes as markers of oxidative stress in vivo: an overview. *Biomarkers,* 10 Suppl 1**,** S10-23.

MONTUSCHI, P., BARNES, P. J. & ROBERTS, L. J., II 2004. Isoprostanes: markers and mediators of oxidative stress. *FASEB J.,* 18**,** 1791-1800.

MORROW, J. D., AWAD, J. A., BOSS, H. J., BLAIR, I. A. & ROBERTS, L. J., 2ND 1992. Non-cyclooxygenase-derived prostanoids (F2-isoprostanes) are formed in situ on phospholipids. *Proc Natl Acad Sci U S A,* 89**,** 10721-5.

MORROW, J. D., HILL, K. E., BURK, R. F., NAMMOUR, T. M., BADR, K. F. & ROBERTS, L. J., 2ND 1990. A series of prostaglandin F2-like compounds are produced in vivo in humans by a non-cyclooxygenase, free radical-catalyzed mechanism. *Proc Natl Acad Sci U S A,* 87**,** 9383-7.

MORROW, J. D. & ROBERTS, L. J. 1996. The isoprostanes : Current knowledge and directions for future research. *Biochemical Pharmacology,* 51**,** 1-9.

MUNGRUE, I. N., BREDT, D. S., STEWART, D. J. & HUSAIN, M. 2003. From molecules to mammals: what's NOS got to do with it? *Acta Physiol Scand,* 179**,** 123-35.

MURPHY, R. C., BARKLEY, R. M., ZEMSKI BERRY, K., HANKIN, J., HARRISON, K., JOHNSON, C., KRANK, J., MCANOY, A., UHLSON, C. & ZARINI, S. 2005. Electrospray ionization and tandem mass spectrometry of eicosanoids. *Analytical Biochemistry,* 346**,** 1-42.

NIKOLAIDIS, M. G., KYPAROS, A. & VRABAS, I. S. 2011. F2-isoprostane formation, measurement and interpretation: The role of exercise. *Progress in Lipid Research,* 50**,** 89-103.

PARK, J. Y., PILLINGER, M. H. & ABRAMSON, S. B. 2006. Prostaglandin E2 synthesis and secretion: The role of PGE2 synthases. *Clinical Immunology,* 119**,** 229-240.

PASIKANTI, K. K., HO, P. C. & CHAN, E. C. 2008. Gas chromatography/mass spectrometry in metabolic profiling of biological fluids. *J Chromatogr B Analyt Technol Biomed Life Sci,* 871**,** 202-11.

PEDRO MENA 1EMAIL, L. C. E., CHIARA DALL'ASTA 3EMAIL, GIANNI GALAVERNA 3EMAIL, CRISTINA GARCÍA-VIGUERA 1, RENATO BRUNI 3EMAIL, ALAN CROZIER 4EMAIL AND DANIELE DEL RIO 2,* EMAIL 2012. Rapid and Comprehensive Evaluation of (Poly)phenolic Compounds in Pomegranate (Punica granatum L.) Juice by UHPLC-MSn

Molecules, 17**,** 14821-14840.

PRAKASH, C., ZHANG, J. Y., FALCK, J. R., CHAUHAN, K. & BLAIR, I. A. 1992. 20-Hydroxyeicosatetraenoic acid is excreted as a glucuronide conjugate in human urine. *Biochemical and Biophysical Research Communications,* 185**,** 728-733.

RABBANI, N. & THORNALLEY, P. J. 2008. Assay of 3-nitrotyrosine in tissues and body fluids by liquid chromatography with tandem mass spectrometric detection. *Methods Enzymol,* 440**,** 337-59.

RADABAUGH, M. R., NEMIROVSKIY, O. V., MISKO, T. P., AGGARWAL, P. & MATHEWS, W. R. 2008. Immunoaffinity liquid chromatography-tandem mass spectrometry detection of nitrotyrosine in biological fluids: Development of a clinically translatable biomarker. *Analytical Biochemistry,* 380**,** 68-76.

RAGO, B. & FU, C. 2013. Development of a high-throughput ultra performance liquid chromatography–mass spectrometry assay to profile 18 eicosanoids as exploratory biomarkers for atherosclerotic diseases. *Journal of Chromatography B,* 936**,** 25-32.

RIVERA, J., WARD, N., HODGSON, J., PUDDEY, I. B., FALCK, J. R. & CROFT, K. D. 2004. Measurement of 20-hydroxyeicosatetraenoic acid in human urine by gas chromatography-mass spectrometry. *Clin Chem,* 50**,** 224-6.

ROBERTS, L. J., II & MILNE, G. L. 2009. Isoprostanes. *J. Lipid Res.,* 50**,** S219-223.

ROBERTS, L. J. & MORROW, J. D. 2000. Measurement of F(2)-isoprostanes as an index of oxidative stress in vivo. *Free Radic Biol Med,* 28**,** 505-13.

ROKACH, J., KHANAPURE, S. P., HWANG, S. W., ADIYAMAN, M., LAWSON, J. A. & FITZGERALD, G. A. 1997a. The Isoprostanes: A Perspective. *Prostaglandins,* 54**,** 823-851.

ROKACH, J., KHANAPURE, S. P., HWANG, S. W., ADIYAMAN, M., LAWSON, J. A. & FITZGERALD, G. A. 1997b. Nomenclature of Isoprostanes: A Proposal. *Prostaglandins,* 54**,** 853-873.

ROUX, A., LISON, D., JUNOT, C. & HEILIER, J.-F. Applications of liquid chromatography coupled to mass spectrometry-based metabolomics in clinical chemistry and toxicology: A review. *Clinical Biochemistry,* In Press, Corrected Proof.

RYBERG, H. & CAIDAHL, K. 2007. Chromatographic and mass spectrometric methods for quantitative determination of 3-nitrotyrosine in biological samples and their application to human samples. *Journal of Chromatography B,* 851**,** 160-171.

SCHWEDHELM, E., BENNDORF, R. A., BOGER, R. H. & TSIKAS, D. 2007. Mass Spectrometric Analysis of F2-Isoprostanes: Markers and Mediators in Human Disease. *Current Pharmaceutical Analysis,* 3**,** 39-51.

SCHWEDHELM, E., TSIKAS, D., GUTZKI, F.-M. & FRÖLICH, J. C. 1999. Gas Chromatographic-Tandem Mass Spectrometric Quantification of Free 3-Nitrotyrosine in Human Plasma at the Basal State. *Analytical Biochemistry,* 276**,** 195-203.

SCORLETTI, E. & BYRNE, C. D. 2013. Omega-3 fatty acids, hepatic lipid metabolism, and nonalcoholic fatty liver disease. *Annu Rev Nutr,* 33**,** 231-48.

SHAIK, J. S. B., MILLER, T. M., GRAHAM, S. H., MANOLE, M. D. & POLOYAC, S. M. 2014. Rapid and simultaneous quantitation of prostanoids by UPLC–MS/MS in rat brain. *Journal of Chromatography B,* 945–946**,** 207-216.

SHIGENAGA, M. K., LEE, H. H., BLOUNT, B. C., CHRISTEN, S., SHIGENO, E. T., YIP, H. & AMES, B. N. 1997. Inflammation and NO(X)-induced nitration: assay for 3-nitrotyrosine by HPLC with electrochemical detection. *Proc Natl Acad Sci U S A,* 94**,** 3211-6.

SICILIA, T., MALLY, A., SCHAUER, U., PÄHLER, A. & VÖLKEL, W. 2008. LC-MS/MS methods for the detection of isoprostanes (iPF2[alpha]-III and 8,12-iso-iPF2[alpha]-VI) as biomarkers of CCl4-induced oxidative damage to hepatic tissue. *Journal of Chromatography B,* 861**,** 48-55.

SIRCAR, D. & SUBBAIAH, P. V. 2007. Isoprostane Measurement in Plasma and Urine by Liquid Chromatography-Mass Spectrometry with One-Step Sample Preparation. *Clin Chem,* 53**,** 251-258.

STAFFORINI, D. M., SHELLER, J. R., BLACKWELL, T. S., SAPIRSTEIN, A., YULL, F. E., MCINTYRE, T. M., BONVENTRE, J. V., PRESCOTT, S. M. & ROBERTS, L. J. 2006. Release of Free F2-isoprostanes from Esterified Phospholipids Is Catalyzed by Intracellular and Plasma Platelet-activating Factor Acetylhydrolases. *Journal of Biological Chemistry,* 281**,** 4616-4623.

STRASSBURG, K., HUIJBRECHTS, A. L., KORTEKAAS, K., LINDEMAN, J., PEDERSEN, T., DANE, A., BERGER, R., BRENKMAN, A., HANKEMEIER, T., DUYNHOVEN, J., KALKHOVEN, E., NEWMAN, J. & VREEKEN, R. 2012. Quantitative profiling of oxylipins through comprehensive LC-MS/MS analysis: application in cardiac surgery. *Analytical and Bioanalytical Chemistry,* 404**,** 1413-1426.

TAYLOR, A., BRUNO, R. & TRABER, M. 2008. Women and Smokers Have Elevated Urinary F₂-Isoprostane Metabolites: A Novel Extraction and LC–MS Methodology. *Lipids,* 43**,** 925-936.

TAYLOR, A. W., BRUNO, R. S., FREI, B. & TRABER, M. G. 2006. Benefits of prolonged gradient separation for high-performance liquid chromatography-tandem mass spectrometry quantitation of plasma total 15-series F2-isoprostanes. *Analytical Biochemistry,* 350**,** 41-51.

TAYLOR, A. W. & TRABER, M. G. 2010. Quantitation of plasma total 15-series F2-isoprostanes by sequential solid phase and liquid-liquid extraction. *Analytical Biochemistry,* 396**,** 319-321.

THEODOROU, V., SKOBRIDIS, K., TZAKOS, A. G. & RAGOUSSIS, V. 2007. A simple method for the alkaline hydrolysis of esters. *Tetrahedron Letters,* 48**,** 8230-8233.

TOURDOT, B. E., AHMED, I. & HOLINSTAT, M. 2014. The emerging role of oxylipins in thrombosis and diabetes. *Front Pharmacol,* 4**,** 176.

TRAPPE, T. A., STANDLEY, R. A., JEMIOLO, B., CARROLL, C. C. & TRAPPE, S. W. 2013. *Prostaglandin and myokine involvement in the cyclooxygenase-inhibiting drug enhancement of skeletal muscle adaptations to resistance exercise in older adults*.

TSIKAS, D. 2010a. Analytical methods for 3-nitrotyrosine quantification in biological samples: the unique role of tandem mass spectrometry. *Amino Acids*.

TSIKAS, D. 2010b. Measurement of nitrotyrosine in plasma by immunoassays is fraught with danger: commercial availability is no guarantee of analytical reliability. *Clinical Chemistry and Laboratory Medicine,* 48**,** 141-143.

TSIKAS, D. 2010c. Quantitative analysis of biomarkers, drugs and toxins in biological samples by immunoaffinity chromatography coupled to mass spectrometry or tandem mass spectrometry: A focused review of recent applications. *Journal of Chromatography B,* 878**,** 133-148.

TSIKAS, D., MITSCHKE, A., SUCHY, M.-T., GUTZKI, F.-M. & STICHTENOTH, D. O. 2005. Determination of 3-nitrotyrosine in human urine at the basal state by gas chromatography-tandem mass spectrometry and evaluation of the excretion after oral intake. *Journal of Chromatography B,* 827**,** 146-156.

TSIKAS, D., SCHWEDHELM, E., STUTZER, F. K., GUTZKI, F.-M., RODE, I., MEHLS, C. & FRÖLICH, J. C. 2003. Accurate quantification of basal plasma levels of 3-nitrotyrosine and 3-nitrotyrosinoalbumin by gas chromatography-tandem mass spectrometry. *Journal of Chromatography B,* 784**,** 77-90.

TSIKAS, D. & ZOERNER, A. A. 2014. Analysis of eicosanoids by LC-MS/MS and GC-MS/MS: A historical retrospect and a discussion. *Journal of Chromatography B,* 964**,** 79-88.

VAYA, J. 2008. Novel designed probes for the characterization of oxidative stress in biological fluids, cells, and tissues. *Methods Mol Biol,* 477**,** 3-13.

WANG, X., XIE, Y., HU, X., LI, Y., HU, P., WANG, Y., LIANG, Q. & LUO, G. 2013. Qualitative and quantitative analysis of glucosinolates and nucleosides in Radix Isatidis by HPLC and liquid chromatography tandem mass spectrometry. *Acta Pharmaceutica Sinica B,* 3**,** 337-344.

WEIßENBACHER, B. 2013. *Selection of a solid phase extraction procedure for the measurement of oxidative stress pa-rameters in assisted reproduction technology (ART).* Master, FH JOANNEUM.

WINNIK, W. M. & KITCHIN, K. T. 2008. Measurement of oxidative stress parameters using liquid chromatography-tandem mass spectroscopy (LC-MS/MS). *Toxicology and Applied Pharmacology,* 233**,** 100-106.

WOO, H. M., KIM, K. M., CHOI, M. H., JUNG, B. H., LEE, J., KONG, G., NAM, S. J., KIM, S., BAI, S. W. & CHUNG, B. C. 2009. Mass spectrometry based metabolomic approaches in urinary biomarker study of women's cancers. *Clinica Chimica Acta,* 400**,** 63-69.

YAN, Z., MAS, E., MORI, T. A., CROFT, K. D. & BARDEN, A. E. 2010. A significant proportion of F2-isoprostanes in human urine are excreted as glucuronide conjugates. *Analytical Biochemistry,* 403**,** 126-128.

YIN, H., PORTER, N. A. & MORROW, J. D. 2005. Separation and identification of F2-isoprostane regioisomers and diastereomers by novel liquid chromatographic/mass spectrometric methods. *Journal of Chromatography B,* 827**,** 157-164.

Appendix

Table 5-1 reagents of the validation of 8-iso-PGF2a in human plasma

Reagent	Brand	Art. #
Methanol LC-MS grade	VWR	83638.320
Water LC-MS grade	VWR	83645.320
Sodium hydroxide	Roth	6771.1
2 N hydrochloric acid	Merck	1.09063.1000
Formic acid	Fluka	06440
8-iso Prostaglandin F2α Quant-PAK	Cayman chemical	10007652

Table 5-2 instruments of the validation of 8-iso-PGF2a in human plasma

Instrument	Brand	Type
Centrifuge	Heraeus Sepatech	Megafuge 1.0
Vortex	Heidolph	
Rotary shaker	Heidolph	Reax 2000
Pipette	Eppendorf	1-10 mL
Stepper	Eppendorf	100µL
Pipette	Eppendorf	10-100 µL
Dispenser	VWR	Volupette 0-30 mL

Table 5-3 reagents of the validation of 8-OHdG in urine

Reagent	Brand	Art. #
Methanol LC-MS grade	VWR	83638.320
Water LC-MS grade	VWR	83645.320
Formic acid	Fluka	06440
8-hydroxy-2'-deoxyguanosine	Sigma	H5653-1MG
8-mercaptoguanosine	Sigma	M7772-250MG

Table 5-4 instruments of the validation of 8-OHdG in urine

Instrument	Brand	Type
Vortex	Heidolph	
Rotary shaker	Heidolph	Reax 2000
Pipette	Eppendorf	1-10 mL
Stepper	Eppendorf	100µL
Pipette	Eppendorf	10-100 µL
Dispenser	VWR	Volupette 0-30 mL

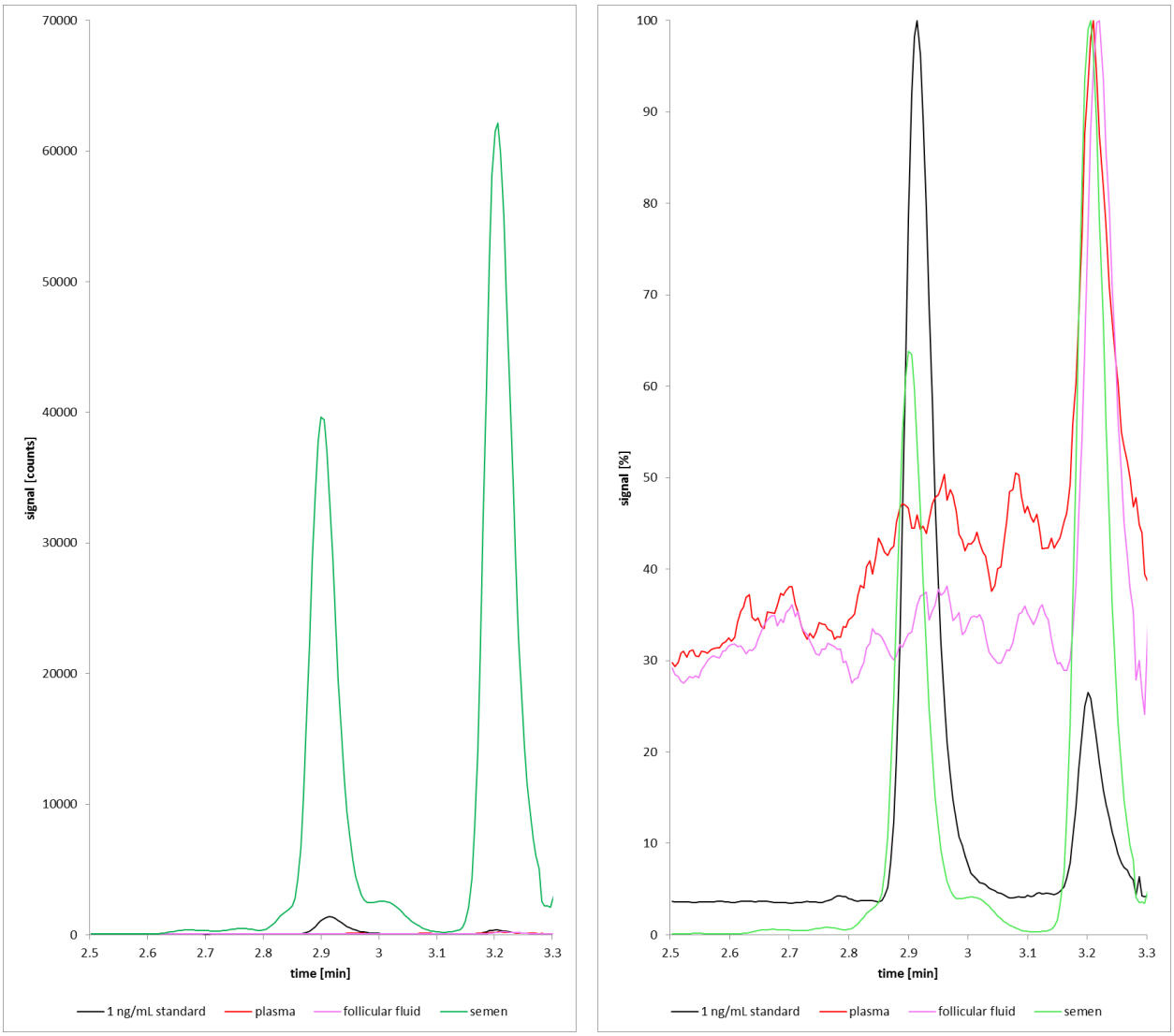

Figure 5-1 2,3-dinor-8-iso-PGF$_{2\alpha}$ measured in 1 ng/mL standard, plasma, follicular fluid and semen plasma

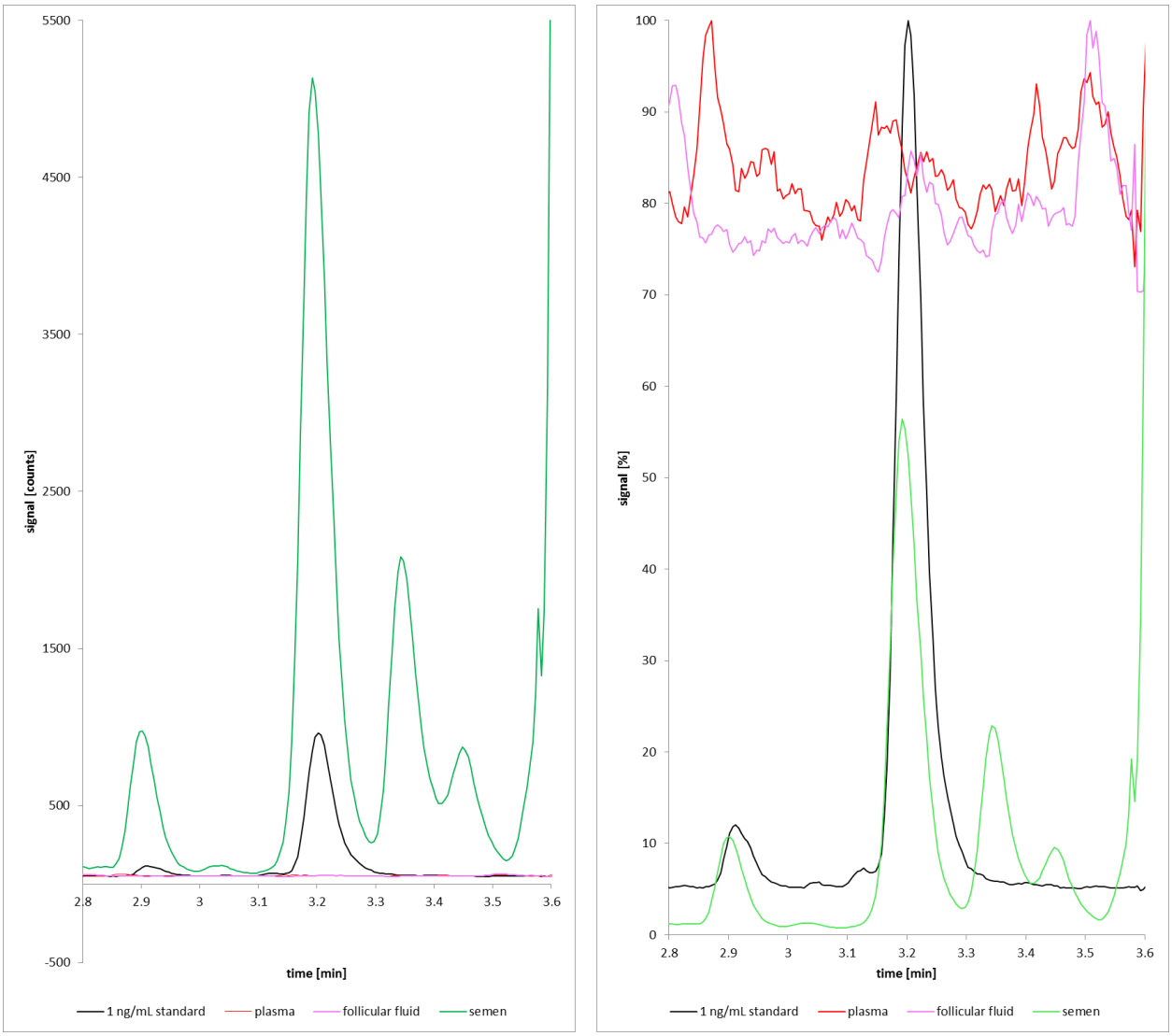

Figure 5-2 2,3-dinor-11-beta-PGF$_{2\alpha}$ measured in 1 ng/mL standard, plasma, follicular fluid and semen plasma

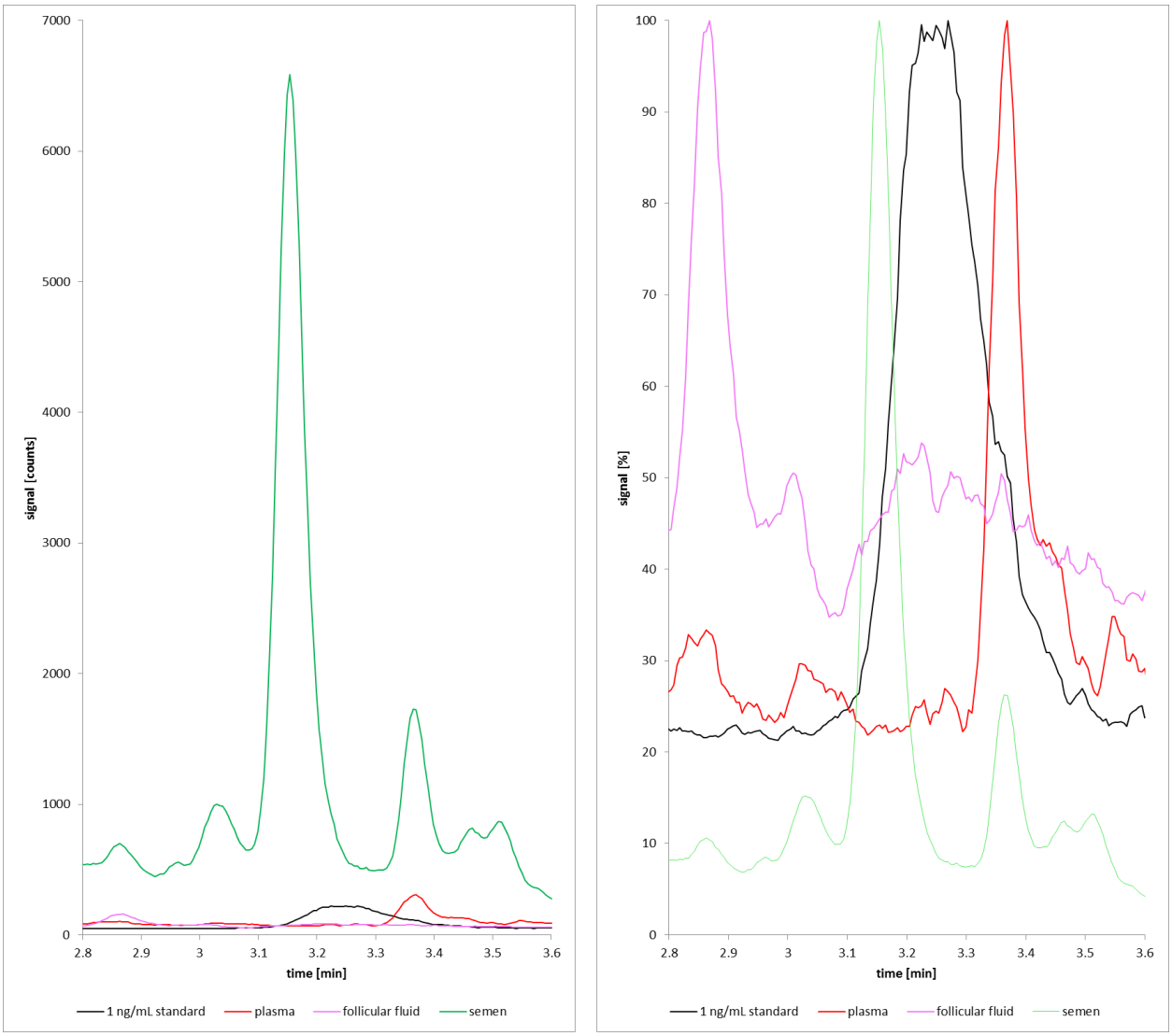

Figure 5-3 6-keto-PGF$_{1\alpha}$ measured in 1 ng/mL standard, plasma, follicular fluid and semen plasma

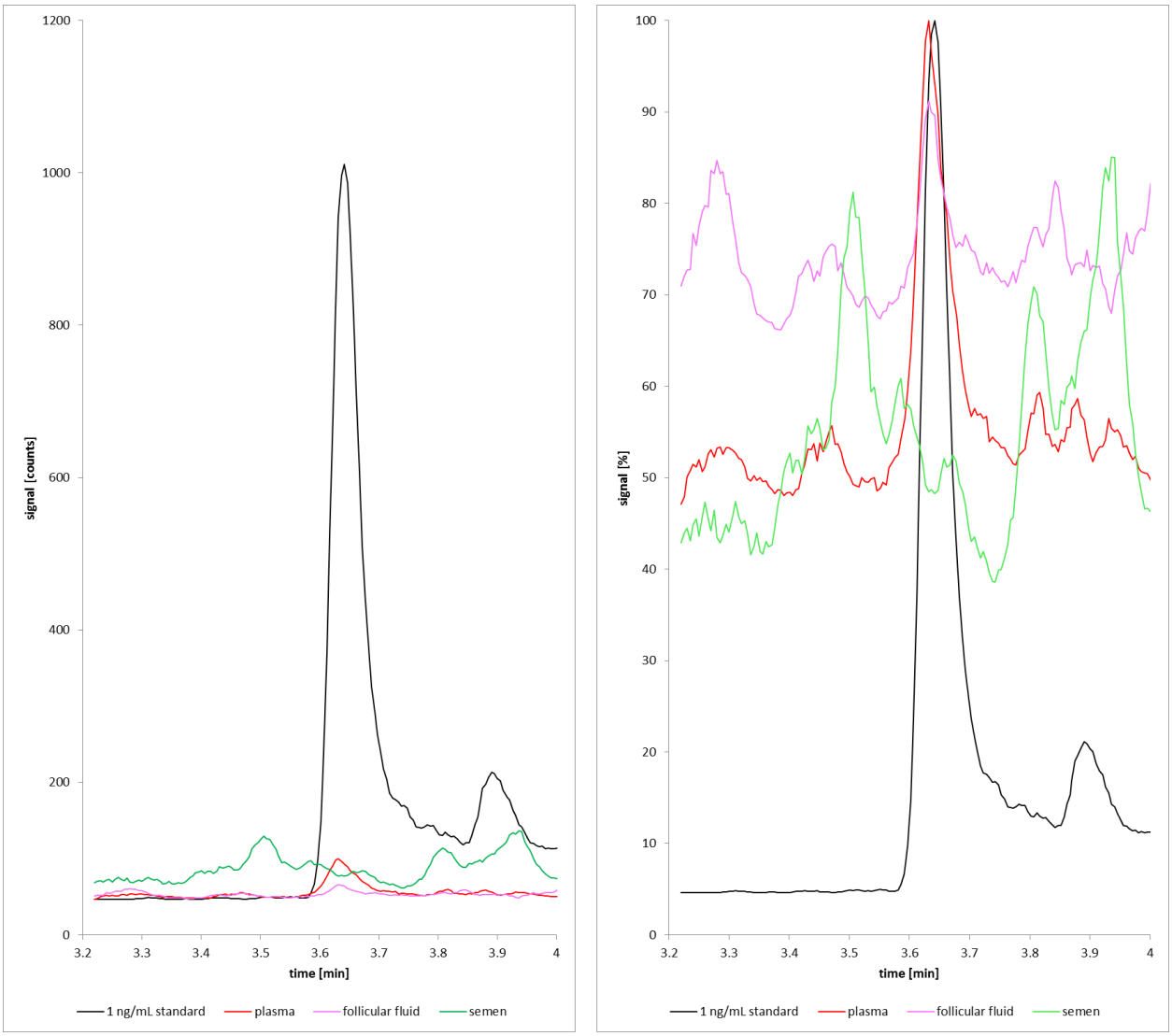

Figure 5-4 Thromboxane B_3 measured in 1 ng/mL standard, plasma, follicular fluid and semen plasma

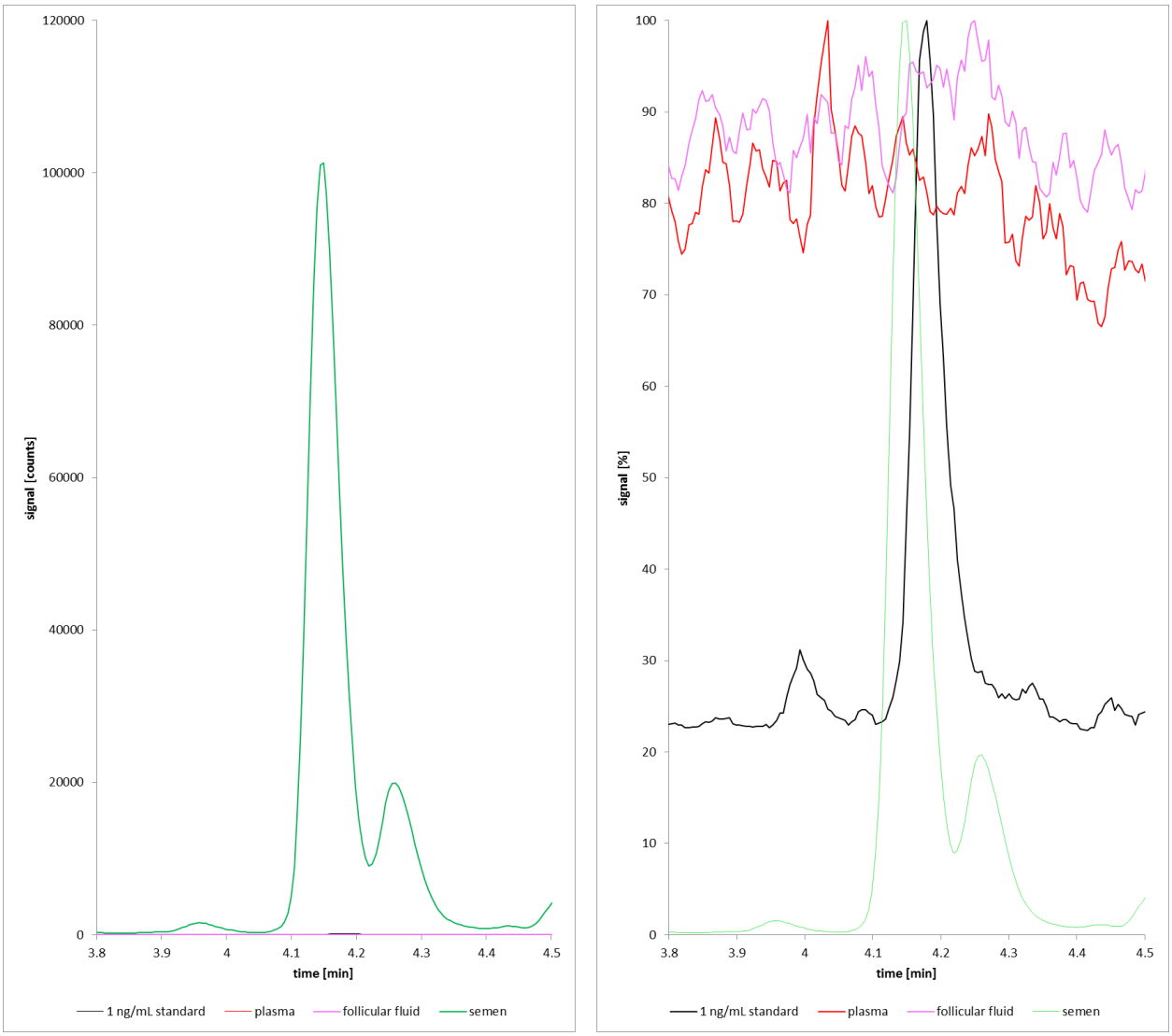

Figure 5-5 Prostaglandin $F_{3\alpha}$ measured in 1 ng/mL standard, plasma, follicular fluid and semen plasma

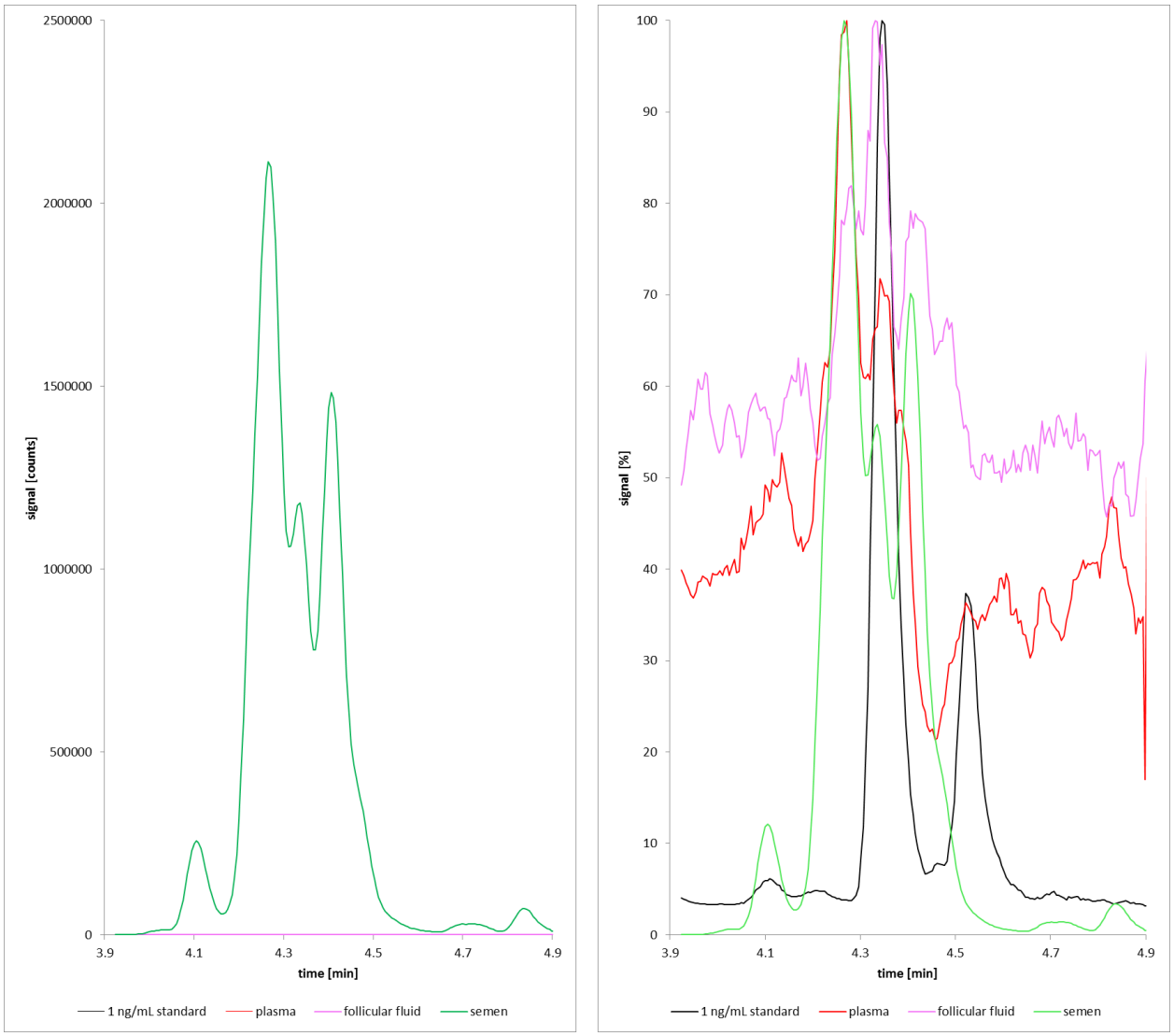

Figure 5-6 Prostaglandins E_3 and D_3 (elution order) measured in 1 ng/mL standard, plasma, follicular fluid and semen plasma

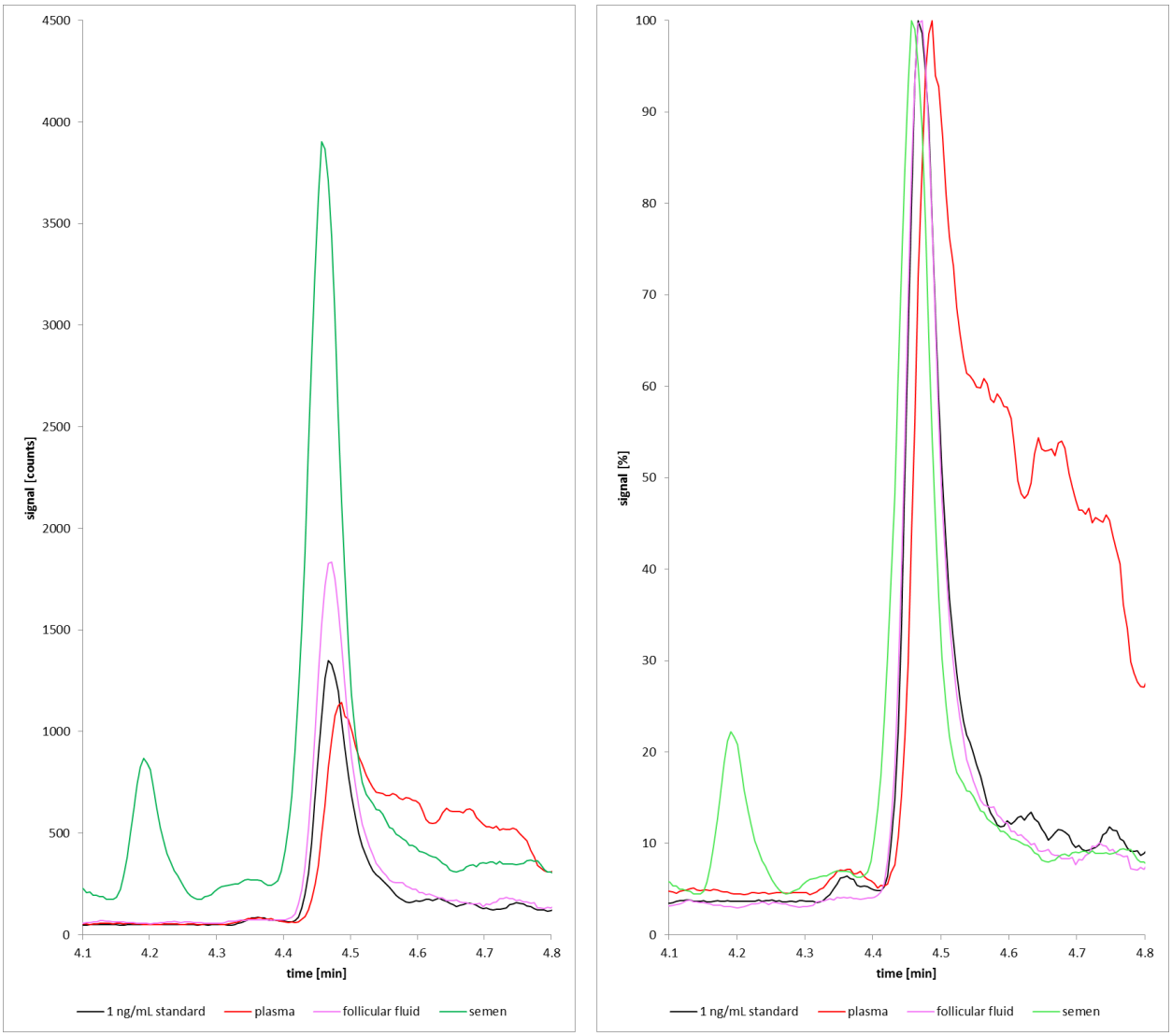

Figure 5-7 Thromboxane B_2 measured in 1 ng/mL standard, plasma, follicular fluid and semen plasma

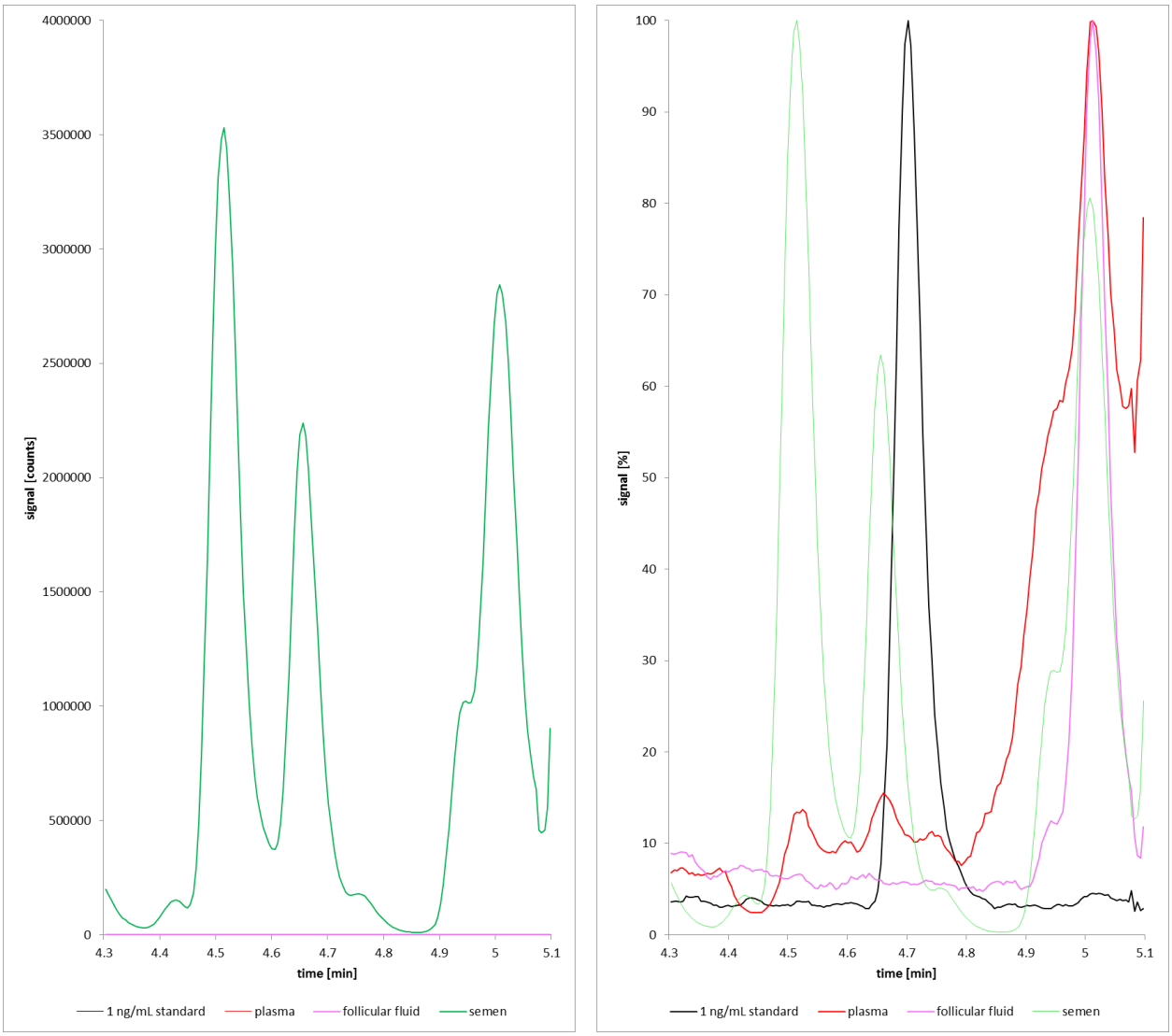

Figure 5-8 8-iso-15-keto-PGF$_{2\alpha}$ measured in 1 ng/mL standard, plasma, follicular fluid and semen plasma

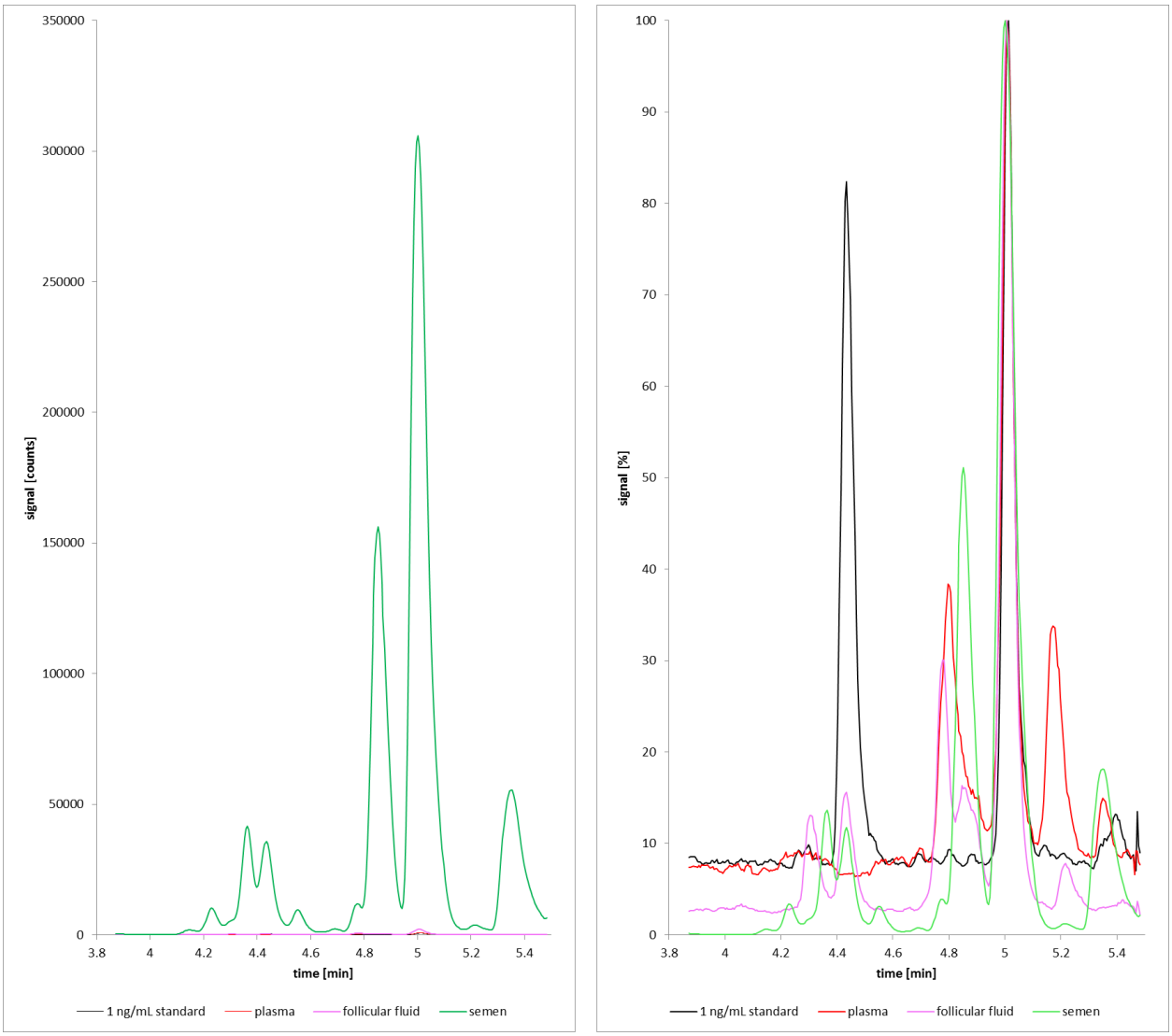

Figure 5-9 8-iso-PGF$_{2\alpha}$ and PGF$_{2\alpha}$ measured in 1 ng/mL standard, plasma, follicular fluid and semen plasma

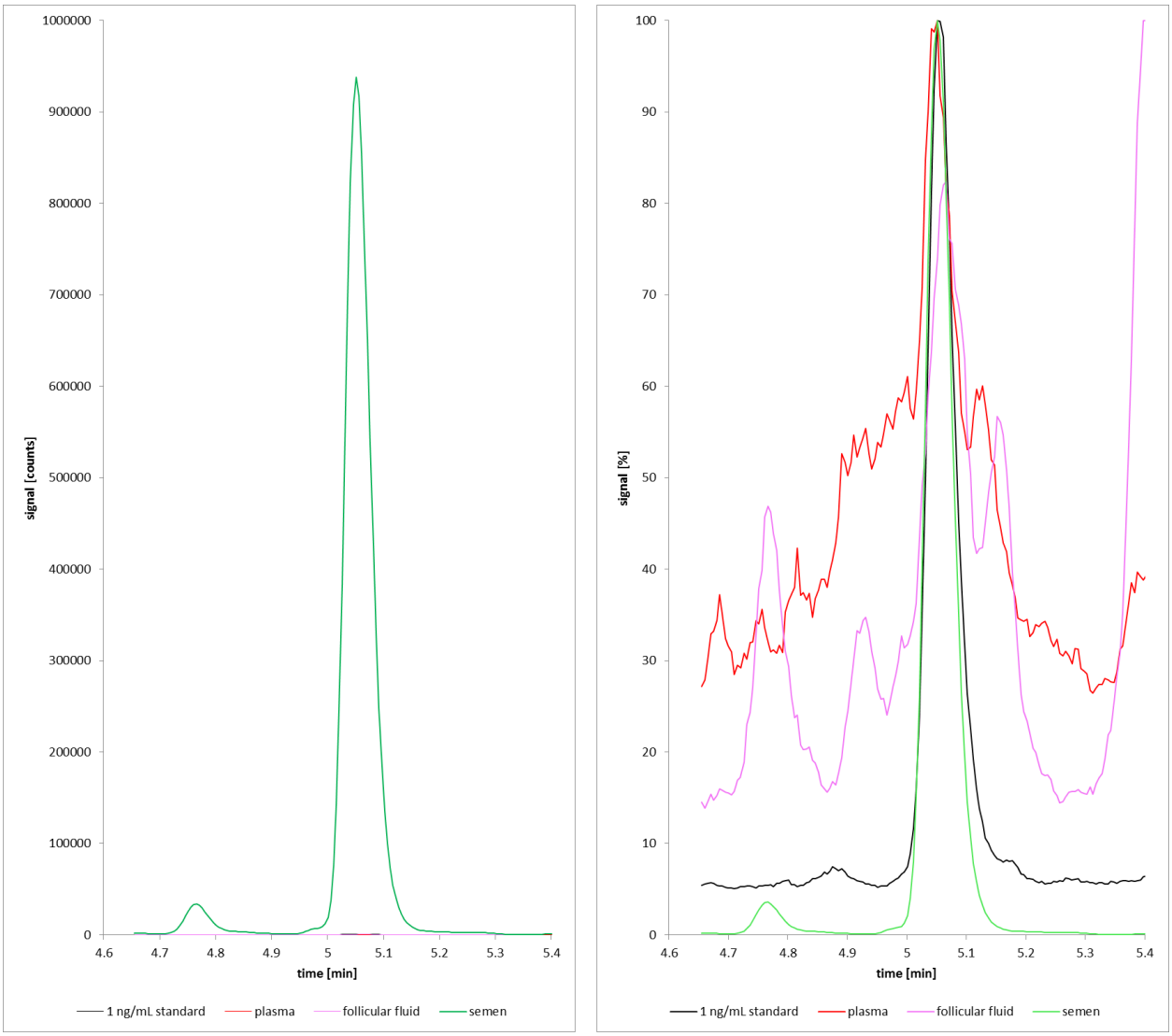

Figure 5-10 $PGF_{1\alpha}$ measured in 1 ng/mL standard, plasma, follicular fluid and semen plasma

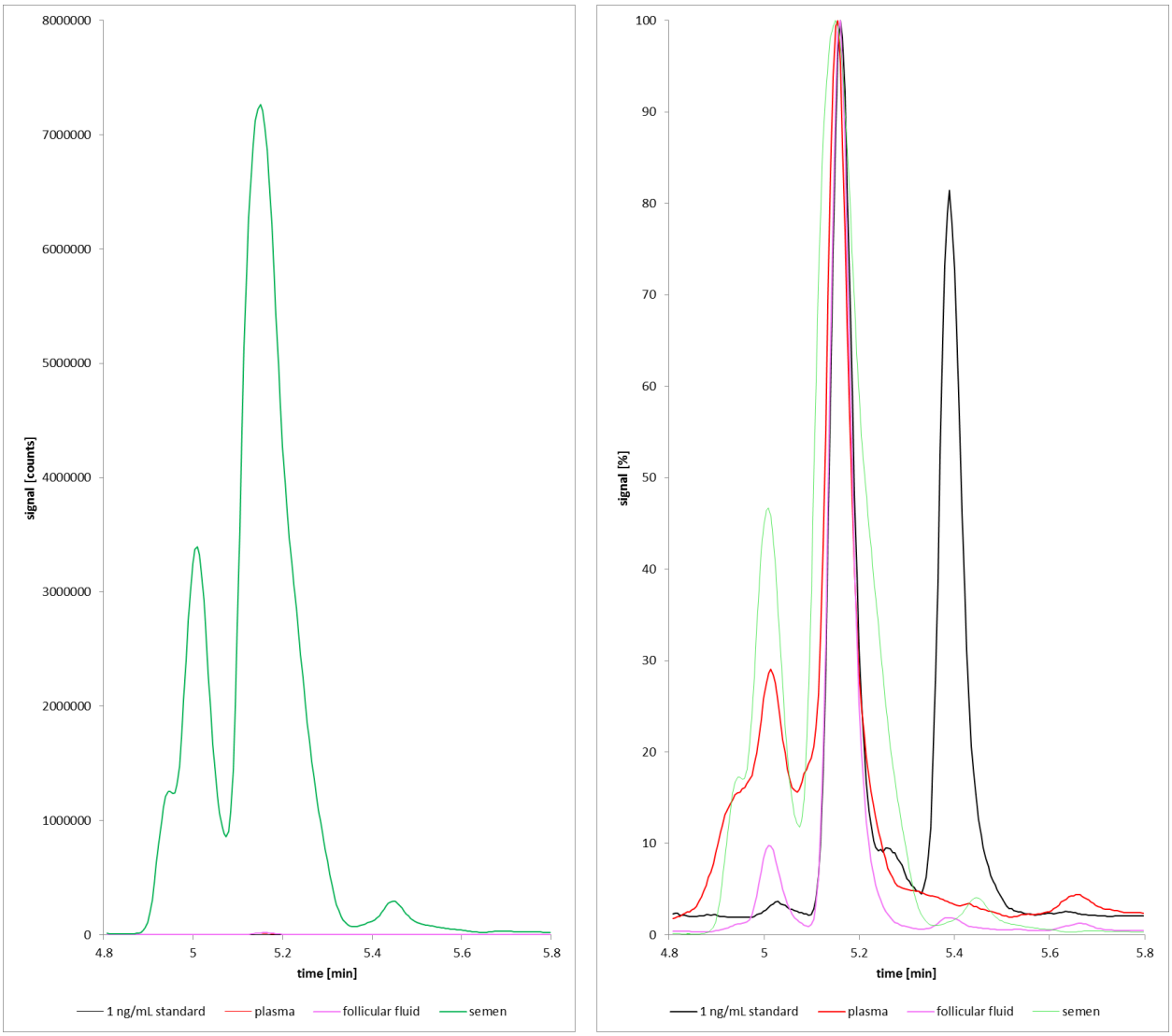

Figure 5-11 PGE_2 and PGD_2 measured in 1 ng/mL standard, plasma, follicular fluid and semen plasma

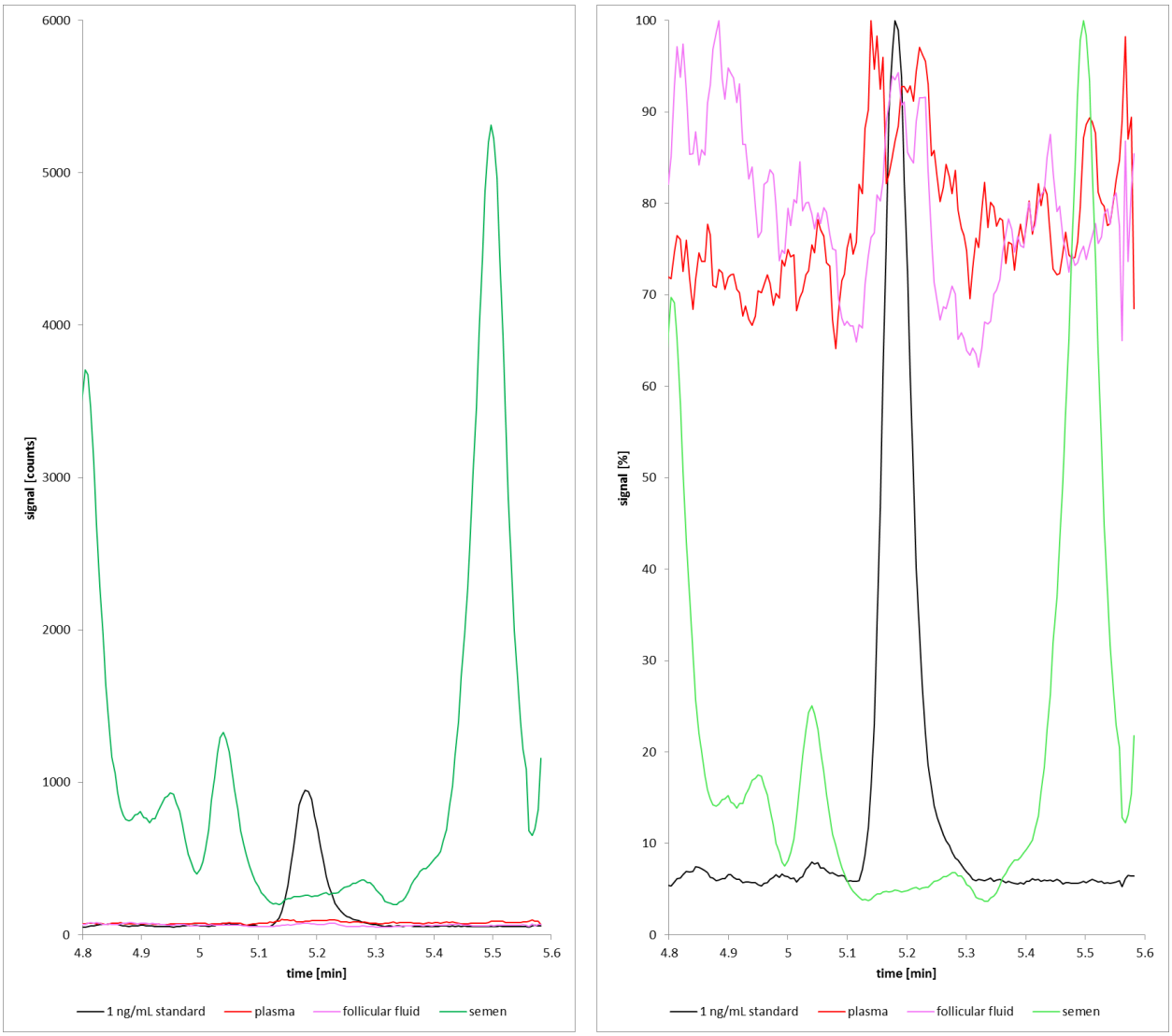

Figure 5-12 11-dehydro-TXB$_2$ measured in 1 ng/mL standard, plasma, follicular fluid and semen plasma

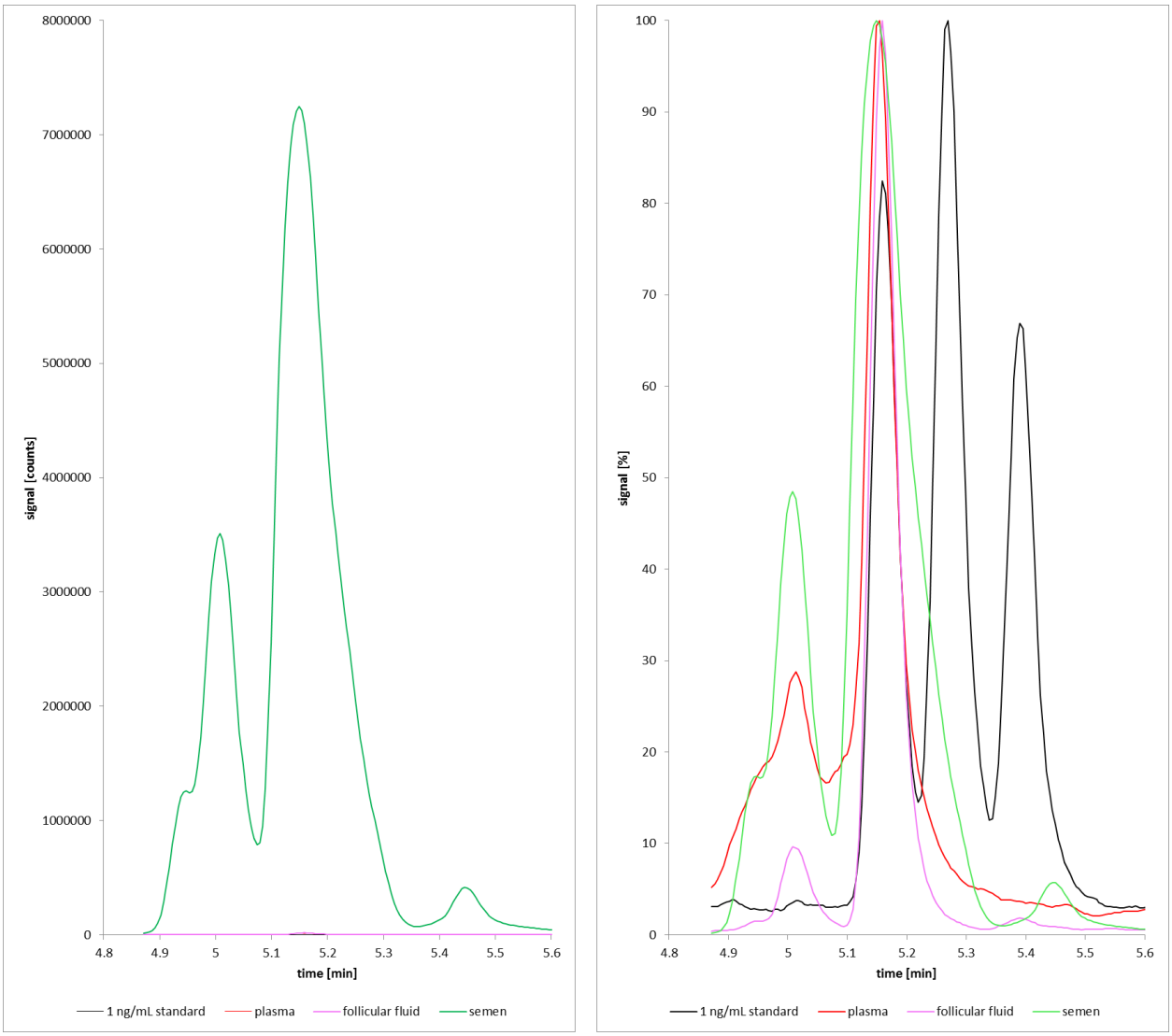

Figure 5-13 15-keto- $PGF_{2\alpha}$ dehydro-TXB_2 measured in 1 ng/mL standard, plasma, follicular fluid and semen plasma

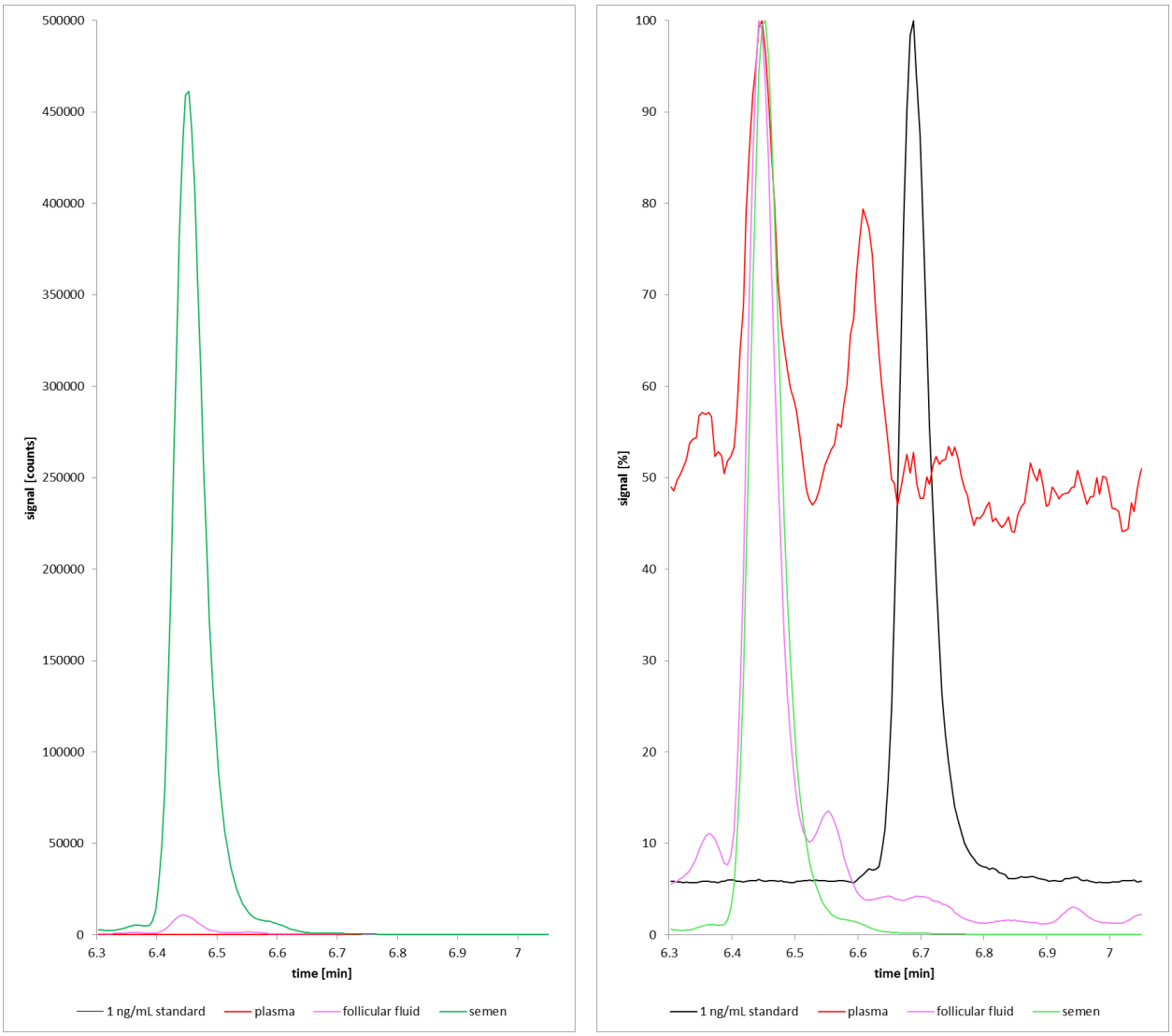

Figure 5-1416,16-dimethyl- $PGF_{2\alpha}$ measured in 1 ng/mL standard, plasma, follicular fluid and semen plasma

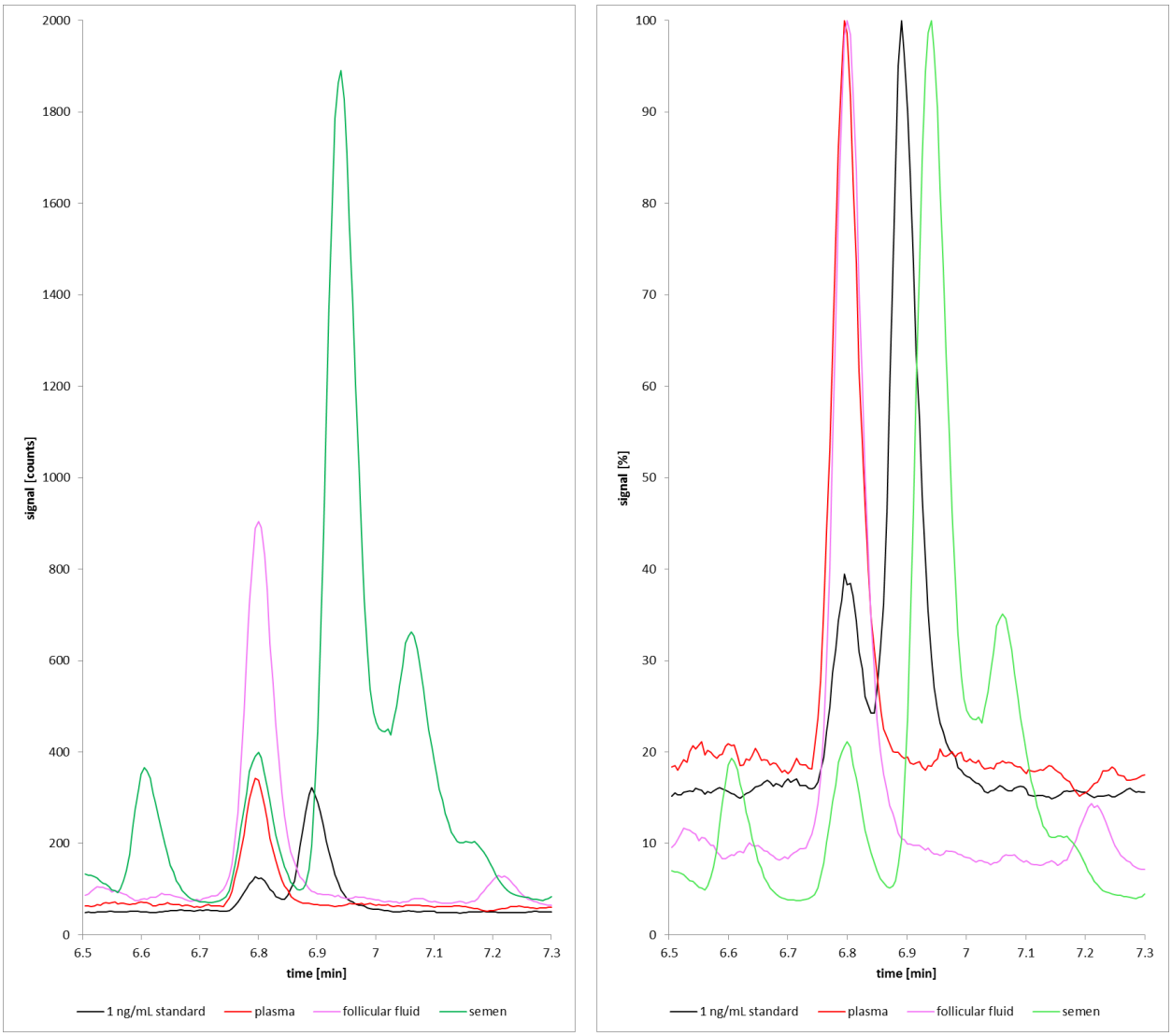

Figure 5-15 11-deoxy-PGF$_{2\alpha}$ measured in 1 ng/mL standard, plasma, follicular fluid and semen plasma

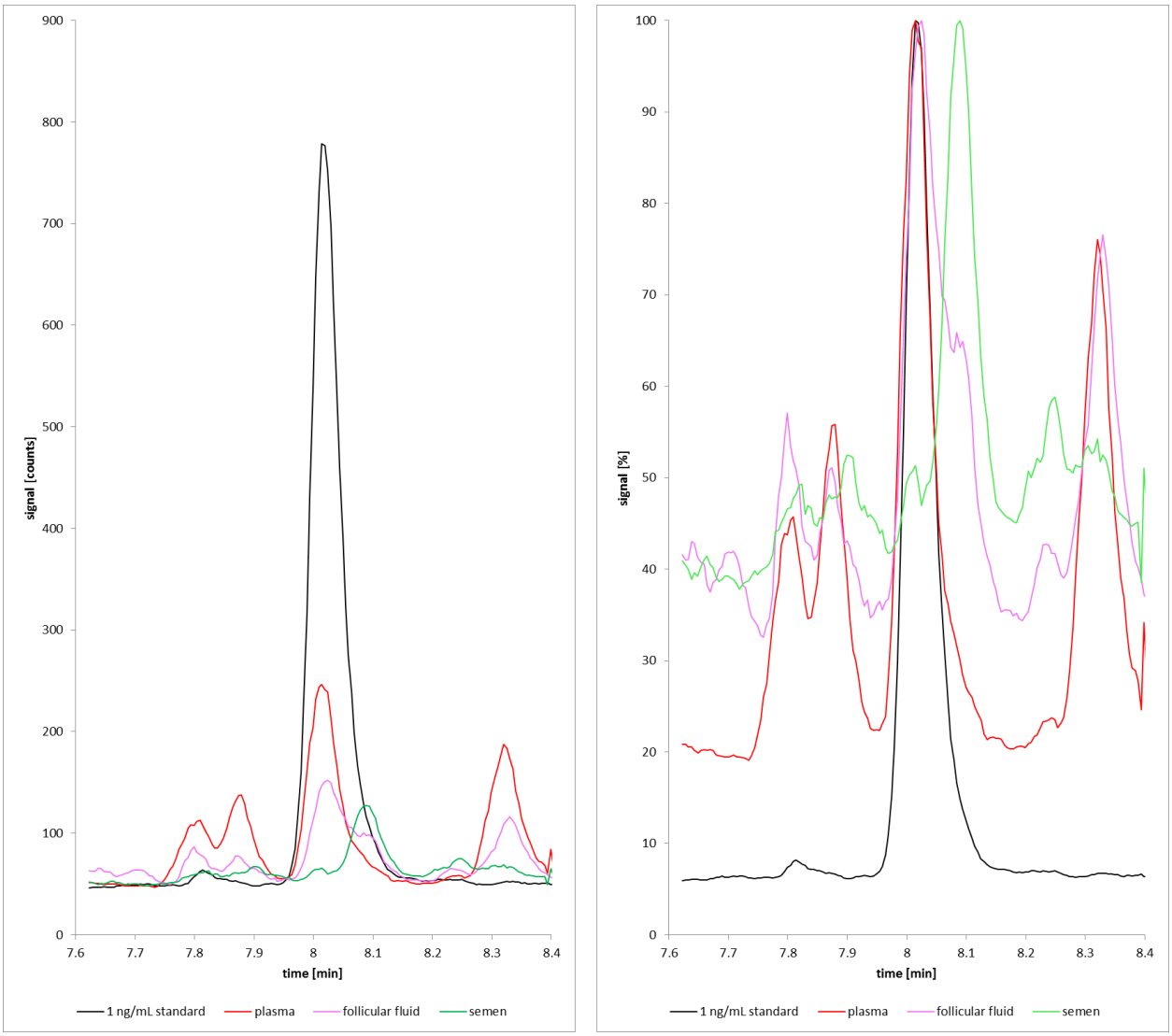

Figure 5-16 LTB_4 measured in 1 ng/mL standard, plasma, follicular fluid and semen plasma

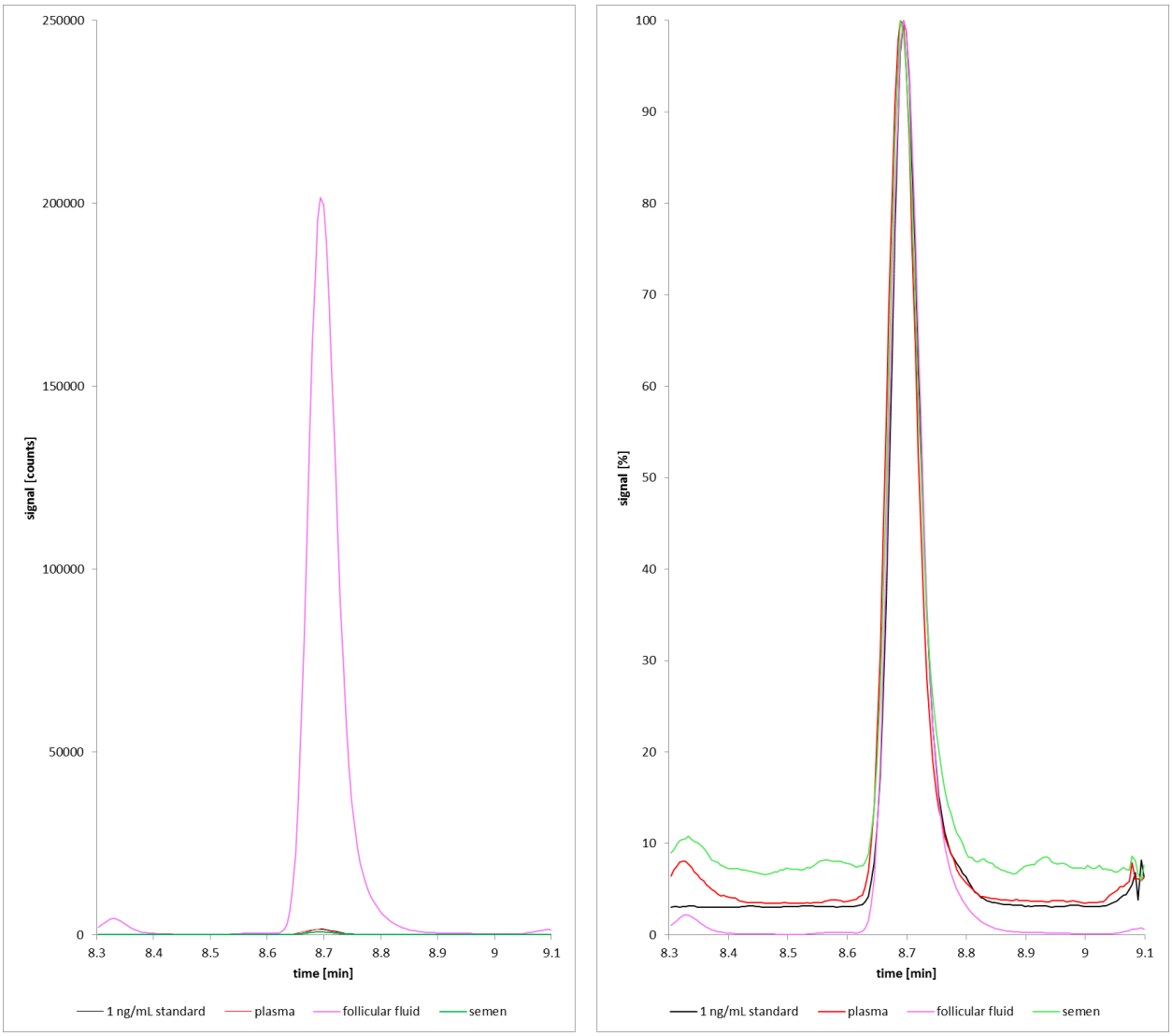

Figure 5-17 14,15-DHET measured in 1 ng/mL standard, plasma, follicular fluid and semen plasma

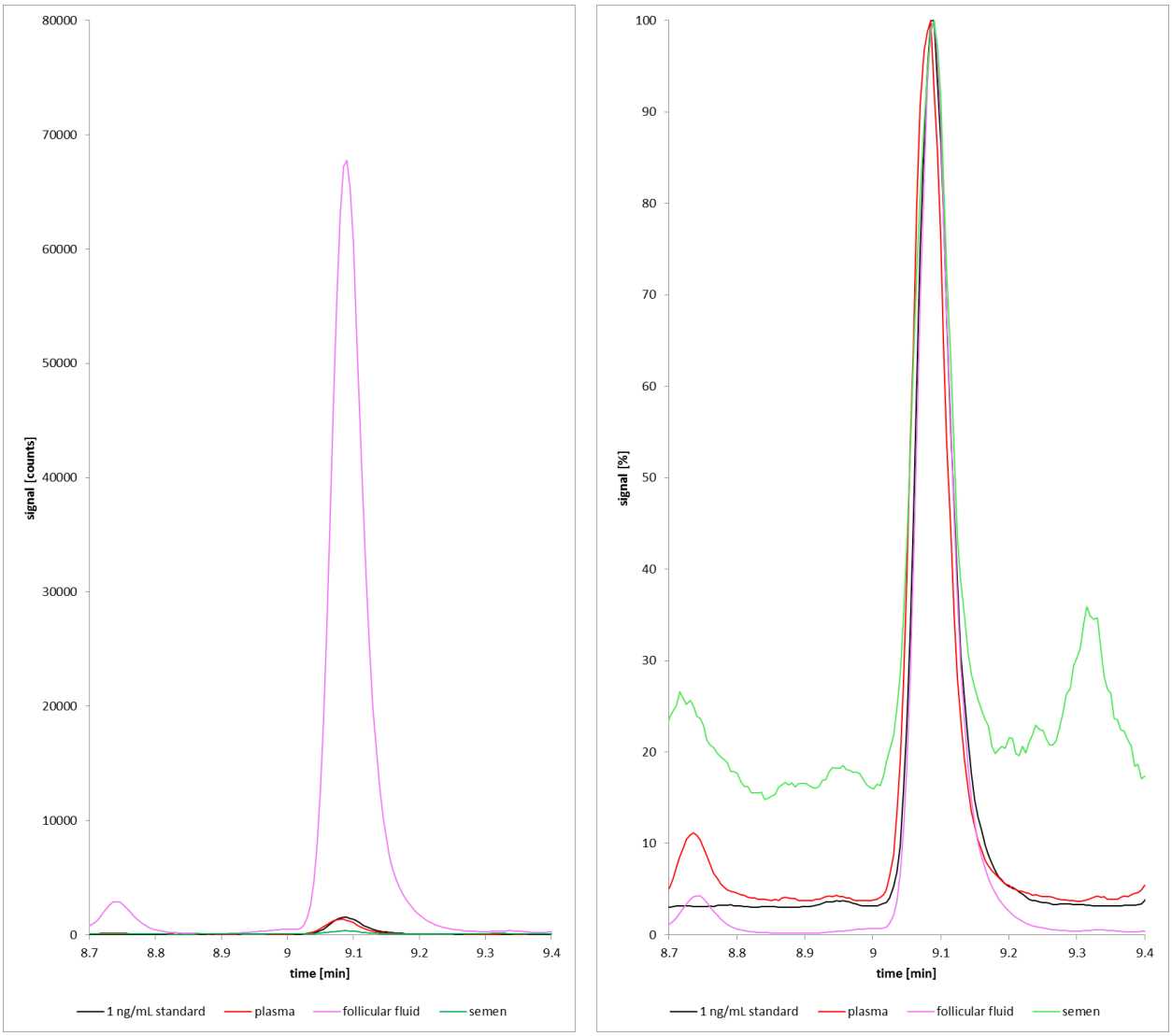

Figure 5-18 11,12-DHET measured in 1 ng/mL standard, plasma, follicular fluid and semen plasma

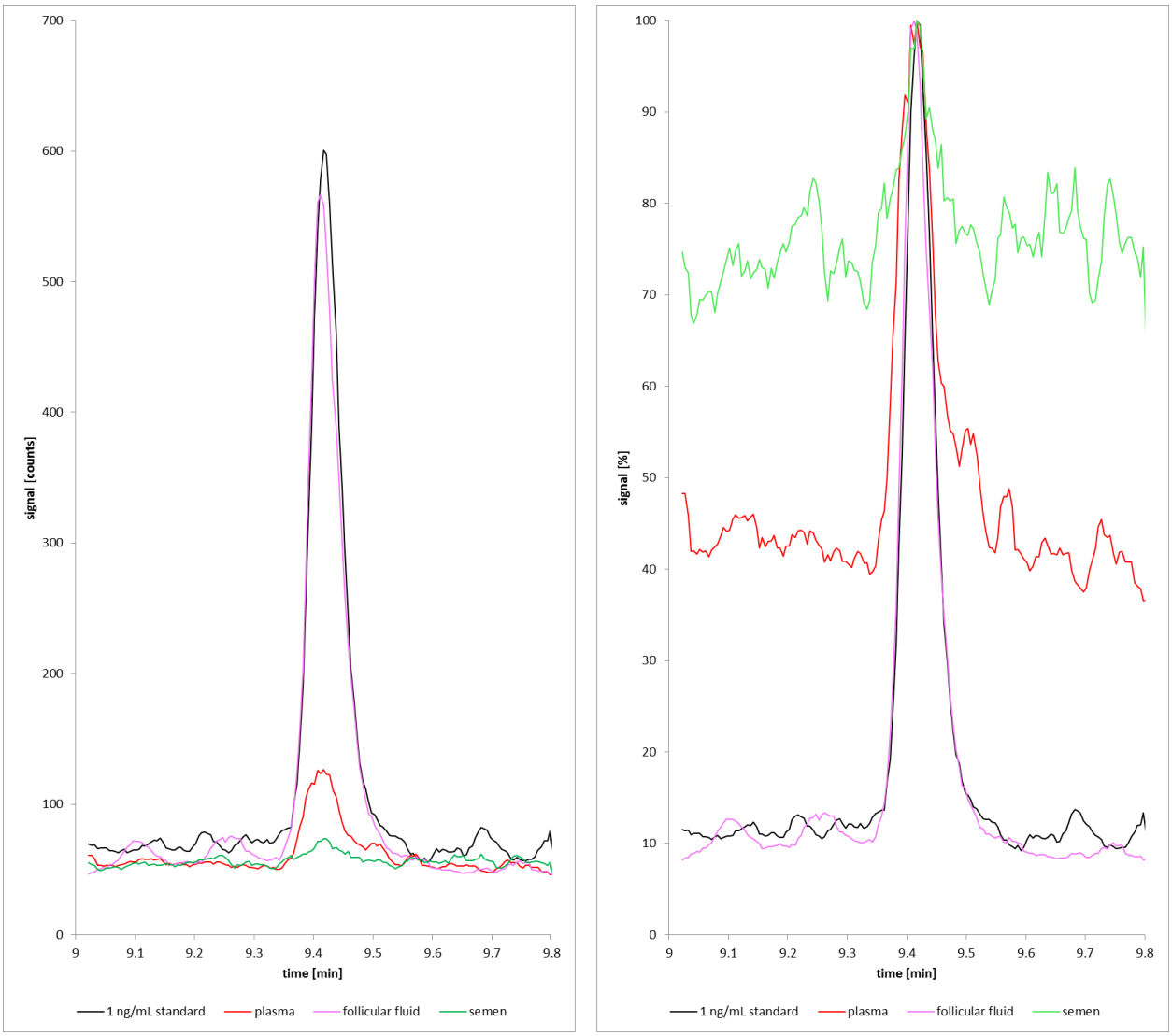

Figure 5-19 18-HEPE measured in 1 ng/mL standard, plasma, follicular fluid and semen plasma

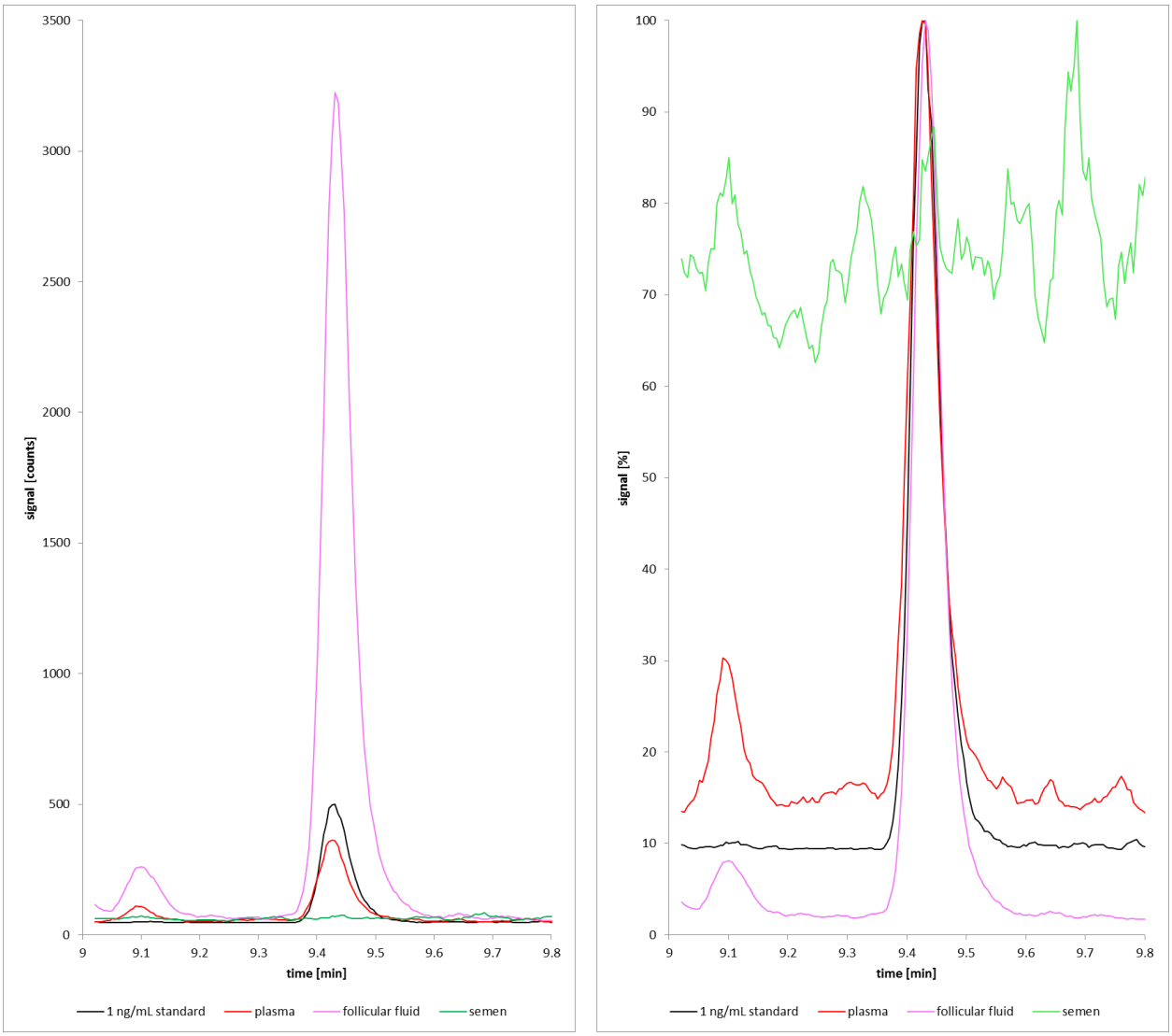

Figure 5-20 8,9-DHET measured in 1 ng/mL standard, plasma, follicular fluid and semen plasma

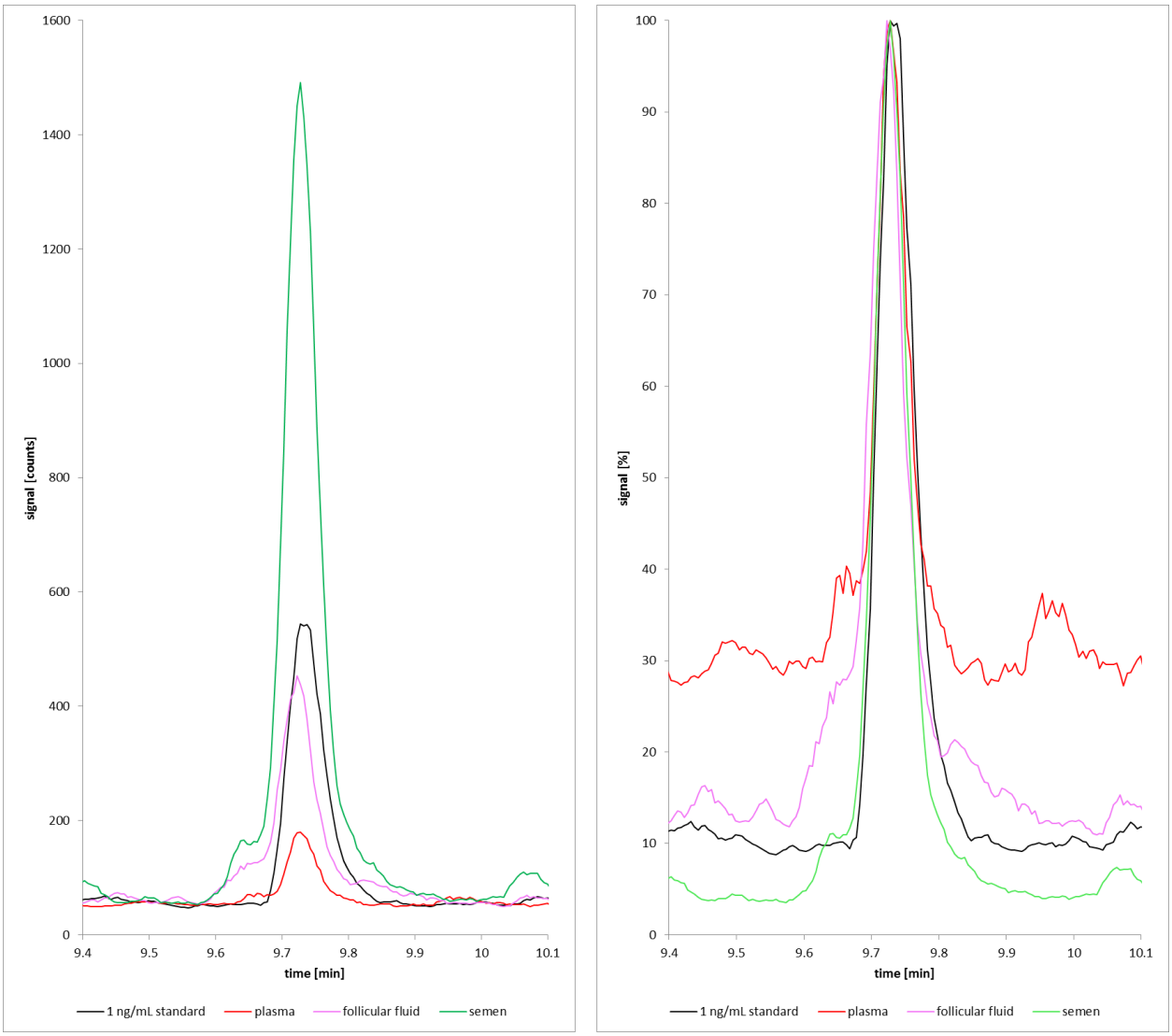

Figure 5-21 15-HEPE measured in 1 ng/mL standard, plasma, follicular fluid and semen plasma

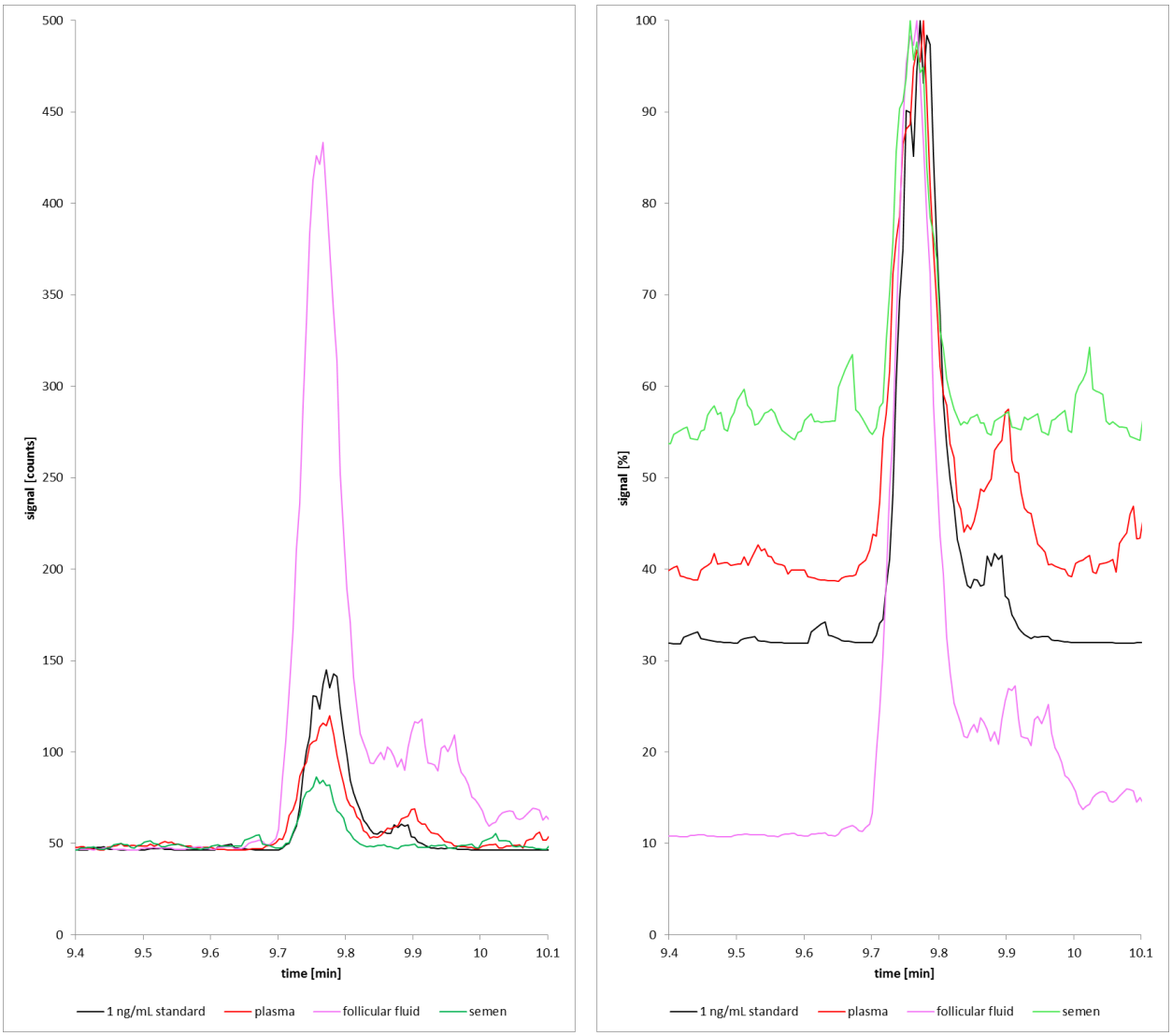

Figure 5-22 20-HETE measured in 1 ng/mL standard, plasma, follicular fluid and semen plasma

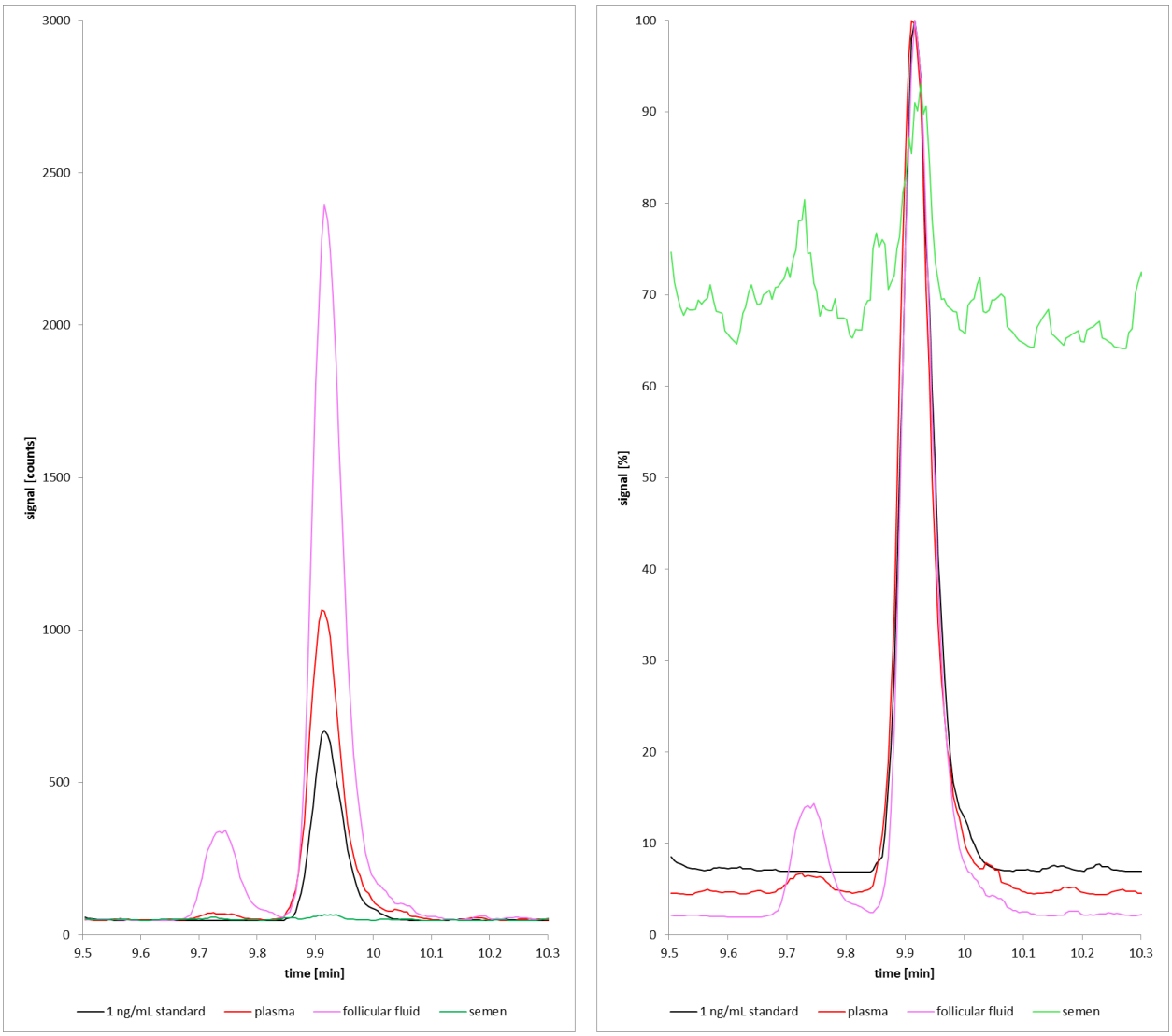

Figure 5-23 5,6-DHET measured in 1 ng/mL standard, plasma, follicular fluid and semen plasma

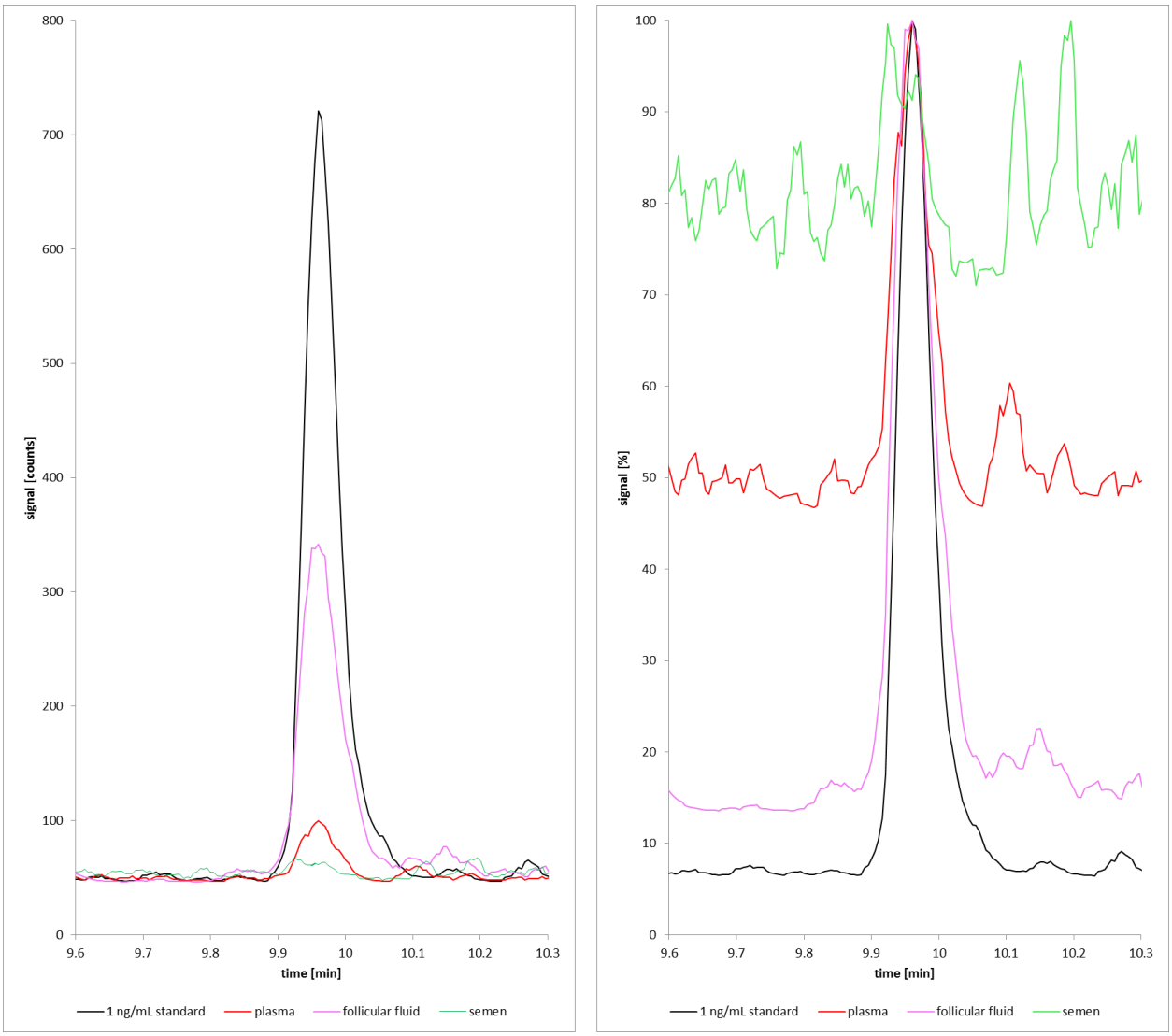

Figure 5-24 8-HEPE measured in 1 ng/mL standard, plasma, follicular fluid and semen plasma

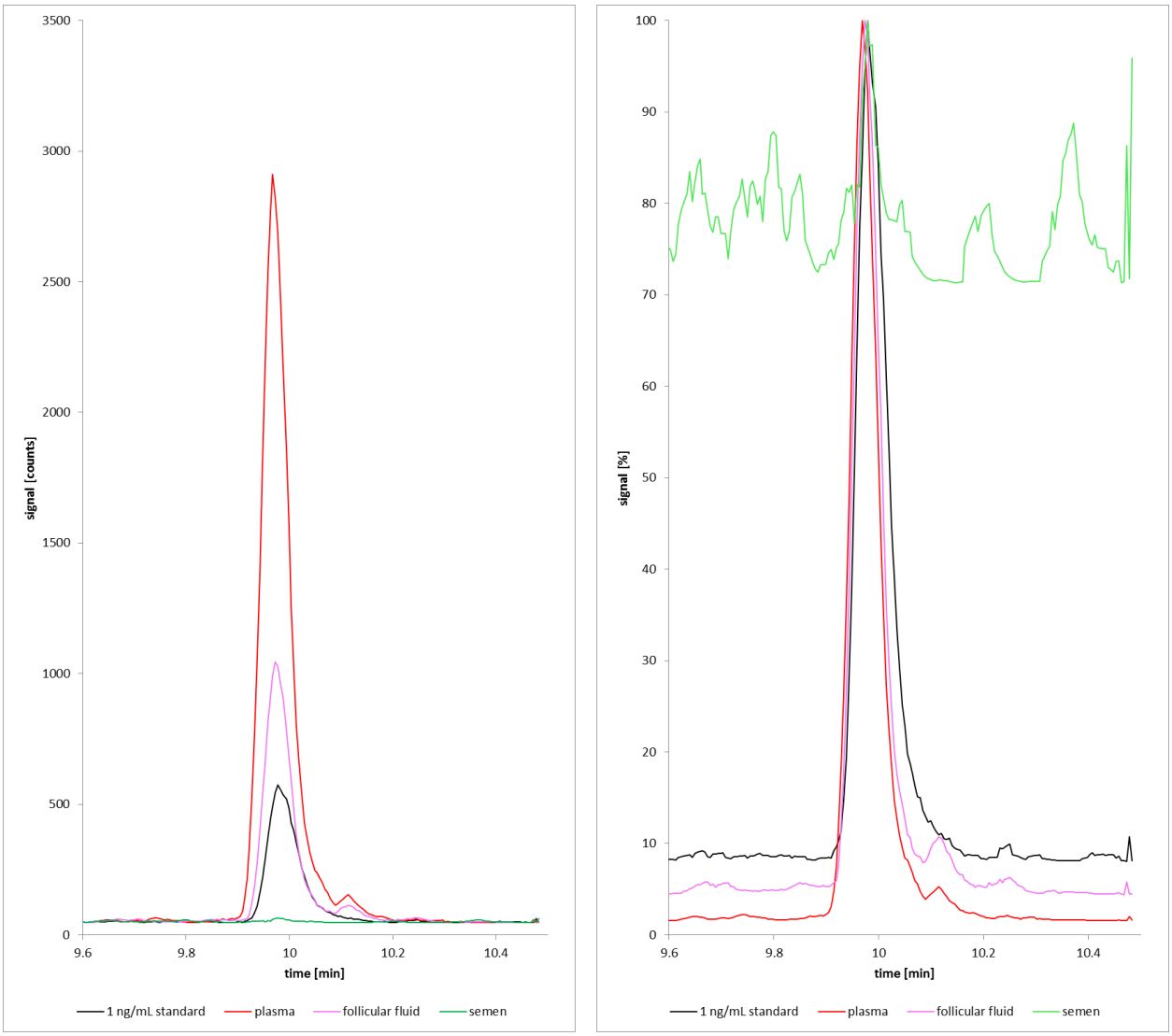

Figure 5-25 12-HEPE measured in 1 ng/mL standard, plasma, follicular fluid and semen plasma

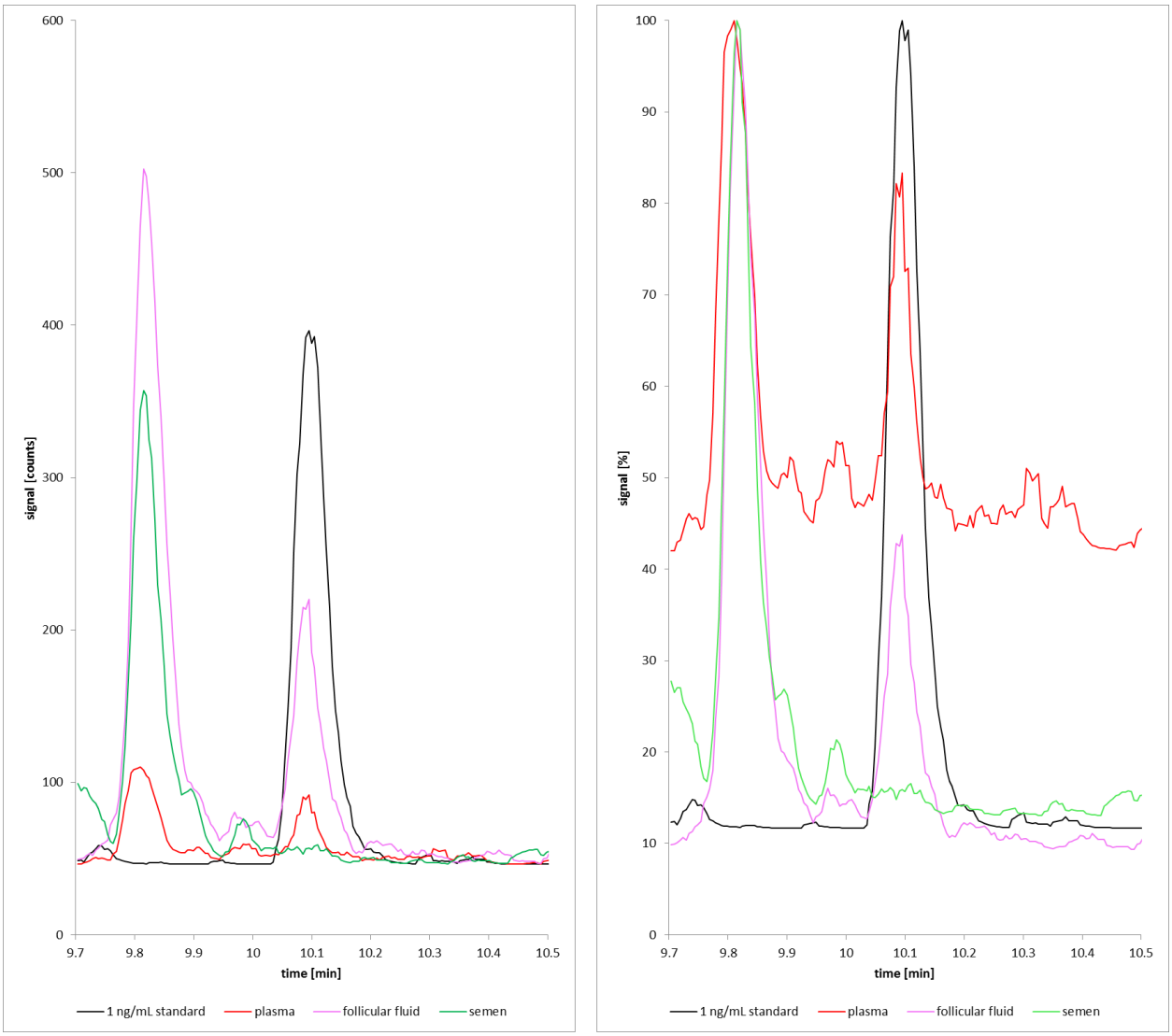

Figure 5-26 9-HEPE measured in 1 ng/mL standard, plasma, follicular fluid and semen plasma

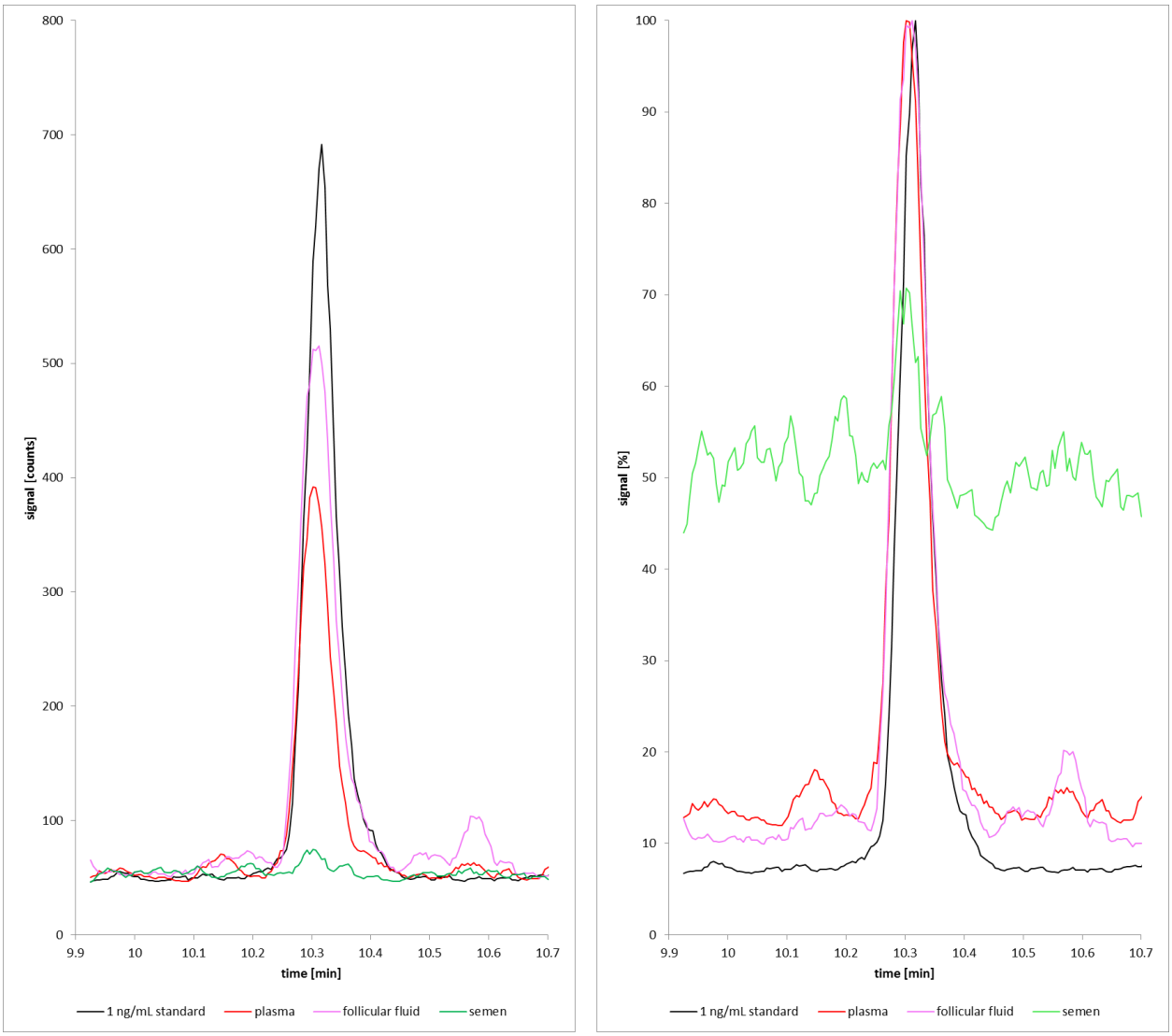

Figure 5-27 5-HEPE measured in 1 ng/mL standard, plasma, follicular fluid and semen plasma

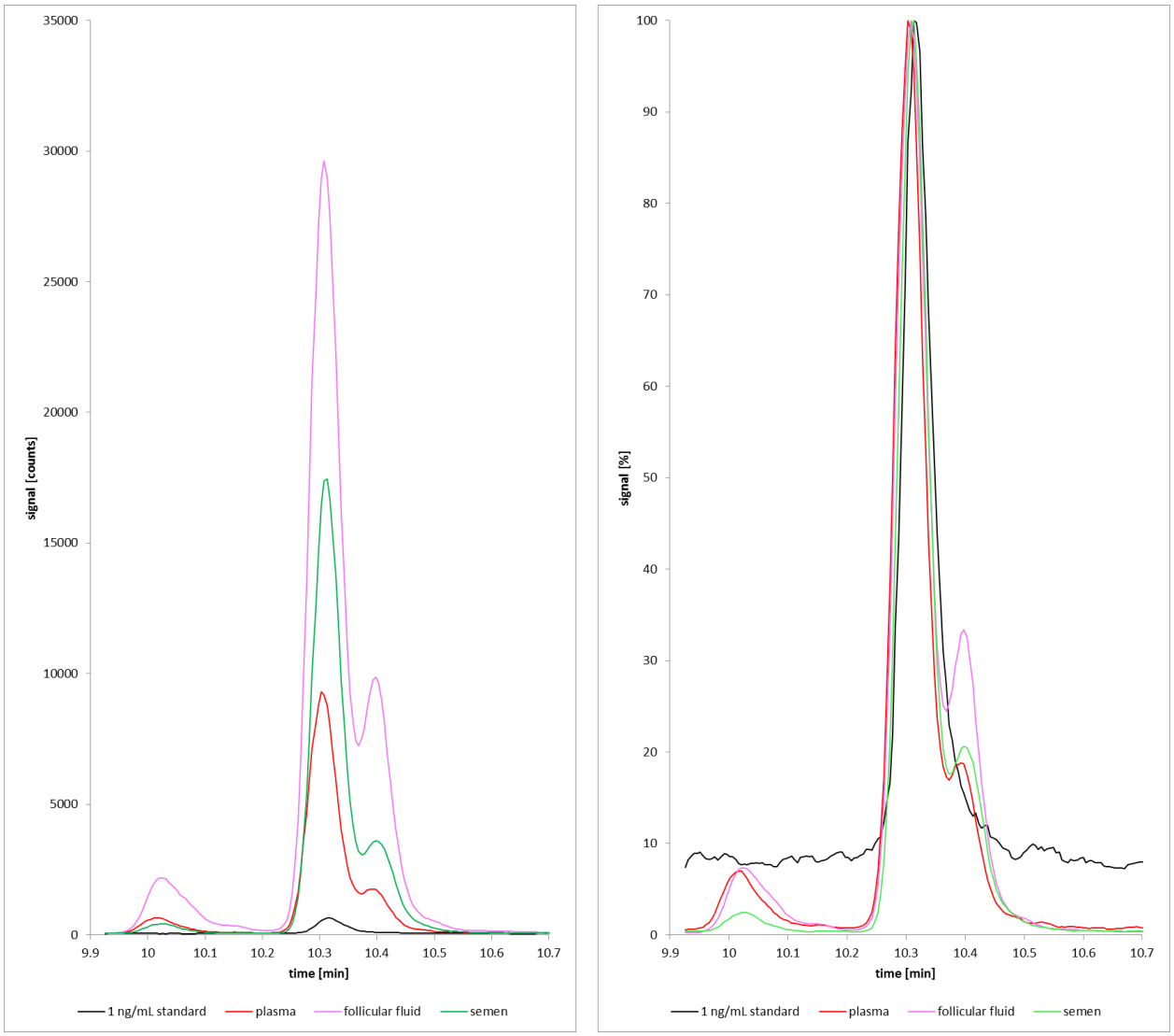

Figure 5-28 13-HODE measured in 1 ng/mL standard, plasma, follicular fluid and semen plasma

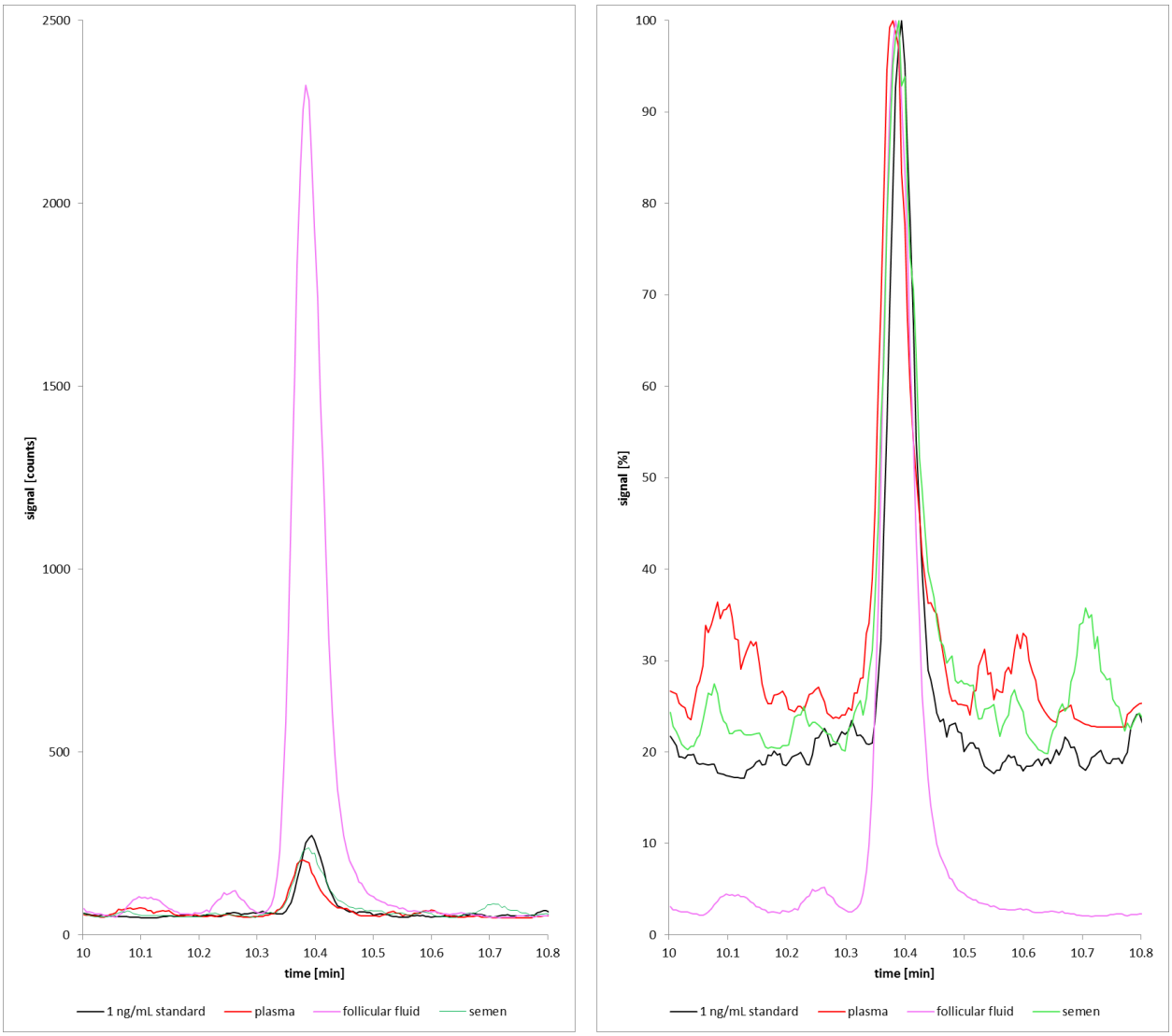

Figure 5-29 20-HDoHE measured in 1 ng/mL standard, plasma, follicular fluid and semen plasma

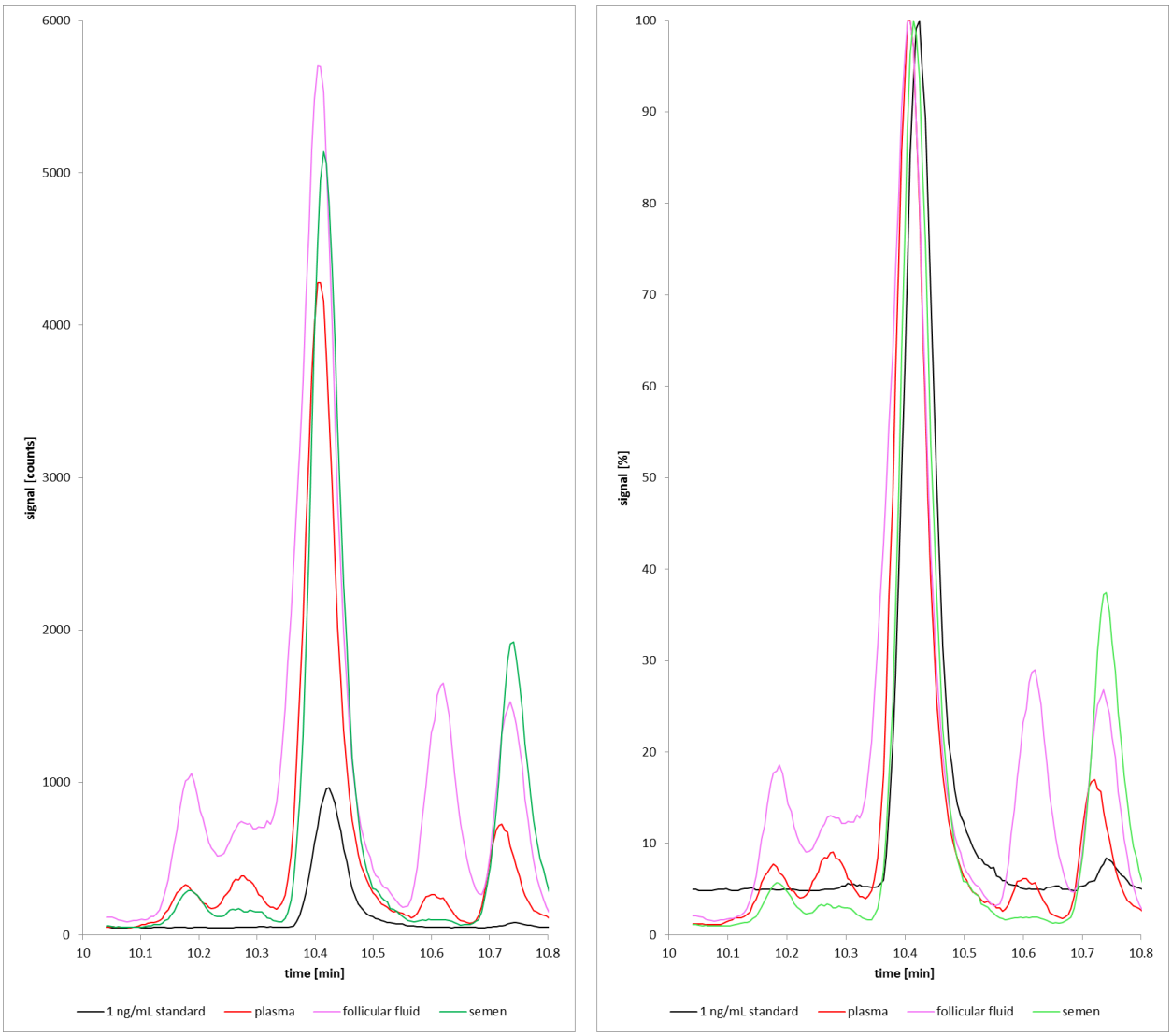

Figure 5-30 9-HODE measured in 1 ng/mL standard, plasma, follicular fluid and semen plasma

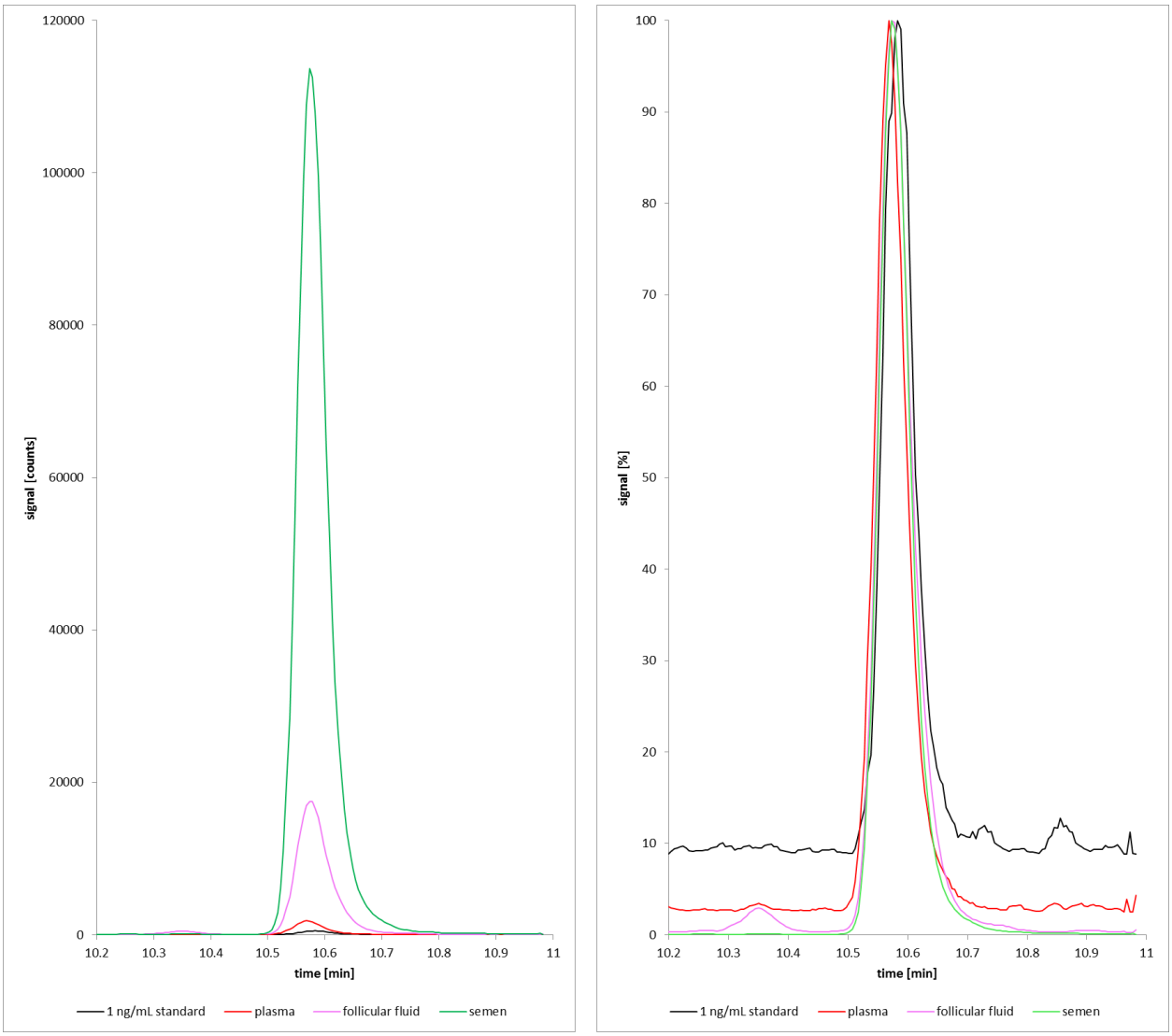

Figure 5-31 15-HETE measured in 1 ng/mL standard, plasma, follicular fluid and semen plasma

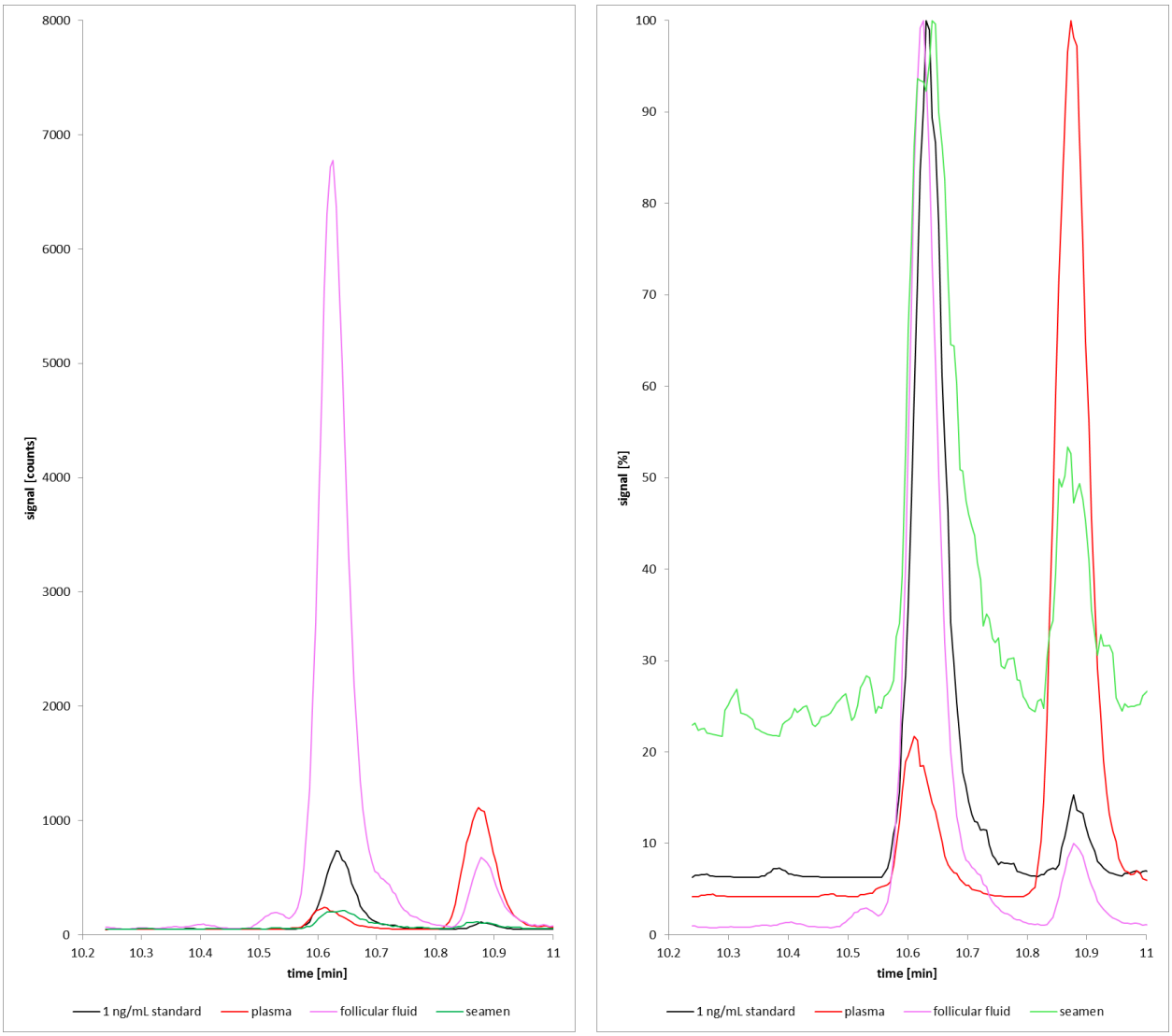

Figure 5-32 16-HDoHE measured in 1 ng/mL standard, plasma, follicular fluid and semen plasma

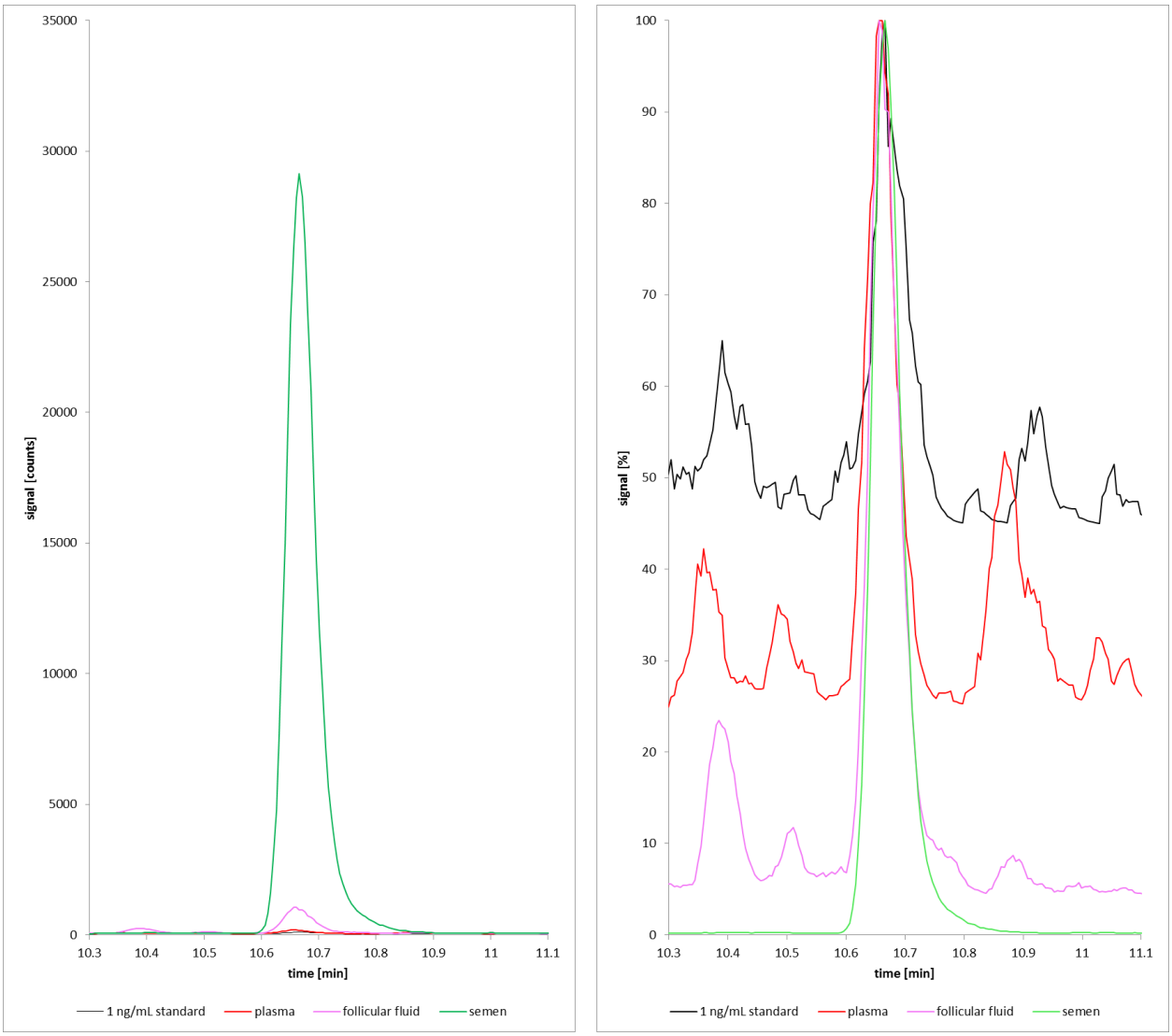

Figure 5-33 17-HDoHE measured in 1 ng/mL standard, plasma, follicular fluid and semen plasma

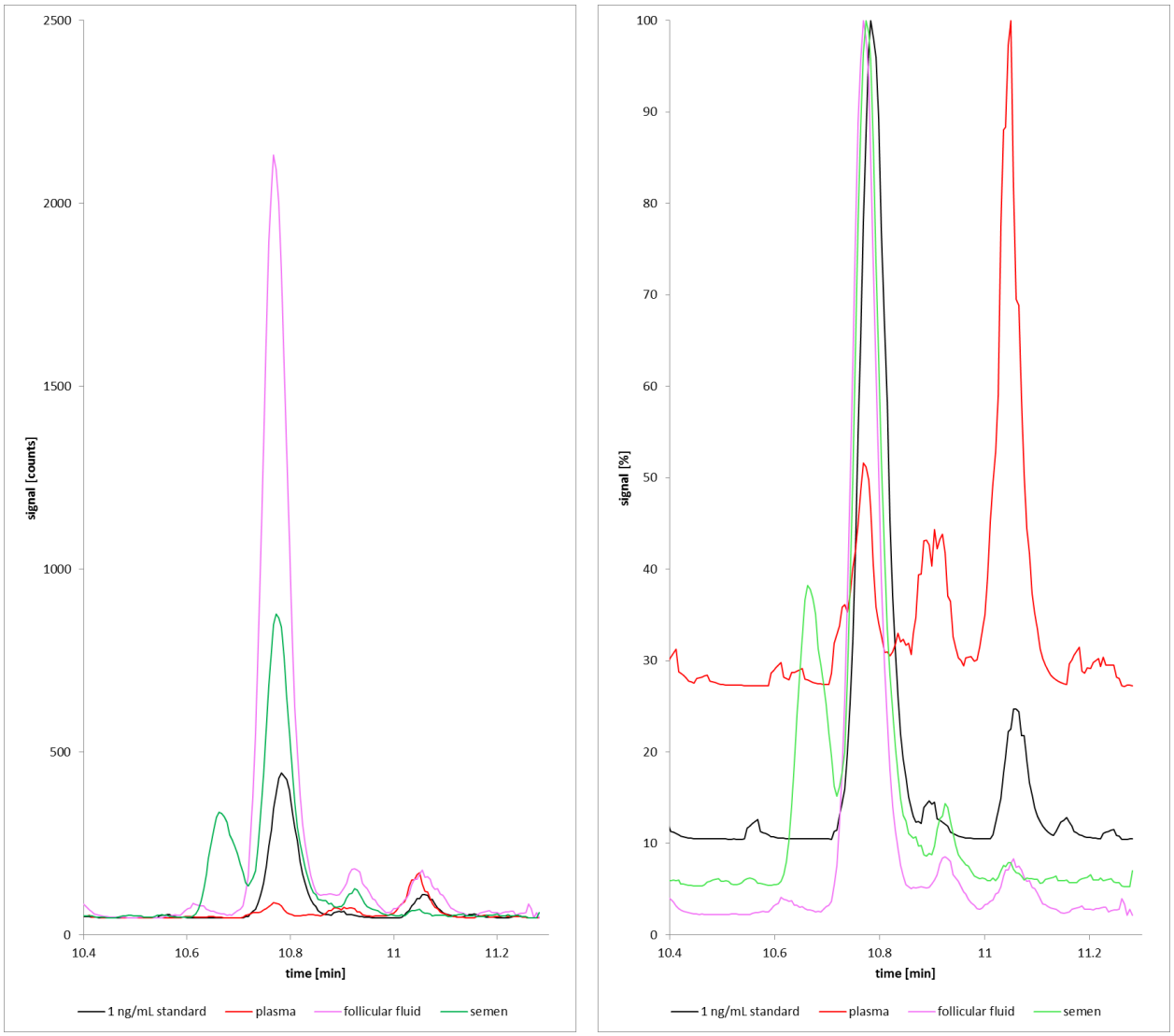

Figure 5-34 13-HDoHE measured in 1 ng/mL standard, plasma, follicular fluid and semen plasma

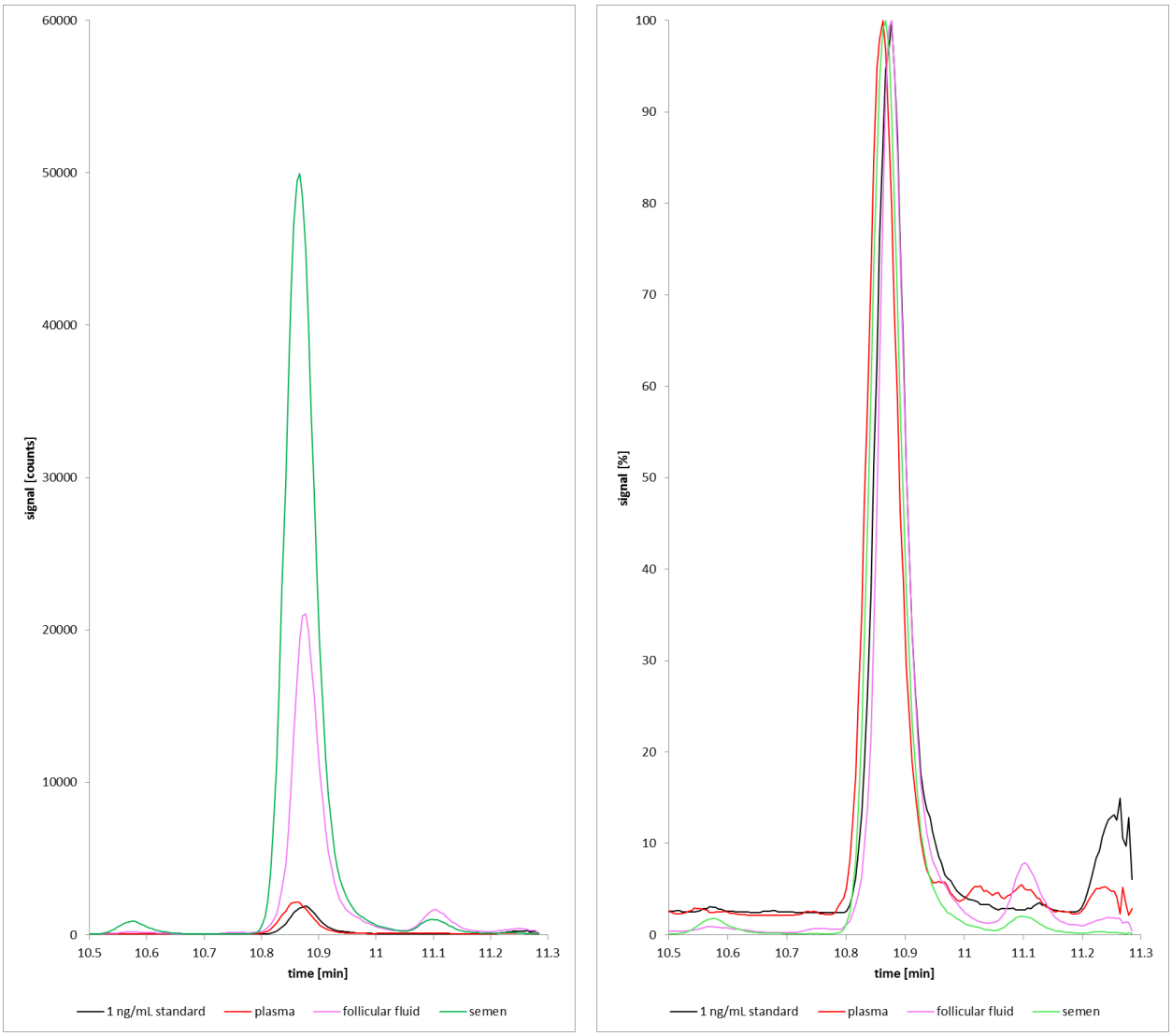

Figure 5-35 11-HETE measured in 1 ng/mL standard, plasma, follicular fluid and semen plasma

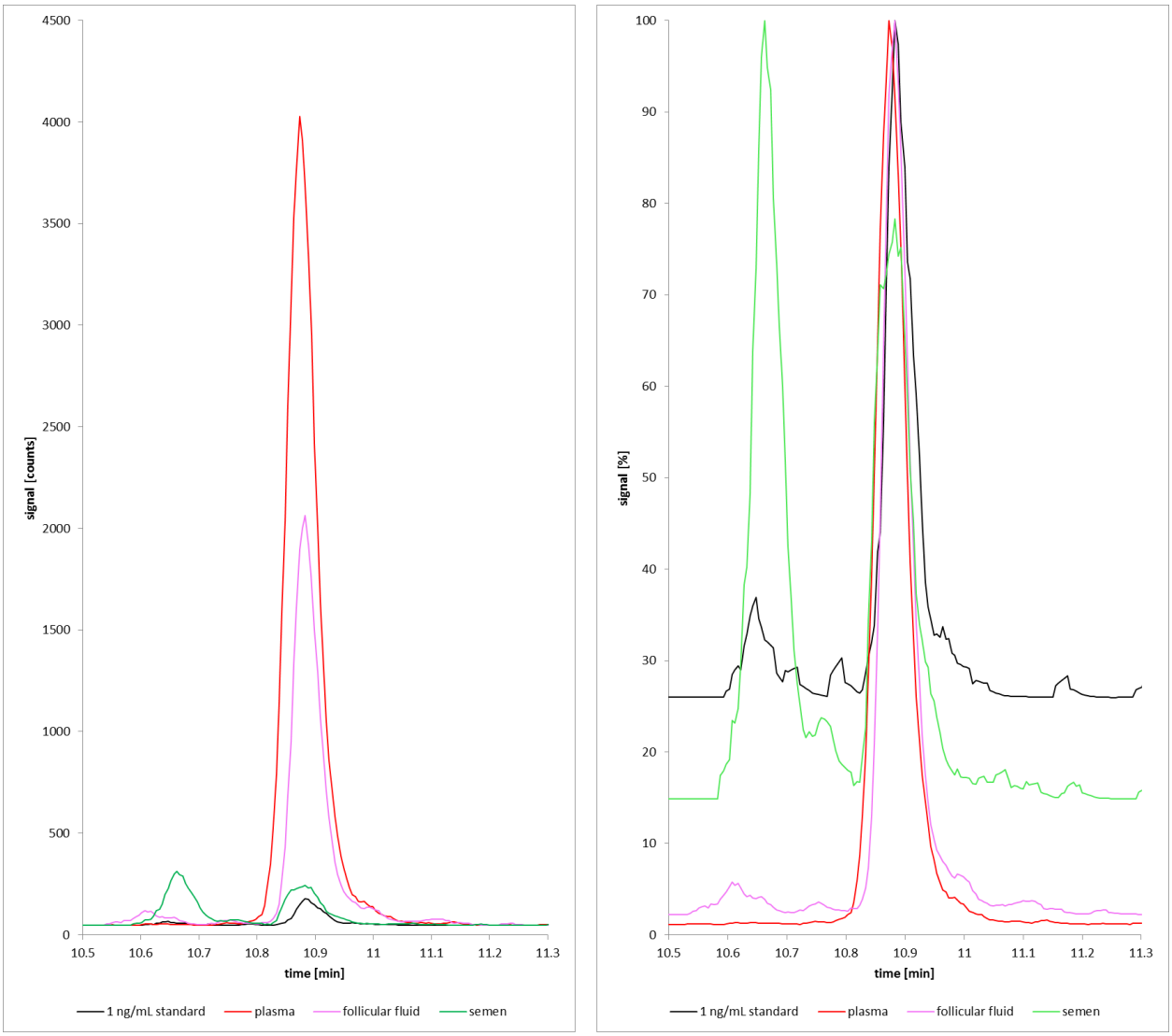

Figure 5-36 14-HDoHE measured in 1 ng/mL standard, plasma, follicular fluid and semen plasma

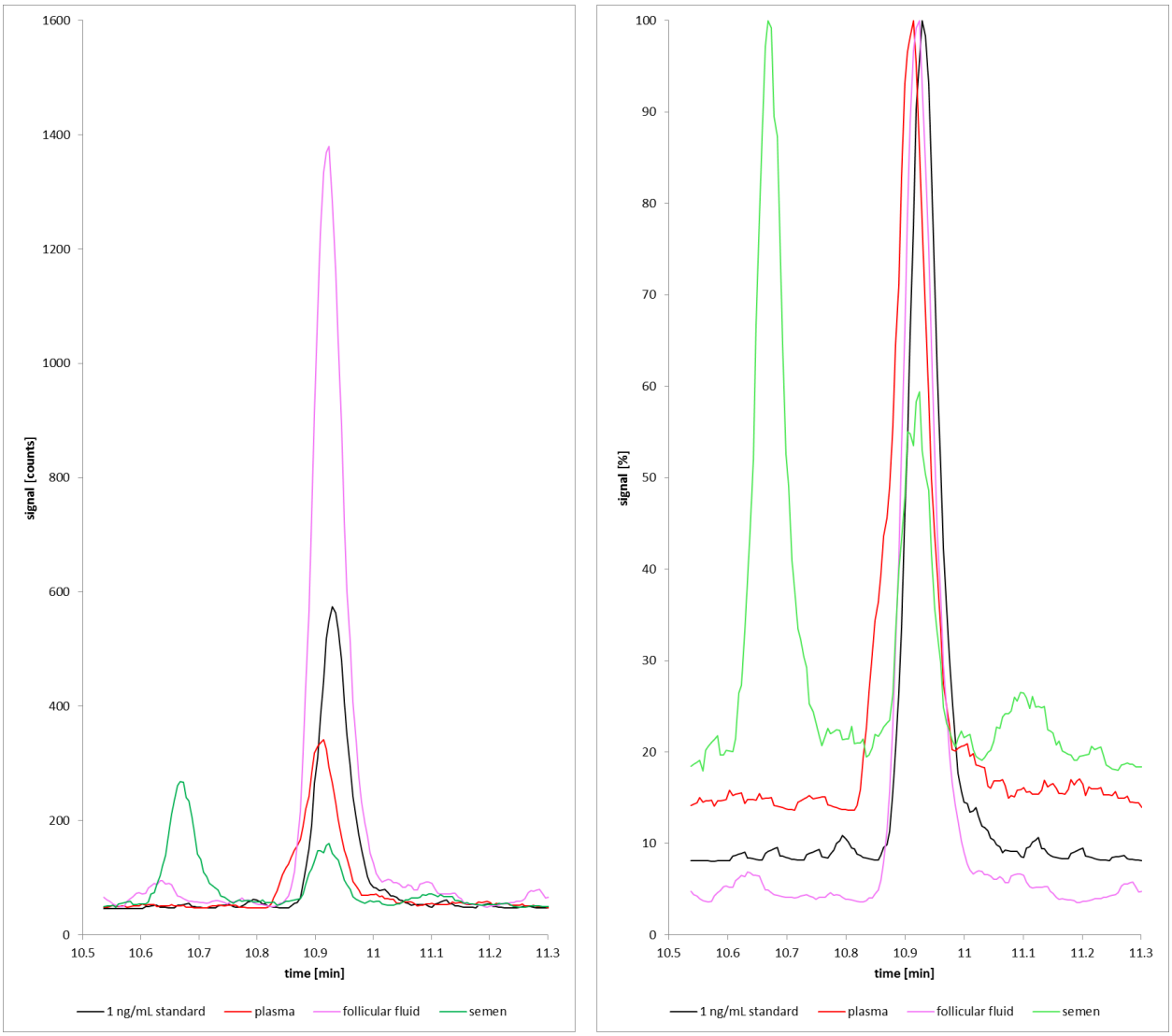

Figure 5-37 10-HDoHE measured in 1 ng/mL standard, plasma, follicular fluid and semen plasma

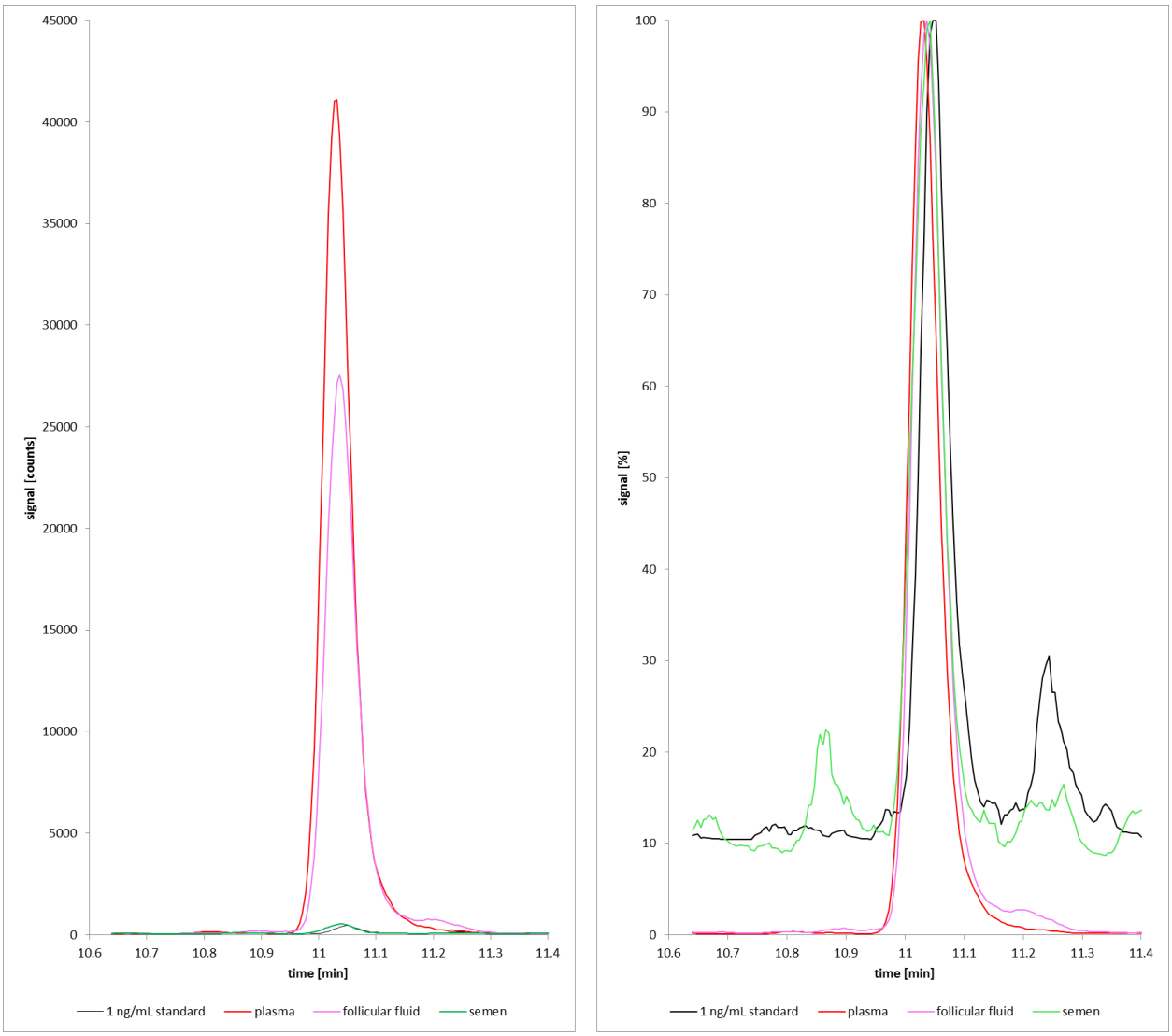

Figure 5-38 12-HETE measured in 1 ng/mL standard, plasma, follicular fluid and semen plasma

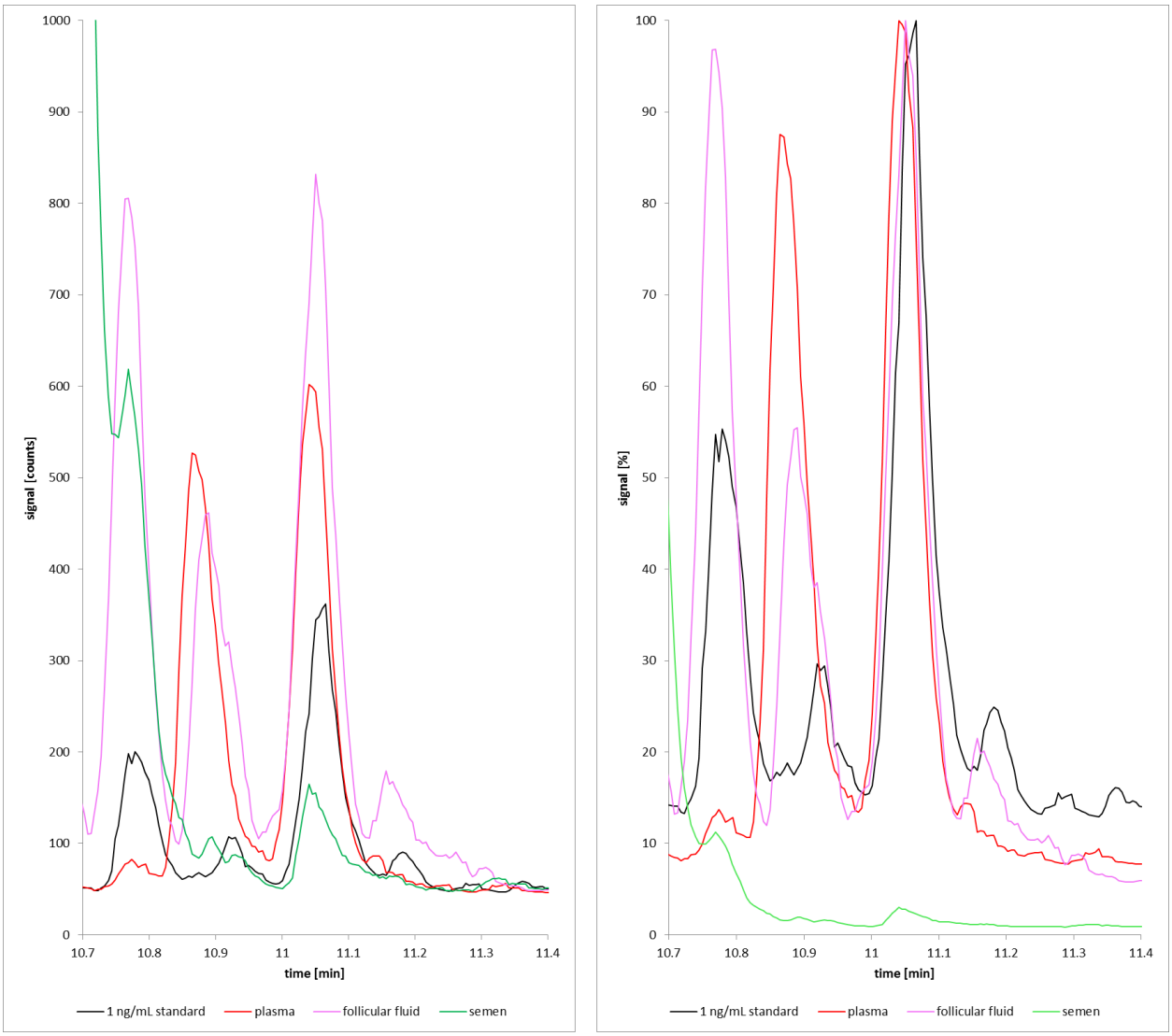

Figure 5-39 11-HDoHE measured in 1 ng/mL standard, plasma, follicular fluid and semen plasma

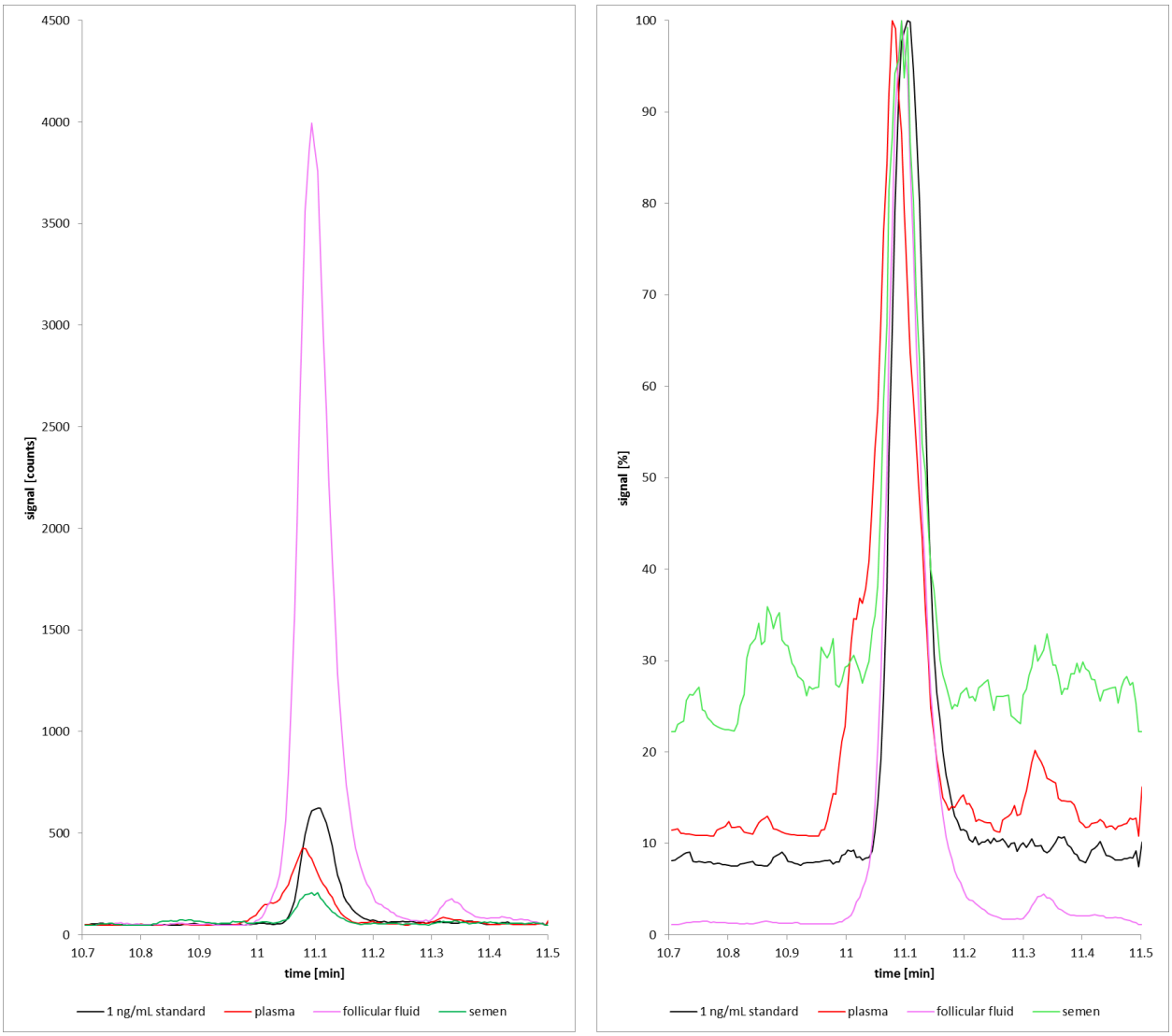

Figure 5-40 8-HETE measured in 1 ng/mL standard, plasma, follicular fluid and semen plasma

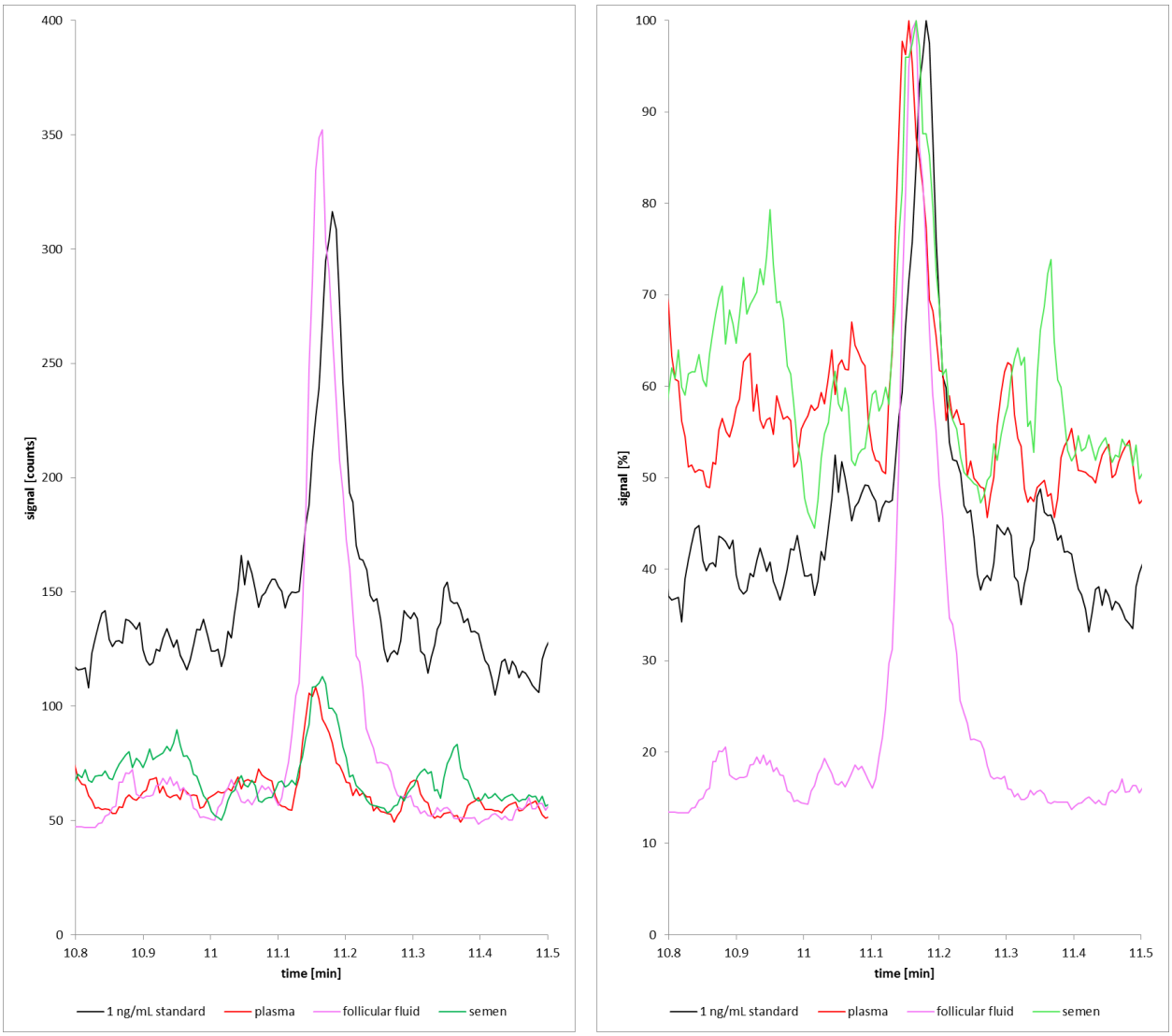

Figure 5-41 7-HDoHE measured in 1 ng/mL standard, plasma, follicular fluid and semen plasma

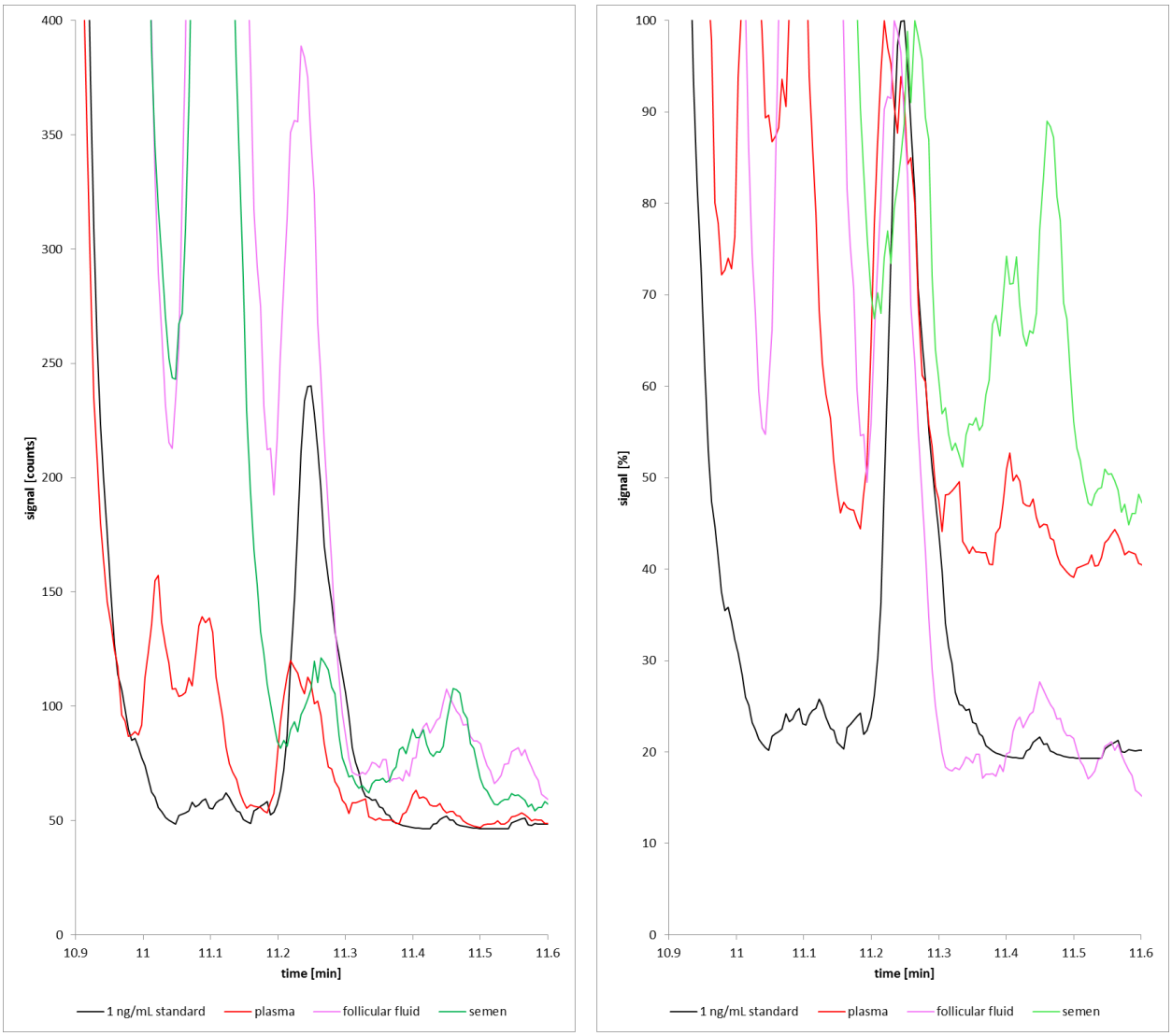

Figure 5-42 9-HETE measured in 1 ng/mL standard, plasma, follicular fluid and semen plasma

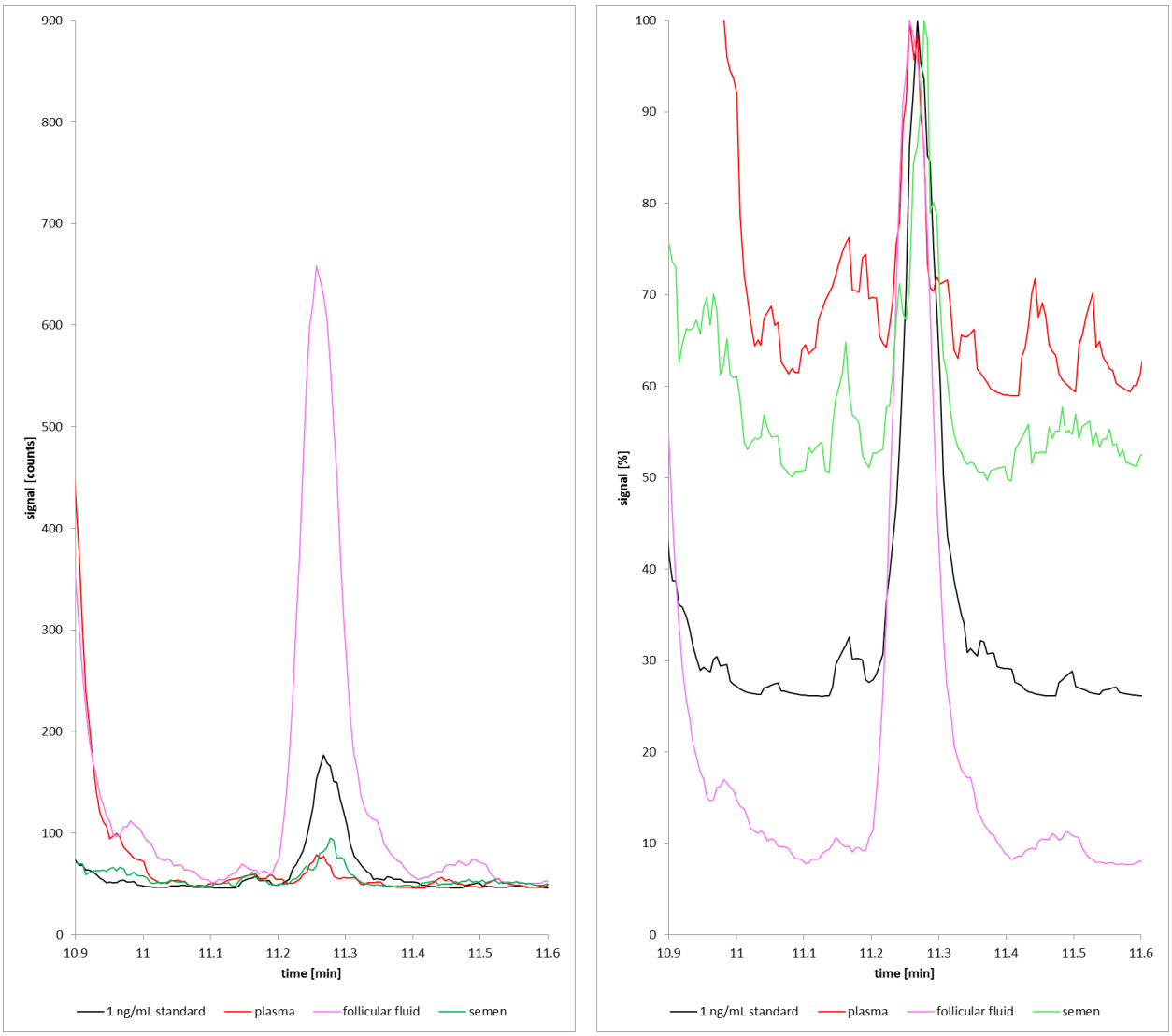

Figure 5-43 8-HDoHE measured in 1 ng/mL standard, plasma, follicular fluid and semen plasma

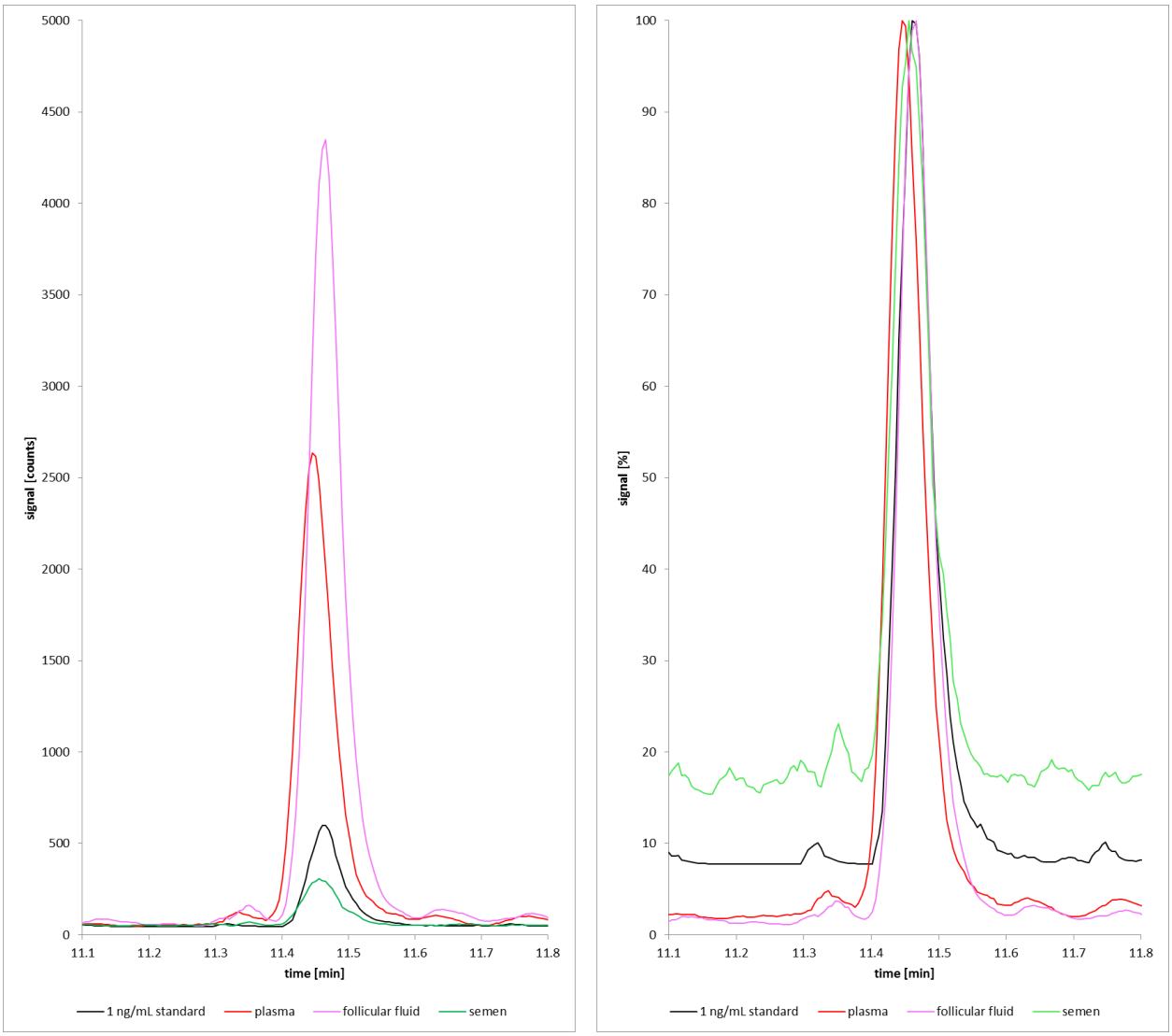

Figure 5-44 5-HETE measured in 1 ng/mL standard, plasma, follicular fluid and semen plasma

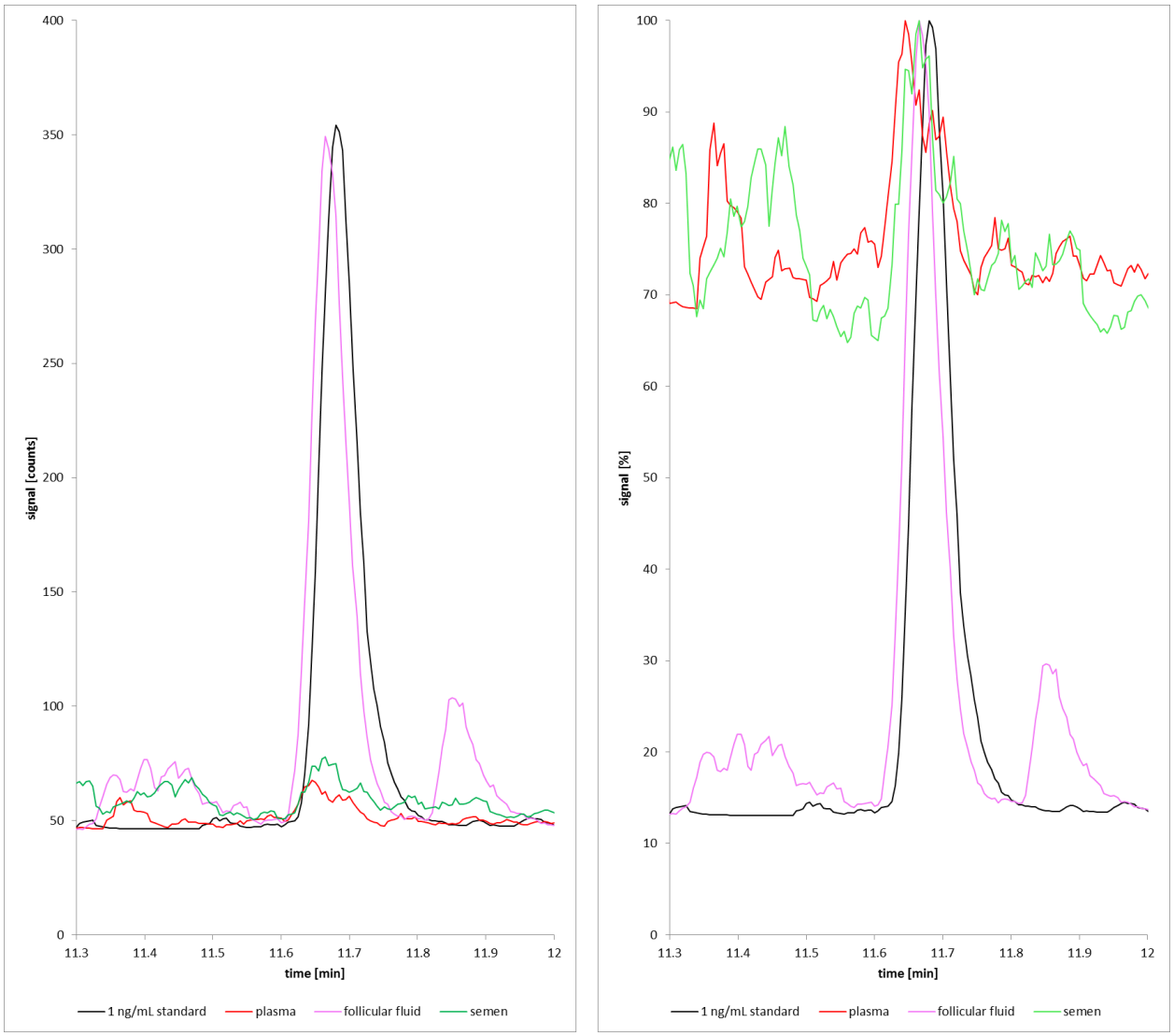

Figure 5-45 14(15)-EET measured in 1 ng/mL standard, plasma, follicular fluid and semen plasma

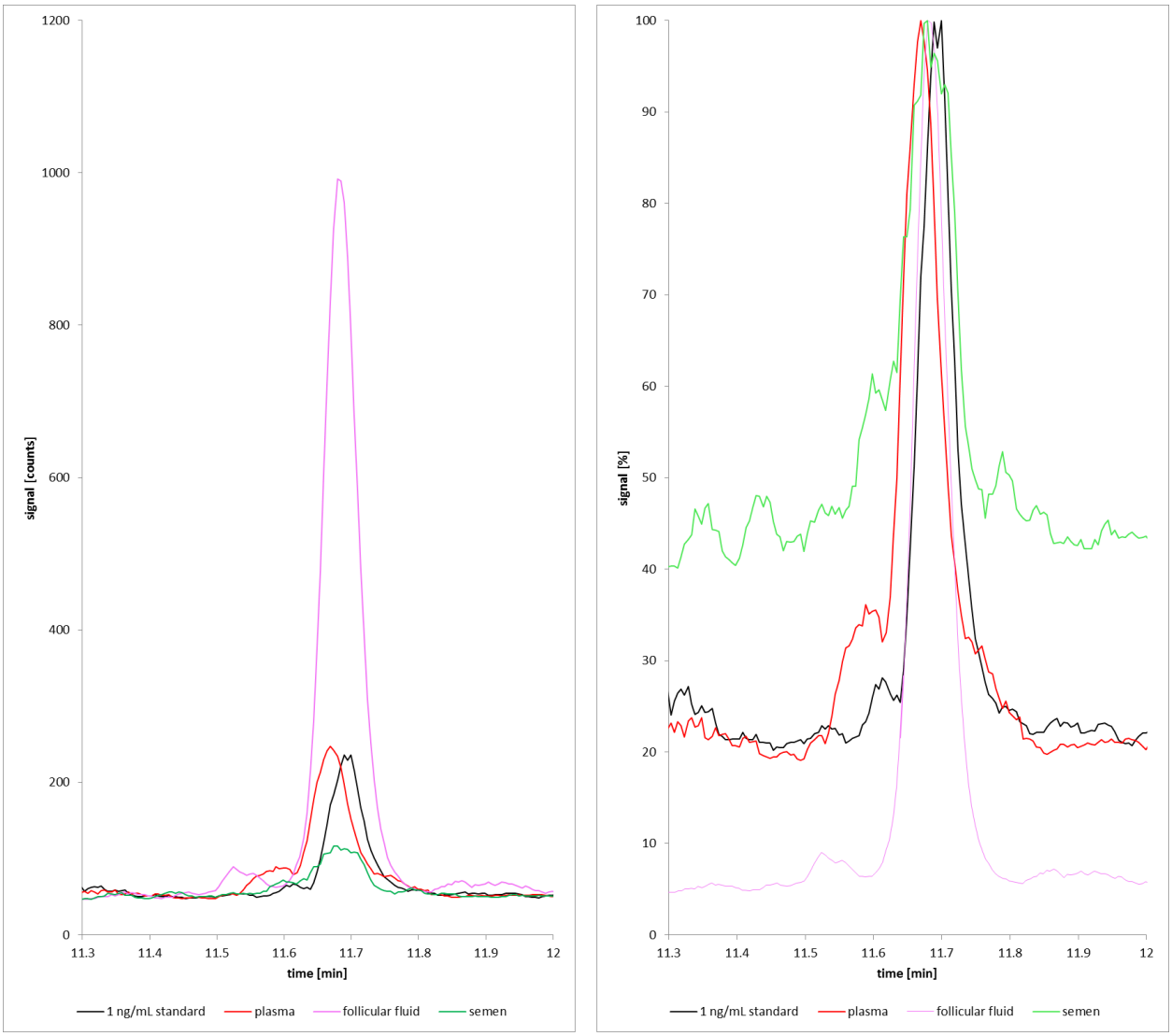

Figure 5-46 4-HDoHE measured in 1 ng/mL standard, plasma, follicular fluid and semen plasma

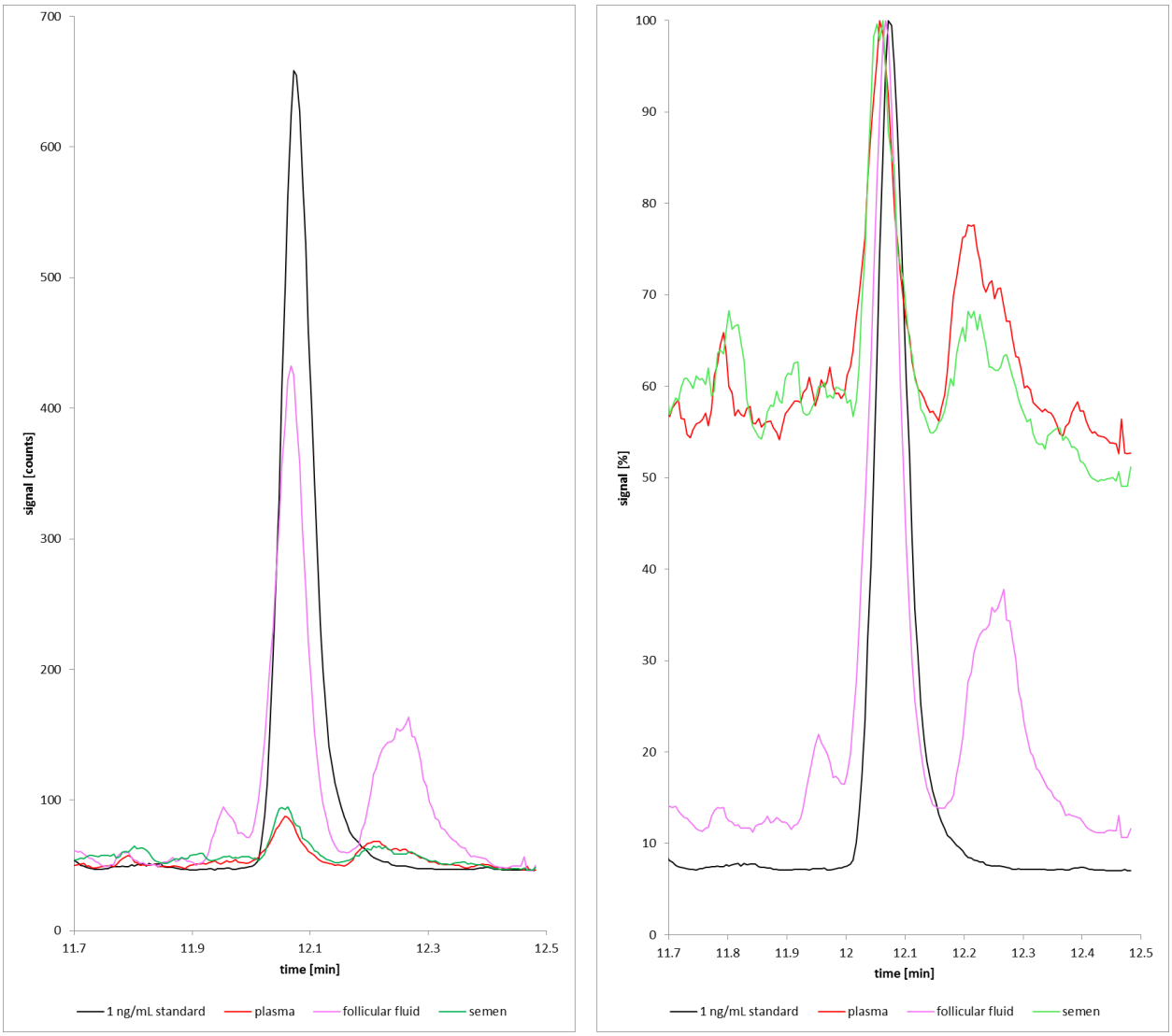

Figure 5-47 11(12)-EET measured in 1 ng/mL standard, plasma, follicular fluid and semen plasma